

***FORWARD AND INVERSE PROBLEM FOR  
NEMATIC LIQUID CRYSTALS***

Al-Humaidi, Saleh

2010

MIMS EPrint: **2017.47**

Manchester Institute for Mathematical Sciences  
School of Mathematics

The University of Manchester

Reports available from: <http://eprints.maths.manchester.ac.uk/>

And by contacting: The MIMS Secretary  
School of Mathematics  
The University of Manchester  
Manchester, M13 9PL, UK

ISSN 1749-9097

# FORWARD AND INVERSE PROBLEM FOR NEMATIC LIQUID CRYSTALS

A DISSERTATION SUBMITTED TO THE UNIVERSITY OF MANCHESTER  
AS A PARTIAL FULFILMENT FOR THE DEGREE OF DOCTOR OF PHILOSOPHY  
IN FACULTY OF ENGINEERING AND PHYSICAL SCIENCES

By

Saleh Al-Humaidi

University of Manchester

School of Mathematics

2010

# Contents

<b>Abstract</b>	<b>16</b>
<b>Declaration</b>	<b>18</b>
<b>Copyright</b>	<b>19</b>
<b>Acknowledgements</b>	<b>20</b>
<b>1 Introduction</b>	<b>21</b>
1.1 The concept of well-posed and ill-posed problems in mathematical physics . . . . .	23
1.2 Fundamental solution of a dynamic system . . . . .	24
1.3 Aims and objectives . . . . .	25
1.4 Thesis organization . . . . .	27
<b>2 Liquid crystals</b>	<b>29</b>
2.1 Some of the properties of liquid crystals . . . . .	29
2.1.1 Concept of anisotropy . . . . .	29
2.1.2 Birefringence . . . . .	30

---

2.1.3	Surface phenomenon . . . . .	31
2.2	Principal values and principal axes . . . . .	32
2.3	Oseen-Frank free-energy equation . . . . .	32
2.3.1	Mechanics of elastic and electric torque in liquid crystal molecules . . . . .	34
2.3.2	Model for director orientation . . . . .	34
2.3.3	Minimizing the Oseen-Frank free energy . . . . .	35
2.3.4	Electrostatic potential . . . . .	39
2.4	Summary . . . . .	40
<b>3</b>	<b>Polarization and Jones treatment</b>	<b>41</b>
3.1	Introduction . . . . .	41
3.2	Equation of polarization . . . . .	43
3.2.1	Linear polarization . . . . .	44
3.2.2	Circular polarization . . . . .	44
3.2.3	Elliptical polarization . . . . .	49
3.3	Jones concept of polarized light . . . . .	50
3.3.1	Jones vector . . . . .	50
3.3.2	The Jones matrix . . . . .	53
3.4	Jones matrix for anisotropic medium with a fixed transmission axis	53
3.5	Relationship between the Jones vector and the Stokes parameters	56
3.5.1	Stokes parameters . . . . .	57
3.5.2	Poincare sphere . . . . .	59

---

3.6	Conclusion . . . . .	60
<b>4</b>	<b>Experiment and Berreman solution</b>	<b>61</b>
4.1	The experimental setup . . . . .	61
4.2	The solution of the Berreman wave equation . . . . .	63
4.2.1	Fundamental matrix for single layer . . . . .	63
4.2.2	Fundamental matrix for the sample . . . . .	65
4.3	Discussion for propagation matrix . . . . .	66
4.3.1	Exponential series expansion method . . . . .	66
4.3.2	Caylay- Hamilton method . . . . .	67
4.4	Conclusion . . . . .	70
<b>5</b>	<b>Maxwell's equations and dielectric tensor</b>	<b>71</b>
5.1	Maxwell's equations . . . . .	71
5.2	Dielectric tensor . . . . .	73
5.3	Dielectric tensor for uniaxial materials . . . . .	75
5.4	Discussion . . . . .	78
5.4.1	Profiles of the elements of dielectric tensor for twisted nematic liquid crystal cell in the off state . . . . .	80
5.4.2	Relationship between the diagonal elements of dielectric tensor . . . . .	81
5.4.3	Positive birefringence . . . . .	82
5.4.4	Negative birefringence . . . . .	86
5.5	Summary . . . . .	90

---

<b>6</b>	<b>Matrix Schrödinger equation</b>	<b>91</b>
6.1	Introduction . . . . .	91
6.2	Our solution for the Schrödinger equation in matrix form . . . . .	92
6.3	Relationship between the Schrödinger equation and the Jones matrix formalism . . . . .	104
6.4	Polarization in Quantum Mechanics . . . . .	105
6.5	Interpretation of our model with Schrödinger model . . . . .	106
6.6	Floquet's theory . . . . .	107
6.7	Existence of the solution of the Schrödinger equation . . . . .	108
6.8	Eigenvalues and the corresponding potential for the Schrödinger equation . . . . .	109
6.8.1	Potential for isotropic sample . . . . .	110
6.8.2	Potential for anisotropic sample with a fixed transmission axis . . . . .	111
6.8.3	Potential for anisotropic sample with a twisted transmission axis . . . . .	112
6.9	Conclusion . . . . .	112
<b>7</b>	<b>Equation of propagation</b>	<b>114</b>
7.1	Introduction . . . . .	114
7.2	Detailed derivation for the Berreman equation from Maxwell's equations . . . . .	115
7.2.1	Berreman in the presence of a source . . . . .	120
7.2.2	Solution of Berreman in the presence of a source . . . . .	121

---

7.3	Derivation of a $2 \times 2$ differential equation from Berreman . . . . .	122
7.3.1	Modes inside the infinitesimal layer . . . . .	124
7.3.2	Elements of $2 \times 2$ system . . . . .	126
7.4	Modes of propagation . . . . .	128
7.4.1	Modes of propagation when $H(x)$ is constant . . . . .	128
7.4.2	Modes of propagation when $H(z)$ is a function of $z$ . . . . .	129
7.5	Propagation matrix . . . . .	132
7.6	Application to isotropic medium . . . . .	133
7.6.1	Two waves with phase shift zero . . . . .	135
7.6.2	Two waves with phase shift ninety . . . . .	135
7.7	Application to a non-twisted medium . . . . .	137
7.7.1	Discussion . . . . .	140
7.7.2	linear polarization with phase shift zero . . . . .	143
7.7.3	a circular polarization . . . . .	145
7.8	Application to a medium with a twisted transmission axis . . . . .	147
7.8.1	Normal incident . . . . .	147
7.8.2	Oblique incident . . . . .	150
7.9	Berreman approximation . . . . .	150
7.10	Conclusion . . . . .	154
<b>8</b>	<b>Forward and inverse problem</b>	<b>159</b>
8.1	Derivation from Maxwell's equations . . . . .	159
8.1.1	Ordinary and extraordinary matrices . . . . .	160

---

8.1.2	Derivation of the Schrödinger Equation . . . . .	161
8.2	Discussion . . . . .	163
8.2.1	The Solution of the Schrödinger equation with a vanishing potential . . . . .	164
8.2.2	The Solution of the Schrödinger equation with a constant potential . . . . .	165
8.2.3	The Solution of the Schrödinger equation with a non-vanishing potential . . . . .	167
8.3	Inverse problem for Berreman . . . . .	169
8.4	Linearized inverse problem for Berreman . . . . .	171
8.5	Summary . . . . .	172
<b>9</b>	<b>Conclusions and future work</b>	<b>174</b>
9.1	conclusion . . . . .	174
9.2	Future work . . . . .	176
9.2.1	Non-vanishing tilt angles . . . . .	176
9.2.2	Reconstruction of the potential . . . . .	177
	<b>Bibliography</b>	<b>178</b>

# List of Tables

3.1	Shows the normalized form of the Jones vector for some selected polarization states. . . . .	52
5.1	This table shows the values of the dielectric tensor elements at some different locations for calcite $\text{CaCO}_3$ which is has a negative birefringence. . . . .	89
6.1	The possible direction for the transmission axis together with corresponding potential and eigenvalues of the Schrödinger equation for anisotropic sample with a fixed transmission axis. . . . .	111

# List of Figures

2.1	In uniaxial materials, light decomposes into two components traveling in two different directions and at two different velocities. . .	30
2.2	Nematic liquid crystal cell sandwiched between two glasses:(a)Without electric field, (b) An electric field is applied across the cell. . . . .	33
3.1	Two waves propagates inside isotropic medium with phase difference zero. . . . .	45
3.2	The above two waves propagate perpendicular to each other . . .	45
3.3	Shows the sum of these two waves . . . . .	46
3.4	This figure shows the resultant linear polarization. . . . .	46
3.5	Two waves propagates inside isotropic medium with ninety degrees phase shift between them. . . . .	47
3.6	The above two waves propagate perpendicular to each other. . . .	48
3.7	Shows the sum of these two waves together with the type of resulting polarization. . . . .	48
3.8	This figure shows the type of polarization which is a circular polarization. . . . .	49

---

3.9	The representation of the state of polarization by the Poincare sphere using the Stokes parameters. . . . .	59
4.1	This figure shows the experiment setup used at Hewlett Packard Laboratories in Bristol(HPLB). The nematic liquid crystal sample is fixed inside the cylindrical mount and the incident angle can be changed by rotating the cylindrical mount. . . . .	62
4.2	The nematic liquid crystal sample is divided into thin layers with thickness $h$ . For each layer, the orientation of the director is considered to be constant. . . . .	64
5.1	The axes of the ellipse give us the direction of the principal axes for $z = 0.2$ , in which the dielectric tensor has a diagonal form. . .	76
5.2	The axes of the ellipse give us the direction of the principal axes for $z = 0.6$ , in which the dielectric tensor has a diagonal form. . .	76
5.3	Director orientation inside the sample with tilt angle $\theta$ and azimuthal angle $\phi$ . . . . .	77
5.4	The twist(Green) and tilt(Blue) angles profiles for some voltages applied across the sample. The voltage in the above graph are 0.2, 0.4, 1.2, 1.9, 2.9, and high voltage 5 . . . . .	80
5.5	The profile of the optical axis which coincides with the director as a function of position. . . . .	81
5.6	The profile of the first diagonal element of the dielectric tensor in the off state as we travel though the sample with a positive birefringence. . . . .	84

5.7 The profile of the second diagonal element of the dielectric tensor in the off state as we travel through the sample with a positive birefringence. . . . . 84

5.8 The profiles of all diagonal elements of the dielectric tensor in the off state as we travel through the sample with a positive birefringence. 85

5.9 This graph shows the profiles of all remaining off diagonal elements of the dielectric tensor in the off state for a sample with a positive birefringence. . . . . 85

5.10 The profiles of all elements of a dielectric tensor in the off-state after re-scaling the diagonal elements. . . . . 86

5.11 The profile of the first diagonal element of the dielectric tensor in the off state as we travel through the sample with a negative birefringence. . . . . 87

5.12 The profile of the second diagonal element of the dielectric tensor in the off state as we travel through the sample with a negative birefringence. . . . . 88

5.13 The profiles of all diagonal elements of the dielectric tensor in the off state as we travel through the sample with a negative birefringence. 88

5.14 This graph shows the profiles of all remaining off diagonal elements of the dielectric tensor in the off state for a sample with a negative birefringence. . . . . 89

5.15 The profiles of all elements of a dielectric tensor in the off-state with a negative dielectric tensor after re-scaling. . . . . 90

---

6.1	This graph shows the $x$ -component for the exact and numerical solution of the Schrödinger equation. . . . .	95
6.2	This graph shows the $y$ -component for the exact and numerical solution of the Schrödinger equation. . . . .	96
6.3	This graph shows both $x$ -component and $y$ -component for the numerical solution of the Schrödinger equation as they propagate through the medium. . . . .	97
6.4	This graph shows both $x$ -component and $y$ -component for the exact solution of the Schrödinger equation as they propagate through the medium. . . . .	98
6.5	This graph shows the $x$ -component for the exact and numerical solution of the Schrödinger equation. . . . .	100
6.6	This graph shows the $y$ -component for the exact and numerical solution of the Schrödinger equation. . . . .	101
6.7	This graph shows both the $x$ -component and $y$ -component for the numerical solution of the Schrödinger equation as they propagate through the medium. . . . .	102
6.8	This graph shows both $x$ -component and $y$ -component for the exact solution of the Schrödinger equation as they propagate through the medium. . . . .	103
7.1	This figure illustrates the change in the orientation of the local birefringence axes from the initial input at the position $z$ to the new position $z + \Delta z$ . . . . .	123

---

7.2	This figure shows the modes that propagate in isotropic medium with a circular polarization input. These modes propagate in the eigen-direction that is along the molecular axes. . . . .	129
7.3	This figure shows the local modes for a sample with a fixed axis of anisotropy. . . . .	130
7.4	This figure shows the local modes for a sample with a twisted axis of anisotropy. . . . .	131
7.5	Dependence of the eigenvalue on the incident angle of a sample with refractive index $n_o = 1.400$ . . . . .	134
7.6	The propagation of the plan waves inside isotropic medium with phase shift zero according the above solution. . . . .	136
7.7	The directions of propagation of the waves inside the medium. . .	136
7.8	The resulting type of polarization at any location inside the medium with input phase shift zero. . . . .	137
7.9	The propagation of the plan waves inside the isotropic medium with phase shift ninety. . . . .	138
7.10	The directions of propagation of the waves inside the medium with input phase shift ninety. . . . .	138
7.11	The resulting type of polarization at any location inside the medium with input phase shift ninety. . . . .	139
7.12	Illustration of the polarization in terms of the ratio of electric field components inside a medium with a fixed transmission axis of anisotropy. . . . .	141

---

7.13	This figure shows the behavior of the eigenvalues with incident angle for a positive birefringence. . . . .	141
7.14	This figure shows the behavior of the eigenvalues with incident angle for a negative birefringence. . . . .	142
7.15	This figure shows the difference between the eigenvalues as the incident angle increases for a positive birefringence. . . . .	142
7.16	This figure shows the difference between the eigenvalues as the incident angle increases for a negative birefringence. . . . .	143
7.17	This figure shows the propagation of the wave inside anisotropic medium with a fixed transmission axis of anisotropy and a linear polarization input. . . . .	144
7.18	This figure illustrates the state of polarization at any location inside the medium together with the orthogonal waves. . . . .	144
7.19	The state of polarization at any location inside the medium. . . .	145
7.20	This figure shows the propagation of the wave inside anisotropic medium with a fixed transmission axis of anisotropy and a circular polarization input. . . . .	146
7.21	This figure illustrates the state of polarization at any location inside the medium together with the orthogonal waves. . . . .	146
7.22	The state of polarization at any location inside the medium. . . .	147
7.23	This figure shows how the waves propagate inside a sample with a twisted axis of anisotropy. . . . .	151
7.24	Berreman approaches to solve the Maxwell equations for inhomogeneous medium anisotropic medium. . . . .	152

---

7.25	The first electric field component of Berreman approximated solution is not converging to the analytical solution for inhomogeneous sample with twist $22.5^\circ$ . . . . .	153
7.26	The second electric field component of Berreman approximated solution is not converging to the analytical solution for inhomogeneous sample with twist $22.5^\circ$ . . . . .	153
7.27	This figure shows the convergence of Berreman approximated solution to the exact solution of an inhomogeneous sample of length $8.666\mu m$ . In this figure, the number of partition is 83557 . . . . .	155
7.28	The error of the first component of the electric field $E_x$ for a fixed medium with seven different wavelengths. . . . .	155
7.29	The error of the first component of the electric field $E_y$ for a fixed medium with seven different wavelengths. . . . .	156
7.30	The error of the electric field for a fixed medium with the same seven different wavelengths. . . . .	156
7.31	The log-log plot for the error of the electric field the same seven different wavelengths. . . . .	157

# Abstract

This thesis starts with an introduction to liquid crystal properties, which are needed to proceed with this research. From the dielectric tensor which appears in the Maxwell equations, we were able to obtain a relationship between the elements on the main diagonal of the dielectric tensor. This relationship has been discussed and illustrated with some examples for both positive and negative birefringence.

By introducing a constrain on the Berreman model, we were able to derive a  $2 \times 2$  differential equation in matrix form which works for both normal and oblique incident. This equation gives us a simple and intuitive means to analyze the evolution of light through all sorts of media i.e. isotropic, anisotropic with a fixed transmission axis and anisotropic with a twisted transmission axis of anisotropy.

One of the objectives of this research was to find the right technique to solve the  $2 \times 2$  dynamic equation. Fortunately, the classic Floquet's theory guarantees the existence of the solution and it gives some of its characteristics. In fact, we were able to solve the  $2 \times 2$  Schrödinger equation by a new method which we called it in this thesis a rotational frame method. The obtained solution is consistent with Floquet's theory and agrees totally with the Jones solutions. Also, this solution allows us to test the Berreman approximation.

Finally, in this research we were able to encode the orientation of the optical axis inside a liquid crystal sample, into the potential of the Schrödinger equation. As a consequence of that, solving the inverse problem of the Schrödinger equation that is recovering the potential, is indeed recovering the orientation of the director inside the sample. The Berreman inverse problem and its corresponding linearized problem has been considered in this thesis. In these sections, we give a rigorous derivation for the Fréchet derivative.

# Declaration

No portion of the work referred to in this thesis has been submitted in support of an application for another degree or qualification of this or any other university or other institution of learning.

# Copyright

Copyright in text of this thesis rests with the Author. Copies (by any process) either in full, or of extracts, may be made **only** in accordance with instructions given by the Author and lodged in the John Rylands University Library of Manchester. Details may be obtained from the Librarian. This page must form part of any such copies made. Further copies (by any process) of copies made in accordance with such instructions may not be made without the permission (in writing) of the Author.

The ownership of any intellectual property rights which may be described in this thesis is vested in The University of Manchester, subject to any prior agreement to the contrary, and may not be made available for use by third parties without the written permission of the University, which will prescribe the terms and conditions of any such agreement.

Further information on the conditions under which disclosures and exploitation may take place is available from the Head of School of Mathematics.

© Copyright 2010

by

Saleh Al-Humaidi

University of Manchester

# Acknowledgements

There are several people to whom I feel the need to acknowledge them for their role in the preparation of this thesis. First of all, I am thankful to GOD ALLAH who provided me with great health, energy and education while preparing this work.

I would like to express my thanks and gratitude to my supervisor Prof. Bill Lionheart for his help, guidance and high standard friendship. He is one of the most active members of the British Inverse Problem Society and it was a great honor to have my PhD with him. I would like to express my thanks to Dr. Chris Newton at Hewlett Packard Laboratories in Bristol (HPLB), for his help and willingness to introduce me to the experiment. Special thanks to Mr. Darren Micklewright at Wilbraham Primary School in Manchester for his advice and help. Particular thanks go to the Royal Commission in Jubail and Saudi Cultural Bureau in London for the financial support throughout the four years.

I also extend my thanks to all my family in general, my parents for their continuous support and advice and mainly for their Doa'a without which this work would not be accomplished, my sisters and brothers, for their help and support. I would like to acknowledge my wife Awal for her cooperation, support and patience. Finally, special thanks to my lovely kids Ali and Karrar whose smiles give me a great hope in life.

# Chapter 1

## Introduction

It is well known that material scientists classified the matter into three different states: gas, liquid and solid. The main basis of this classification is the orientation and the position of the molecules in the matter. Last century a new state of matter has been reported under the name of liquid crystal. As it can be easily seen that the formalism of this name appears since the new state lies between liquid phase and solid phase. Indeed the molecules in liquid crystal tend to have an average degree of orientation and this average of orientation is known as the director of the liquid crystal. However, the molecules in the liquid crystal phase do not have any degree of positioning order.

In short, liquid crystal consist of elongated rod shape molecules in which the long axis of each of the molecules tends to align on average in one direction and this direction is known in optics as the director or the optical axis. In fact, there are many kinds of liquid crystal. However, the twisted nematic liquid crystal is the most common one for applications. An application familiar to most people is the displays, such as calculators, cellular phones, watches, new computer screens and some new large TV screens.

The study of light propagation inside isotropic and anisotropic media, such as a liquid crystal, is of particular importance from a practical application point of view. In practice, the optical properties of liquid crystal have been extensively studied in the literature of numerous papers, see for example [5], [12], [37]. As a consequence of that, several schemes have been proposed to calculate the optical properties of these media.

One of the most important cases which has been treated by several authors is when the wavelength of the propagating light is much smaller than the pitch where the typical distance over which the optical axis changes is significant. In such situations, the reflected light can usually be ignored. By reviewing the literature, it can be easily noticed that the Jones method [27], [58] and the Berreman method [5], [46], [23], [6] are the most commonly used methods to handle and model the optical properties of the liquid crystal devices. Generally speaking, Berreman was able to manipulate Maxwell's equations, as we will see later in this thesis, in order to obtain his equation, which gives us all the information required about the optical properties.

One of the main differences between these methods is that the Berreman method considers both transmitted and reflected waves but the Jones method ignores the reflected and considers only the transmitted waves. A detailed derivation of Jones method is given by Lien [27]. Both of these methods assume that the propagation of the fields vary in one direction which is usually normal to the supporting glasses which sandwich the medium.

In some cases, the Berreman equation can be solved analytically. However, in most cases of interest only a numerical solution is possible. Also, when the sample width is significantly larger than the wavelength of the incident light, then the task of finding a numerical solution to the Berreman equation is time consuming.

Also, from the literature, it can be noticed that both of the above methods can not handle the model for high resolution display devices. The main reason is that the propagation of fields vary in the other directions. A good source for modeling high resolution displays devices can be found in [22]. Finally, the application of an electric field to liquid crystal has the effect to reorient molecules and change the orientation of director inside the liquid crystal devices. This phenomenon leads to a wide range of applications in the field of displays.

## 1.1 The concept of well-posed and ill-posed problems in mathematical physics

Both of the mathematical terms, well-posed and ill-posed were introduced by the the French mathematician Hadamard in the field of partial differential equations. According to Hadamard, the solution of a mathematical model of a certain physical phenomenon has to have certain criteria in order to say that the problem is either well-posed or ill-posed. A problem is said to be well-posed if its solution exists, unique and continuously depends on the data. A good example of the concept of a well-posed problem in the field of partial differential equations is the heat equation with prescribed initial conditions.

On the other hand, a problem is said to be ill-posed if it is simply not well-posed. In other words, an ill-posed problem is a problem which does not have a solution, or the solution exist but it is not unique or the solution does not depend continuously on the data. In reality, a concept has been introduced lately which is the concept of a well-posed problem in the sense of Tikhonov. This concept says that some class of the ill-posed problem can be moved to the class of a well-posed problem. This can be done by reformulating the problem and introducing extra

assumptions. This method is known in mathematics as regularization and was introduced by Tikhonov [49].

## 1.2 Fundamental solution of a dynamic system

The major objective of this section is to introduce the concept of a fundamental matrix of a linear dynamic system. Basically, a linear dynamic system is a set of first order linear differential equations . These equations can be written in vector form as:

$$\psi(z)' = A(z)\psi(z). \quad (1.1)$$

where  $A(z)$  is a square matrix known as the dynamic coefficient matrix. If the elements of the coefficient matrix are continuous, then a fundamental matrix exists for the above dynamic linear system on the interval  $[0, z]$  if

$$T(z)' = A(z)T(z), \quad (1.2)$$

and  $T(0) = I$ . This solution of the dynamic system which is called a fundamental matrix is also known in some contexts as a transition matrix. The matrix is a square matrix that satisfies the differential equation of a dynamic system and equals to an identity at the initial state. One of the main properties of this matrix is the ability to transfer any possible initial state of a dynamic system to another state

$$\psi(z) = T(z)\psi(0). \quad (1.3)$$

In other words, if  $\psi(z) = T(z)\psi(0)$  is the solution of the dynamic system with initial state  $\psi(0)$  then

$$\psi(z)' = \frac{d}{dz}\{T(z)\psi(0)\} \quad (1.4)$$

$$= \frac{d}{dz}\{T(z)\}\psi(0) \quad (1.5)$$

$$= \{A(z)T(z)\}\psi(0) \quad (1.6)$$

$$= A(z)\{T(z)\psi(0)\} \quad (1.7)$$

$$= A(z)\psi(z). \quad (1.8)$$

is indeed the solution of the differential equation of the system.

### 1.3 Aims and objectives

Nowadays, a lot of research has been done in the field of liquid crystals, to explore their optical properties. One of the main reasons of these researches is the wide range of their applications, which range from illuminated sensors, watches to large TV displays, which can be seen in the market these days. Understanding the evolution of the state of polarization is the most important key for their optimum operations.

The main objective of this research is to investigate the forward and inverse problem for the Berreman model which has been derived from Maxwell's equations. A theoretical investigation around the propagation of light inside both isotropic and anisotropic media is carried out. This investigation leads us to study a system of ordinary differential equations which arises in the field of optics

$$\frac{d\mathbf{E}}{dz} + i\frac{\omega}{c}n_o\mathbf{E} = V(z)\mathbf{E}, \quad (1.9)$$

where  $V(z)$  is called potential in Quantum Mechanics. According to the research carried out by X. Zhu and R. Jain [61], there is no analytical solution to the matrix equation when the potential is a function of position. The main reason is that these equations are coupled-mode equations and the coupling coefficients are functions of position.

In this thesis, the coupling between the eigen-states when potential is a function of position i.e. twisted nematic liquid crystal has been investigated to gain detailed information about how the state of polarization evolves as the wave propagates. This has been done as we will see later by using a new technique which has been named as a rotational frame method and has been illustrated graphically for some different input state of polarizations.

Before considering the inverse problem, let us first state the forward problem. Suppose that the potential  $V(z)$  for the above differential equation is given, then  $E_x = E_x(z, \lambda)$  and  $E_y = E_y(z, \lambda)$  are the solutions of the matrix equation

$$\frac{d\mathbf{E}}{dz} + i\frac{\omega}{c}n_o\mathbf{E} = V(z)\mathbf{E}, \quad (1.10)$$

with initial conditions  $E_x(0, \lambda) = a$ , and  $E_y(0, \lambda) = b$ , where  $a$  and  $b$  depend on the initial state of polarization. The forward problem is not an easy to solve when the Schrödinger equation has a non-vanishing potential. A major part of this thesis is to overcome this task. In fact, a new method has been obtained in this research to solve the forward problem with different types of potentials.

On the other hand, the inverse problem for this system of differential equation is to recover the potential of the schrödinger equation. For the solution of the inverse problem, one might need to apply the techniques used to solve inverse problem of the Schrödinger equation to recover the potential. The main reason

is that the orientation of the optical axis inside the liquid crystal sample was encoded inside the potential. In fact, recovering the potential will lead to recover the director. As a consequence of that, it will lead eventually to recover the dielectric tensor inside the material.

## 1.4 Thesis organization

In the context of this thesis, the first chapter starts with a brief introduction to liquid crystals. In this introduction, the two most popular methods in literature used to handle the propagation of light inside the liquid crystal are mentioned and compared.

Chapter **2** introduces a brief description to some technical terms relating to liquid crystal such as anisotropy, birefringence and principal axes. Understanding these concepts is vital to formulate and proceed with the main problem discussed in this thesis.

Chapter **3** presents the concept of polarization with all different possible types of polarizations. After that, this chapter discusses the first method used to handle the propagation of light in materials that is the Jones method. Also, the relationship between the Stokes parameters, which measure the intensity of light, and Jones vector is presented in this chapter.

Chapter **4** is dedicated to the experiment which is used in Hewlett Packard Laboratories in Bristol (HPLB). It, also, introduces the basic method used by Berreman to solve the forward problem. A simple example has been worked out to show the method used by Berreman to obtain the solution for the forward problem.

Chapter **5** introduces the basic equations which govern the propagation of

electromagnetic waves in materials known as Maxwell's equations. Also, the concept of dielectric tensors is discussed in some detail. In this chapter, we obtained a relationship between the diagonal elements of dielectric tensor. This relationship has been verified and illustrated with some graphs, for the case of a twisted nematic liquid crystal, in off-state with a positive and negative birefringence.

Chapter **6** addresses the polarization states from the Quantum Mechanics point of view. This chapter compares the strong relationship between the Jones analysis in optics and the Schrödinger equation in Quantum Mechanics. Floquet's theory guarantee the existence of the solution of our model and gives some of its characteristics specially when there is a coupling between the differential equations. This chapter concludes by discussing all possible types of potentials we might obtain for different types of liquid crystal samples.

Chapter **7** provides a detail derivation of a  $2 \times 2$  differential equation from the Berreman model. This system,  $2 \times 2$  differential equation, allows us to visualize the propagating modes in twisted anisotropic sample. Also, in this chapter we obtained a new technique to solve the  $2 \times 2$  system when there is a coupling between the differential equations. Also, in this chapter, we make use of this equation to study the local modes propagating in the medium for different types of potentials.

In chapter **8** we obtained the general form of a spectral equation from the Maxwell equations. This equation has exactly the same form as the second order Schrödinger equation. The solutions for this equation with different types of potentials has been presented and discussed. Also, this chapter concludes by discussing the inverse problem of Berreman and the corresponding linearized problem.

# Chapter 2

## Liquid crystals

### 2.1 Some of the properties of liquid crystals

#### 2.1.1 Concept of anisotropy

From the microscopic point of view, the molecules in liquid crystal materials have three major axes of symmetry, in which two of them have the same length and the third one is slightly longer, which coincides with the director of the liquid crystals. This special shape of the liquid crystal molecule gives two measurements for many physical properties such as viscosity, conductivity and refractive index, when the measurement is taken over the long axis and the short axis [18]. This leads to introduce the term anisotropy which means that many physical properties have different values when the measurements are taken over different directions. For example, the optical anisotropy term was introduced in optics to indicate that the light propagates at two different speeds along and perpendicular to the director in uniaxial liquid crystals. In other words, there are two refractive indices in uniaxial liquid crystal as we will explain in the coming section.

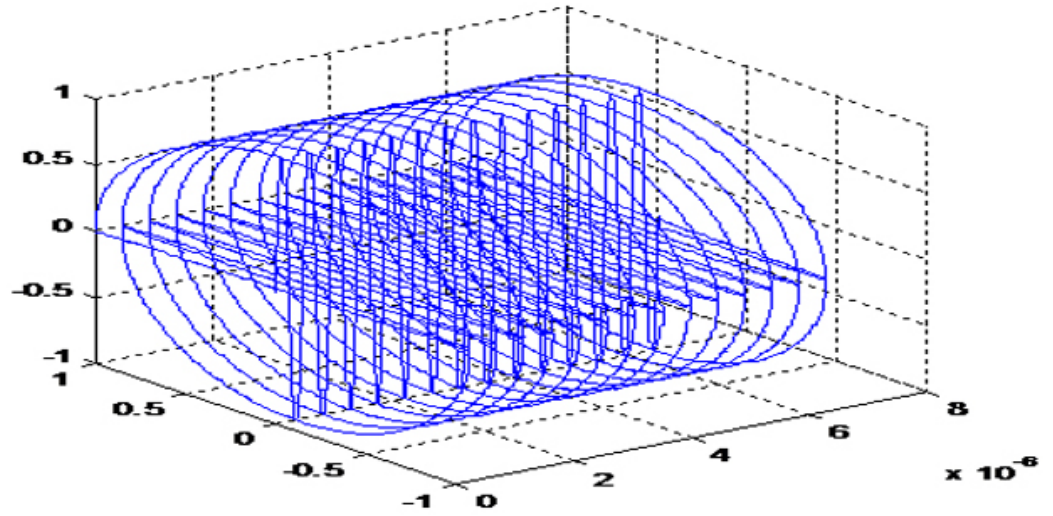


Figure 2.1: In uniaxial materials, light decomposes into two components traveling in two different directions and at two different velocities.

### 2.1.2 Birefringence

In general, the refractive index of most materials is the same regardless of the polarized direction of the light. However, certain materials such as liquid crystals have the ability to decompose the incoming ray of light into two rays, when the light passes through them. Figure 2.1 shows clearly this phenomenon. These rays are known as the ordinary and extraordinary rays. The ordinary ray with a refractive index denoted by  $n_o$  travels perpendicular to the director. On the other hand, the extraordinary ray with a refractive index denoted by  $n_e$  travels parallel to the director.

The decomposition of light inside these materials leads to the concept of birefringence which is defined as [18], [48]

$$\Delta n = n_e - n_o. \quad (2.1)$$

When the magnitude of extraordinary refractive index  $n_e$  is greater than the

magnitude of ordinary refractive index  $n_o$  then the birefringence is said to be positive,

$$\Delta n > 0, \quad (2.2)$$

while it is said to be negative when the magnitude of extraordinary refractive index is less than the magnitude of ordinary refractive index  $n_o$ .

$$\Delta n < 0. \quad (2.3)$$

### 2.1.3 Surface phenomenon

The surface phenomenon has the ability to align the nematic liquid crystal director into three different shapes which are homotropic alignment, planar alignment and inclined alignment. In homotropic alignment sample, the nematic liquid crystal director makes exactly ninety degrees within the boundary of the sample. On the other hand, the director in the planar alignment sample makes zero degrees within the boundary. In other words, the director is perpendicular to the surface in homotropic alignment while it is parallel to the surface in the planar alignment. In the third case which is inclined alignment, the director makes some angle within the boundary.

The uniform parallel alignment of the local director can be easily deformed by several forces such as an electrical field, a magnetic field and the boundaries. In fact, boundaries are used for some small samples, in practice in the range of  $2nm$  to  $100nm$  and this technique is known as the surface phenomenon which been used a long time to control director orientation of the nematic liquid crystal.

## 2.2 Principal values and principal axes

Our goal of this section is to clarify the meaning of the two terms, principal values and principal axes. The dielectric tensor in a non-absorbing medium has symmetric real elements. This means that the dielectric tensor is a Hermitian tensor and its eigenvalues are always real and the corresponding eigenvectors form an orthogonal basis. In other words, the dielectric tensor for nematic liquid crystal and in general for a Hermitian tensor can be always written in a diagonal form with non-negative real elements on the main diagonal. These elements are the eigenvalues which are called the principal values and the corresponding eigenvectors give the directions of the principal axes.

## 2.3 Oseen-Frank free-energy equation

The free-energy of deformation of nematic liquid crystal director follows the Oseen-Frank equation which is given by the following expression [39], [35]

$$F = \int_v \left\{ \frac{1}{2} K_{11} (\nabla \cdot n)^2 + \frac{1}{2} K_{22} (n \cdot \nabla \times n)^2 + \frac{1}{2} K_{33} |n \times \nabla \times n|^2 - \frac{1}{2} \epsilon_o (E \cdot \epsilon_a \cdot E)^2 \right\} dv, \quad (2.4)$$

where  $K_{11}$ ,  $K_{22}$  and  $K_{33}$  are the three elastic constants splay, twist and bend deformations,  $\epsilon_o$  is the dielectric anisotropy constant,  $E$  is the electric field and  $\epsilon_a$  is the difference in dielectric constants between the ordinary and extraordinary axes of the liquid crystal molecules. In fact, this integral composed from two different energy densities. The first three terms of the integral represent the energy density of the liquid crystals and is usually denoted by

$$F_{elastic} = \frac{1}{2} K_{11} (\nabla \cdot n)^2 + \frac{1}{2} K_{22} (n \cdot \nabla \times n)^2 + \frac{1}{2} K_{33} |n \times \nabla \times n|^2, \quad (2.5)$$

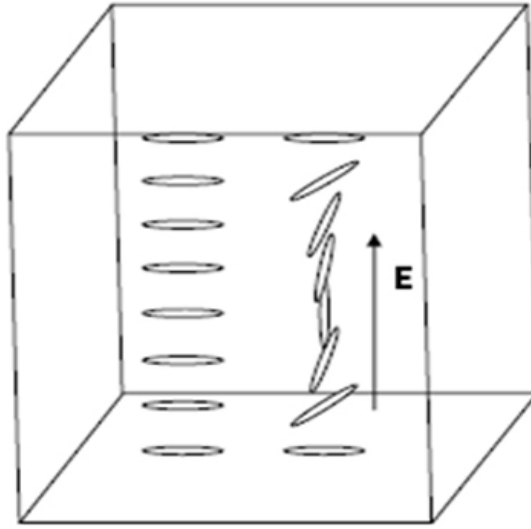


Figure 2.2: Nematic liquid crystal cell sandwiched between two glasses:(a)Without electric field, (b) An electric field is applied across the cell.

while the last term is the contribution of the energy density which comes from the applied external field

$$F_{electric} = \frac{1}{2}D \cdot E. \quad (2.6)$$

The absolute total free energy of the system in fact comes from three factors which are the energy density of liquid crystal, the energy density due to external field and the surface energy density [21]

$$F_{electric} = \int (F_{elastic} + F_{electric})d\mathbf{x} + F_{surface}. \quad (2.7)$$

The surface energy density term  $F_{surface}$  does not appear in the Oseen-Frank model. In fact, this term can be neglected when the anchoring is strong [21]. In the coming section we will explain in some detail how these forces work.

### 2.3.1 Mechanics of elastic and electric torque in liquid crystal molecules

Consider nematic liquid crystal sandwiched between two glasses as illustrated in figure 2.2. In the presence of a low electrical field inside the cell, there is a balancing force between the elastic restoring torque, which is caused by the boundaries and the electrical torque, which is caused by the applied field. When the applied electrical field is below the critical field, which is needed to reorient the liquid crystal molecules, there is no change in the director distribution inside the cell.

In fact, the director distribution below the critical field is similar to director distribution in the off-state field. However, the orientation of director starts to change when the applied electrical field exceeds the critical field. The orientation of the director is no longer similar to the off-state field and varies with the location as illustrated in figure 2.2. The reason is that both the glass boundaries and the applied electrical field exert different forces on the molecule according to its position. The competition between these forces varies with the location and the molecules follow the resulting of these forces. In other words, the torque which is caused by the boundaries decreases toward the center of the cell. As the applied electrical field increase, the molecules will tend toward the direction of the electrical field.

### 2.3.2 Model for director orientation

In this section, we will consider special case for director orientation. let us consider that the electrical field is along the  $z$ -axis. Since the magnitude of the director is not important, it will be considered to equal the unity and the angles between

the director and the  $z$ -axis to be  $\theta(z)$ . To simplify the problem further, it will be considered that there is no twist inside the medium  $\phi(z) = 0$ . In this case the director will have the following components

$$(n_x, n_y, n_z) = (\sin \theta(z), 0, \cos \theta(z)), \quad (2.8)$$

where  $\theta(z)$  is a function of position. In order to calculate the director tensor inside the sample, the tilt angle has to be calculated throughout the cell sample. This can be done by minimizing the elastic energy equation. Before we continue, it should be mentioned that similar idea with magnetic field applied across the sample has been treated by Andrienko [4]

### 2.3.3 Minimizing the Oseen-Frank free energy

By calculating the divergence and curl of the director

$$\nabla \cdot \mathbf{n} = -\sin \theta(z) \frac{d\theta}{dz}, \quad (2.9)$$

$$\nabla \times \mathbf{n} = -j \cos \theta(z) \frac{d\theta}{dz}, \quad (2.10)$$

$$\mathbf{n} \cdot (\nabla \times \mathbf{n}) = 0. \quad (2.11)$$

After the substitution of the above the terms, the Oseen- Frank free energy will take the following form

$$F = \int_0^d \left\{ \frac{1}{2} K_{11} \sin^2 \theta + \frac{1}{2} K_{33} \cos^2 \theta \right\} \left( \frac{d\theta}{dz} \right)^2 - \frac{1}{2} \epsilon_o \Delta \epsilon E^2 \sin^2 \theta \Big\} dz. \quad (2.12)$$

Also, by considering one constant approximation  $K_{11} = K_{22} = K_{33}$ , the elastic energy equation will reduce to

$$F = \int_0^d \left\{ \frac{1}{2} K_{11} \left( \frac{d\theta}{dz} \right)^2 - \frac{1}{2} \epsilon_o \Delta \epsilon E^2 \sin^2 \theta \right\} dz. \quad (2.13)$$

Our goal is to find the function that optimizes the Oseen-Frank free energy. This function which is the equilibrium value can be obtained by using the calculus of variation together with the following boundary conditions

$$\theta(0) = \theta(d) = 0. \quad (2.14)$$

Since our problem is symmetric with respect to the middle of the cell and the desired function achieves its maximum at the middle of the cell, the boundary conditions can be modified and replaced with

$$\theta(0) = 0, \quad (2.15)$$

$$\theta\left(\frac{d}{2}\right) = \rho, \quad (2.16)$$

where  $\rho$  is the maximum of the desired function. From the calculus of variations, the function which optimizes the Oseen-Frank free energy equation has to satisfy the Euler-Lagrangian condition

$$\frac{dL}{d\theta} - \frac{d}{dz} \left( \frac{dL}{dz} \right) = 0. \quad (2.17)$$

The Euler-Lagrangian condition produces the following differential equation

$$K_{11} \frac{d^2\theta}{dz^2} + \epsilon_o \Delta \epsilon E^2 \sin \theta \cos \theta = 0. \quad (2.18)$$

The quantity  $\Omega = \frac{K_{11}}{\epsilon_o \Delta \epsilon E^2}$  is known as the electric coherence length which can be interpreted as the required shortest distance needed by the liquid crystal molecules to tend towards the applied electric field. When the applied electric field is weak, then only the trivial solution exists. In addition, when there is small distortion in the nematic structure, then

$$\theta = \rho_m \sin\left[\frac{z}{\Omega}\right], \quad (2.19)$$

is a good approximate solution for the director distribution. The boundary conditions produce

$$\Omega = \frac{d}{\pi}. \quad (2.20)$$

This result gives us some sense about the measurement of the critical field provided that the quantities  $\epsilon_o$  and  $\Delta \epsilon = \epsilon_{\parallel} - \epsilon_{\perp}$  are known

$$E = \sqrt{\frac{\pi K_{11}}{d \epsilon_o \Delta \epsilon}}. \quad (2.21)$$

Also, it shows that the critical field is inversely proportionate to the length of the sample. The second order differential equation which results from the Euler-Lagrangian condition can be integrated directly to produce the following equation

$$K_{11} \left(\frac{d\theta}{dz}\right)^2 + \epsilon_o \Delta \epsilon E^2 \sin^2 \theta = c, \quad (2.22)$$

where  $c$  is the constant of integration and this constant can be identified by using the modified boundary conditions

$$\epsilon_o \Delta \epsilon E^2 \sin^2 \rho = c. \quad (2.23)$$

Now by substituting the value of the integration constant, the differential equation can be rearranged to separate the variables and as result of that the desired function can be obtained

$$\left(\frac{d\theta}{dz}\right)^2 = \frac{\epsilon_o \Delta \epsilon E^2}{K_{11}} (\sin^2 \rho - \sin^2 \theta). \quad (2.24)$$

Next we will address two cases.

1. The first case is when the electric field is below the critical field. In this case there is no distortion in the structure of the nematic and as a result of that both conditions  $\sin^2 \rho > \sin^2 \theta$  and  $\rho = 0$  will force the differential equation to reduce to

$$\frac{d\theta^2}{dz} = 0. \quad (2.25)$$

By integrating this differential equation and using the boundary conditions, a trivial solution is the only solution that satisfies the boundary conditions.

2. The second case is when the applied electric field is high. In this case,  $\rho = \frac{\pi}{2}$ . Since  $\sin^2 \rho > \sin^2 \theta$  and  $\frac{d\theta}{dz} \neq 0$  in the integration interval, the differential equation can be rearranged as

$$dz = \frac{\tau}{\sqrt{1 - \frac{\sin^2 \theta}{\sin^2 \rho}}} d\theta, \quad (2.26)$$

where

$$\tau = \sqrt{\frac{k_{22}}{\epsilon_{22} \Delta \epsilon E \sin^2 \rho}}. \quad (2.27)$$

Before the integration is carried out, the right hand side of equation (2.26) can be simplified by using the trigonometric identities and direct integration

produces the following equation

$$\begin{aligned} z &= \tau \int_0^\theta |\sec \alpha| d\alpha \\ &= \tau [\ln(\sec \alpha + \tan \alpha)]_0^\theta. \end{aligned}$$

In fact, an explicit function for tilt angle  $\theta$ , can be obtained by using the following identity

$$\sec \alpha + \tan \alpha = \frac{1 + \sin \alpha}{\cos \alpha} = \tan\left(\frac{\alpha}{2} + \frac{\pi}{4}\right), \quad (2.28)$$

and the tilt angle is given by

$$\theta(z) = 2 \arctan\left(\exp\left(\frac{z}{\tau}\right)\right) - \frac{\pi}{2}. \quad (2.29)$$

### 2.3.4 Electrostatic potential

In the case of an electrostatic potential, this explicit function is not quite as simple to solve. The reason is that as the liquid crystal molecules reoriented, the permittivity changes. This change will have some impact on the electric field across the sample. In order to find the effects on the electric field, the Laplace equation must be solved [30]

$$\nabla \cdot \epsilon \cdot \nabla u = 0, \quad (2.30)$$

where  $u$  is the electrical potential

$$E = -\nabla u. \quad (2.31)$$

Since the electric field is applied in the direction of  $z$ -axis, the Laplace equation reduces to

$$\frac{d}{dz}[(\epsilon_{\perp} + \Delta\epsilon \sin^2 \theta) \frac{du}{dz}] = 0. \quad (2.32)$$

Unfortunately, this equation is nonlinear but it can be linearized by introducing the following variables  $u = v_1$  and  $u' = v_2$  which will give us

$$2\Delta\epsilon \sin \theta \cos \theta \frac{d\theta}{dz} v_2 + [(\epsilon_{\perp} + \Delta\epsilon \sin^2 \theta) v_2'] = 0. \quad (2.33)$$

This equation together with the above explicit equation can be solved to obtain the profile of the tilt angle.

## 2.4 Summary

In this chapter, some of the technical terms, such as isotropy, anisotropy, birefringence, principal axes and some other terms, needed to understand the concepts in thesis is discussed in some detail. The mechanics of forces in Oseen-Frank equation is discussed by considering liquid crystal sample. A simple model has been treated and explicit function for the tilt angle is obtained.

# Chapter 3

## Polarization and Jones treatment

### 3.1 Introduction

In this chapter, we will introduce the concept of polarization, which is so important to understand the optical properties behind the propagation of light in materials. To begin with this concept, we start by defining the transverse waves term. By transverse waves, we mean that the waves vibrate perpendicular to direction of propagation. Light, for example, is a good example of transverse waves. Light is also called electromagnetic transverse waves since it consists of electric and magnetic fields. In addition to that, it should be clear from the context of this chapter that we are talking about monochromatic plane waves.

Light can be classified as either polarized or unpolarized. It is said to be unpolarized if the electromagnetic waves vibrate in all possible directions. On the other hand, it is said to be polarized if the light waves vibrate in one single direction [18]. In practice, there are three different types of light polarizations, which depend on the magnitude and phase as they propagate. These types are linear, circular and elliptic polarizations and will be discussed in some detail in

the coming sections.

In the free space or uniform materials, light, in general electromagnetic wave, has the electric and magnetic fields perpendicular to the direction of propagation. According to the experimental evidence, the electric field vector is responsible for all propagation effects behind propagation [18]. As a result of that, the electric field is usually considered and the magnetic field is ignored, since the magnetic field is proportional and perpendicular to the electric field.

In order to polarize a light, a device called a polarizer is used. This device has optical axis which has the ability to change the unpolarized light to polarized. If, for instance, two polarizers are arranged in a series such that their optical axes of polarization are perpendicular, then the polarized light passing from the first polarizer will be blocked by the second polarizer. This configuration is known in optics as the crossed. However, if the angle between the optical axes changes from a right angle i.e as the angle changes from  $90^\circ$  to  $0^\circ$ , the amount of polarized light transmitted by the second polarizer will increase and it will reach maximum if the angle arrived to is zero. In other words, the polarized light will pass through the polarizers if their optical axes are parallel. This phenomenon has numerous applications in the field of data display.

In practical experiments, twisted nematic liquid crystal molecules are placed between two crossed polarizers, but polarized light is passing through them. The reason is that, as the light passes through the first polarizer, the nematic liquid crystal molecules will force the polarized light to travel with the twist direction and will eventually pass through the second polarizer. To clarify the above point, the polarized light by the first polarizer will experience the twist orientation of the nematic liquid crystal molecules placed between the crossed.

## 3.2 Equation of polarization

The state and nature of polarization of a light wave can be fully specified once the propagation direction is identified. If, for example, the  $z$ -axis is assumed to be the direction of propagation, then the electric field of a transverse wave can be uniquely defined in a Cartesian system by the components along the  $x$  and  $y$  axes. These components of electric field can mathematically be defined in terms of phases and amplitudes as:

$$E_x = E_{ox} \cos(\omega t - \delta_x), \quad (3.1)$$

$$E_y = E_{oy} \cos(\omega t - \delta_y), \quad (3.2)$$

where  $\delta_x$  and  $\delta_y$  are the phases,  $E_{ox}$  and  $E_{oy}$  are the amplitudes in the  $x$  and  $y$  directions respectively. If the time is excluded from these equations, one might obtain the equation of polarization [32]

$$\left(\frac{E_x}{E_{ox}}\right)^2 + \left(\frac{E_y}{E_{oy}}\right)^2 - \frac{E_x E_y}{E_{ox} E_{oy}} \cos \delta = \sin^2 \delta, \quad (3.3)$$

where  $\delta = \delta_y - \delta_x$  is the phase difference between the perpendicular components of the electric field.

In the coming sections, we will discuss in some detail the types of polarizations which arise from this equation with application to isotropic medium. The main reason of choosing the isotropic medium, is that this medium has the ability to retain the state of polarization as the wave propagates through it.

### 3.2.1 Linear polarization

There are some special cases for the equation of polarization. The first case occurs when the relative phase difference between the orthogonal components of the wave is  $\delta = 0$  or  $\pi$ . As a result of this difference, the orthogonal components will either arrive to their maximums and minimums exactly at the same time or one will achieve its maximum and the second one will achieve its minimum. The tip of resultant wave vector which come from the sum of these orthogonal waves, will trace a straight line in a plane perpendicular to the direction of propagation [32].

$$\left(\frac{E_x}{A_x}\right)^2 + \left(\frac{E_y}{A_y}\right)^2 \pm \frac{2E_x E_y}{A_x A_y} = 0, \quad (3.4)$$

which can be written as

$$E_y = \pm \frac{A_y}{A_x} E_x. \quad (3.5)$$

To illustrate the linear polarization, we will consider two waves which propagate inside isotropic medium, with phase difference zero as illustrated in figure 3.1 and figure 3.2. Linear polarization is obtained when these two perpendicular waves combine together as illustrated in figure 3.3 and figure 3.4.

### 3.2.2 Circular polarization

The state of polarization is said to be circular, when the tip of the resultant wave vector traces a circle around the origin in a plane perpendicular to the direction of propagation. This case can be achieved when the orthogonal components have exactly the same amplitude and are out of phase by  $90^\circ$ . By replacing the relative

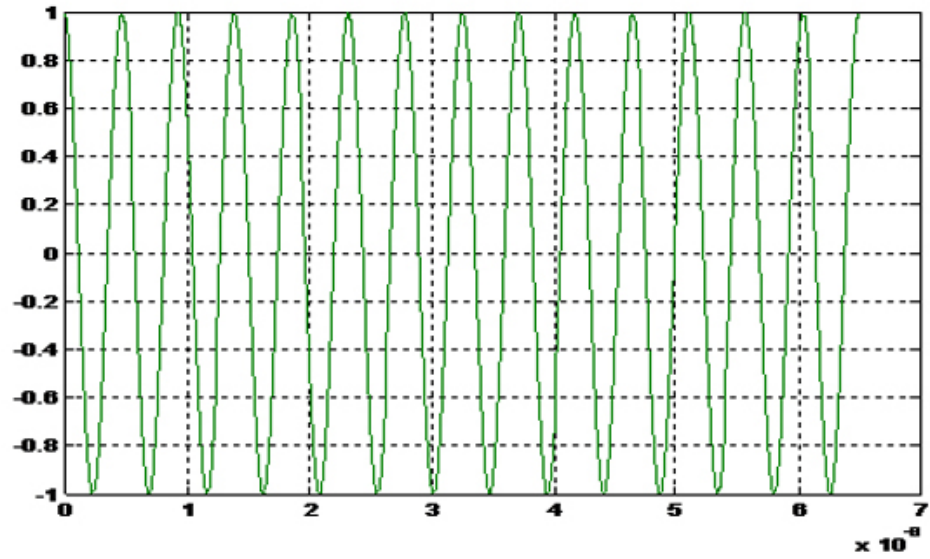


Figure 3.1: Two waves propagate inside isotropic medium with phase difference zero.

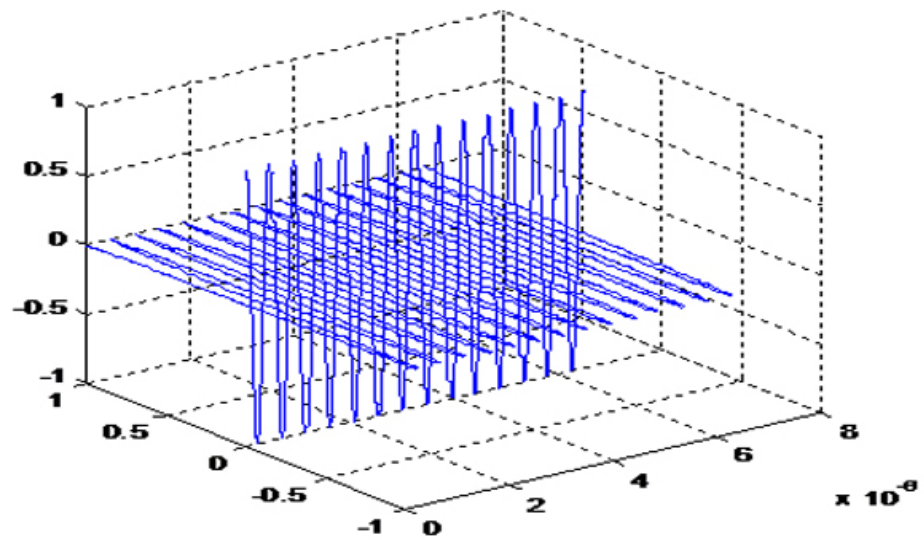


Figure 3.2: The above two waves propagate perpendicular to each other .

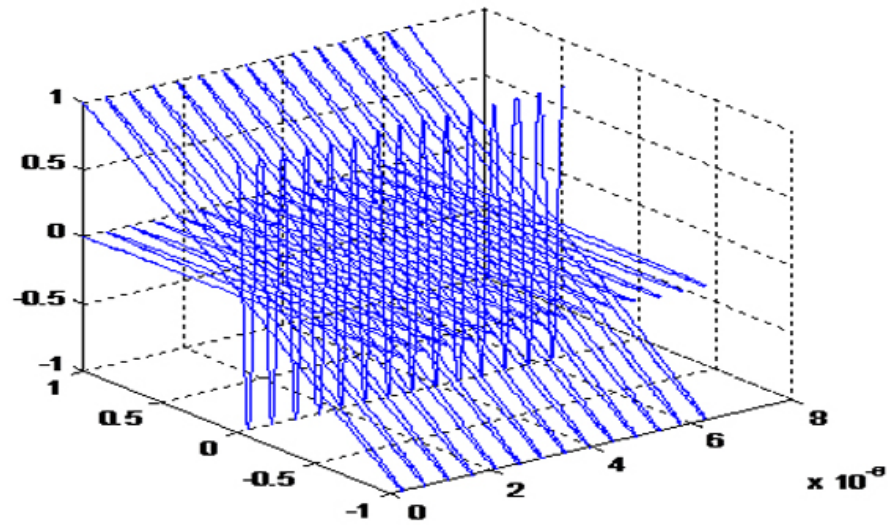


Figure 3.3: Shows the sum of these two waves .

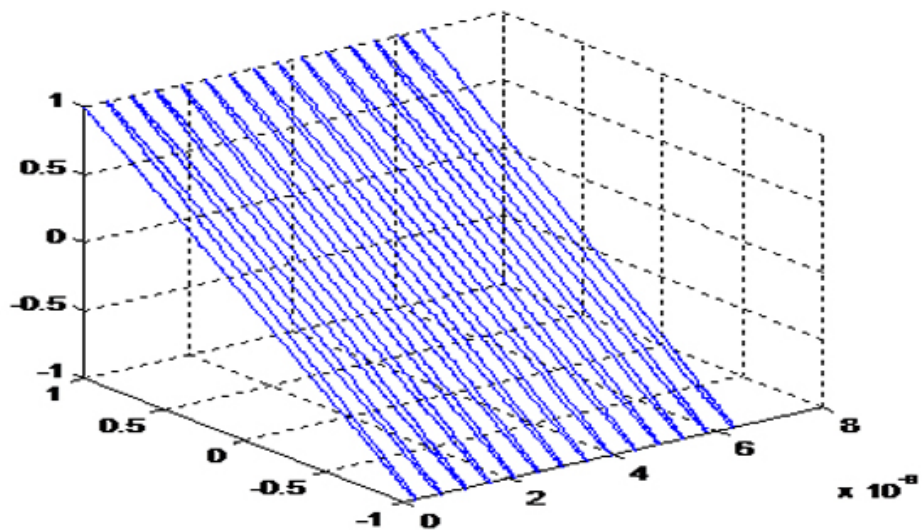


Figure 3.4: This figure shows the resultant linear polarization.

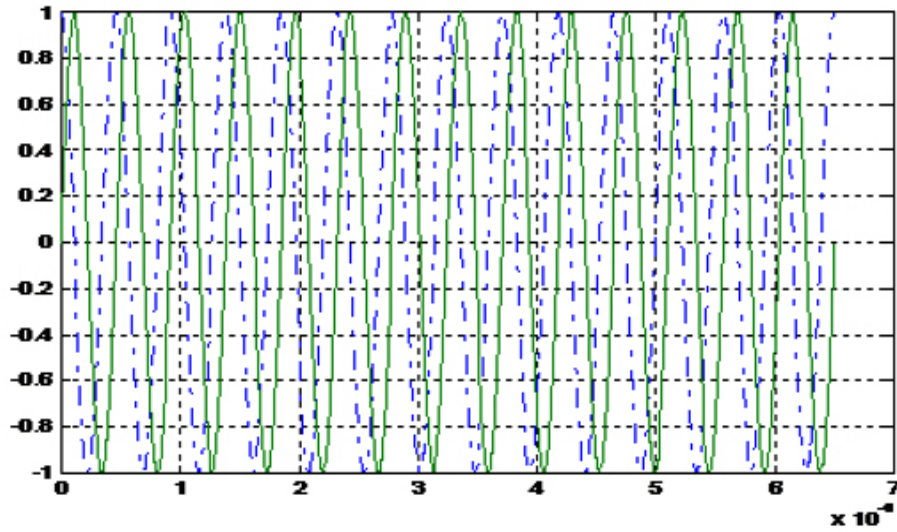


Figure 3.5: Two waves propagate inside isotropic medium with ninety degrees phase shift between them.

phase by 90, the equation of polarization 3.3 reduces to

$$\left(\frac{E_x}{A_x}\right)^2 + \left(\frac{E_y}{A_y}\right)^2 = 1, \quad (3.6)$$

which can be rewritten as

$$E_x^2 + E_y^2 = A_y^2. \quad (3.7)$$

This equation describes a circle with center at origin and radius  $A$ . A good example to illustrate this concept is the isotropic medium. Suppose, for example, that a circular polarization enters isotropic medium, the medium will retain the polarization state throughout the medium. Figure 3.5, figure 3.6, figure 3.7 and figure 3.8 illustrate the circular polarization concept.

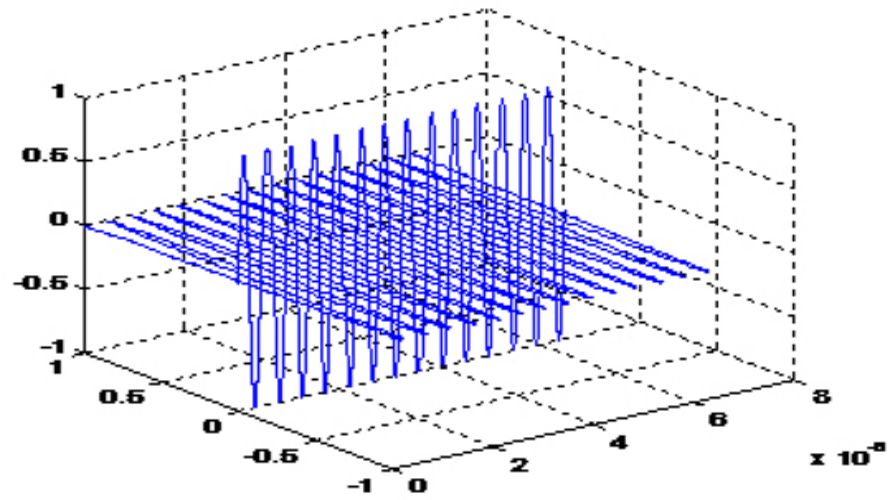


Figure 3.6: The above two waves propagate perpendicular to each other.

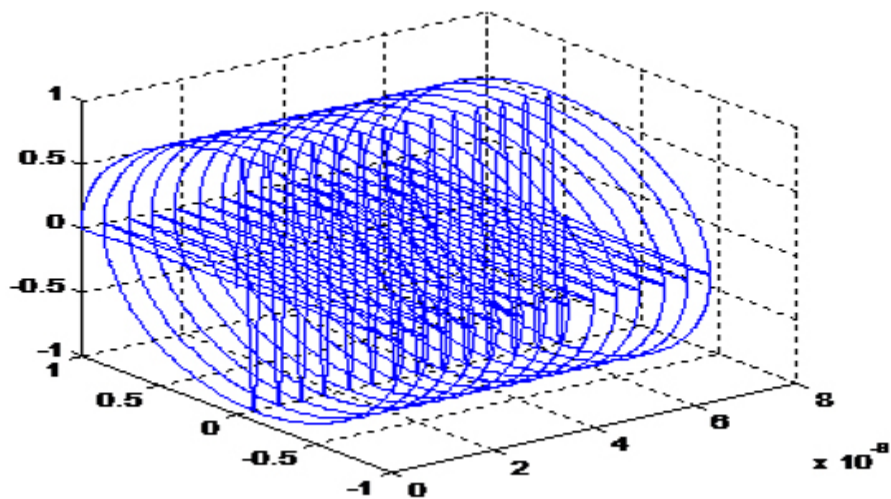


Figure 3.7: Shows the sum of these two waves together with the type of resulting polarization.

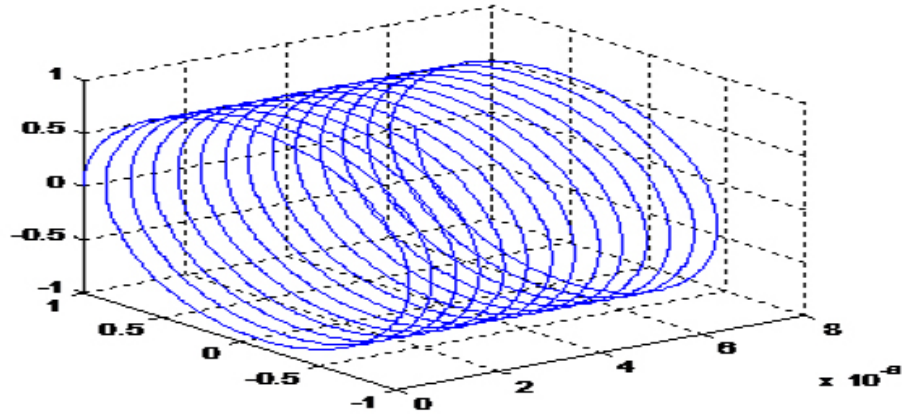


Figure 3.8: This figure shows the type of polarization which is a circular polarization.

### 3.2.3 Elliptical polarization

When the state of polarization is neither linear nor circular, then it is called elliptical polarization. This occurs when the relative phase is not exactly 0 or 90 or the amplitudes of the orthogonal components are not the same. The tip of resultant wave vector in this case will trace an ellipse, in a plane perpendicular to the direction of propagation. In fact, both linear and circular polarizations are special cases of the elliptical polarization. The general equation of the ellipse is

$$\left(\frac{E_x}{E_{ox}}\right)^2 + \left(\frac{E_y}{E_{oy}}\right)^2 - \frac{E_x E_y}{E_{ox} E_{oy}} \cos \delta = \sin^2 \delta. \quad (3.8)$$

The principal axes of the ellipse traced in a plane perpendicular to the propagation direction do not lie in general on the  $xy$ -axes. However, it is not difficult to show that the angle between the  $x$ -axis and the major axis of the ellipse is

$$\tan 2\varphi = \frac{2E_{ox}E_{oy}}{E_{ox}^2 - E_{oy}^2} \cos \delta, \quad (3.9)$$

and the length of these axes are

$$a = \sqrt{E_{ox}^2 \cos^2 \varphi + E_{0y}^2 \sin^2 \varphi + E_{ox} E_{0y} \cos \delta \sin 2\varphi}, \quad (3.10)$$

$$b = \sqrt{E_{ox}^2 \sin^2 \varphi + E_{0y}^2 \cos^2 \varphi - E_{ox} E_{0y} \cos \delta \sin 2\varphi}. \quad (3.11)$$

### 3.3 Jones concept of polarized light

Over the last decades, several methods have been used to describe and characterize the propagation of a light beam through optical devices. Jones matrix method which was introduced by R. C. Jones in 1941, is an effective and a sufficient method to analyze the effect of the optical device on the polarization state, when the incident light beam is completely polarized. This method will be introduced in the coming two sections.

#### 3.3.1 Jones vector

Jones was able to represent a monochromatic plane wave, which propagates in  $z$ -direction and perpendicular to  $xy$ -plane, as a column vector in terms of its complex amplitudes [10], [17]

$$\mathbf{J} = \begin{pmatrix} E_x \\ E_y \end{pmatrix} = \begin{pmatrix} A_{0x} \exp(i\xi_x) \\ A_{0y} \exp(i\xi_y) \end{pmatrix},$$

where  $A_{0x}$  and  $A_{0y}$  are the initial amplitudes of the electric field in the  $x$ -direction and  $y$ -direction respectively,  $\xi_x$  and  $\xi_y$  are the phases of the wave components. This vector is known as the Jones vector which provides us with complete information about intensity, amplitudes and the phase difference between the components

of the electric field. One might notice that if time is added to Jones vector then it is called the Maxwell vector

$$\mathcal{E}(\mathbf{x}, t) = \text{Re} (E(\mathbf{x}) \exp(i\omega t)), \quad (3.12)$$

where  $\omega$  is the angular speed of the light beam. In practice, Jones vector is written in terms of a phase difference of the electric field components

$$\mathbf{J}(z) = \begin{pmatrix} A_{0x} \\ A_{0y} \exp(i[\xi_y - \xi_x]) \end{pmatrix},$$

and this representation gives us exactly the same information about amplitudes and intensity.

Since the state of polarization does not depend on the exact amplitudes of the electric field components, the Jones vector is often written in much more simplified form, by normalizing the components of the vector. This can be done by forcing the Jones vector to satisfy the following condition

$$J^* \cdot J = 1, \quad (3.13)$$

where \* denote the complex conjugate. To show this concept, we will consider, for example, the Jones vector for a left circular polarization which is given by [17]

$$\mathbf{J} = \begin{pmatrix} A_{0x} \exp(i\xi_x) \\ A_{0y} \exp(i[\xi_x + \frac{\pi}{2}]) \end{pmatrix}.$$

The corresponding normalized vector for the above Jones vector representation

is

$$\mathbf{J} = \frac{\sqrt{2}}{2} \begin{pmatrix} 1 \\ i \end{pmatrix}.$$

One might notice that these two representation have different degrees of information, but indeed give us the same state of polarization, which is left circular polarization. In addition, the normalized representation of Jones vector for some selected states of polarization can be found in table 3.1

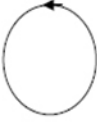
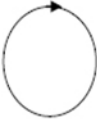
<i>Shape</i>	<i>Type of polarization</i>	<i>Jones representation</i>
	Linear polarization +45	$\mathbf{J} = \begin{pmatrix} 1 \\ 0 \end{pmatrix}$
	Linear polarization along the y-axis	$\mathbf{J} = \begin{pmatrix} 0 \\ 1 \end{pmatrix}$
	Linear polarization +45	$\mathbf{J} = \frac{\sqrt{2}}{2} \begin{pmatrix} 1 \\ 1 \end{pmatrix}$
	Linear polarization -45	$\mathbf{J} = \frac{\sqrt{2}}{2} \begin{pmatrix} 1 \\ -1 \end{pmatrix}$
	Right Circular polarization	$\mathbf{J} = \frac{\sqrt{2}}{2} \begin{pmatrix} 1 \\ i \end{pmatrix}$
	Left Circular polarization	$\mathbf{J} = \frac{\sqrt{2}}{2} \begin{pmatrix} 1 \\ -i \end{pmatrix}$

Table 3.1: Shows the normalized form of the Jones vector for some selected polarization states.

### 3.3.2 The Jones matrix

Mathematically speaking, Jones matrix is simply a linear transformation which transforms the Jones vector of a monochromatic plane wave, from one boundary to the second boundary. This transformation is a square  $2 \times 2$  matrix which is given by

$$\begin{pmatrix} E_x \\ E_y \end{pmatrix} = \begin{pmatrix} J_{11} & J_{12} \\ J_{21} & J_{22} \end{pmatrix} \begin{pmatrix} E_{0x} \\ E_{0y} \end{pmatrix}.$$

The elements of the Jones matrix in fact depend on the optical device. When the optical device has isotropic media for example, then the Jones matrix is given by

$$\mathbf{J} = \begin{pmatrix} \exp\left(\frac{-i\omega}{c}n_oz\right) & 0 \\ 0 & \exp\left(\frac{-i\omega}{c}n_oz\right) \end{pmatrix},$$

where  $n_o$  is the refractive index of the optical device. When an optical system consists of more than one optical device, then one must calculate the Jones matrix for each device and the Jones matrix for the optical system is obtained by multiplying all obtained Jones matrices in a correct order.

## 3.4 Jones matrix for anisotropic medium with a fixed transmission axis

In a non-twisted sample, the liquid crystal molecules in both boundaries align parallel to each other. If the applied voltage is less than the threshold, then the director, which is the vector of average molecular direction remains parallel as we travel from one side of the sample to the other. Since the sample is uniaxial, two eigen-modes will propagate inside the sample with two different velocities,

provided that the Maugin condition is satisfied [36]

$$\Delta n k_o \gg a, \quad (3.14)$$

where  $\Delta n$  is the birefringence,  $k_o$  is the wavelength in vacuum and  $a$  is the twist angle per unit length. While one of the eigen-modes travel along the director, the second eigen-mode will travel perpendicular to the director. The eigen-modes are given by [16], [17], [27], [47]

$$\begin{aligned} & \begin{pmatrix} \exp\left(\frac{-i\omega}{c}n_e z\right) & 0 \\ 0 & \exp\left(\frac{-i\omega}{c}n_o z\right) \end{pmatrix} \\ &= \exp\left(\frac{1}{2}(n_e + n_o)\frac{\omega}{c}z\right) \begin{pmatrix} \exp\left(\frac{i\omega}{c}\Delta n z\right) & 0 \\ 0 & \exp\left(\frac{-i\omega}{c}\Delta n z\right) \end{pmatrix}. \end{aligned}$$

When multiple reflections due to wave propagation are small, then the scalar phase factor is of no consequence and can even be negated [57]. By using the Quantum Mechanics notation, this matrix can even be written further in terms of a spin operator

$$\begin{pmatrix} \exp\left(\frac{-i\omega}{c}\Delta n z\right) & 0 \\ 0 & \exp\left(\frac{-i\omega}{c}\Delta n z\right) \end{pmatrix} = \exp\left(\sigma_z \frac{-i\omega}{c}\Delta n z\right),$$

where  $\sigma_z$  is matrix and given by [44]

$$\sigma_z = \begin{pmatrix} 1 & 0 \\ 0 & -1 \end{pmatrix}.$$

This is one of the well known matrices which are known as the Pauli matrices  $\sigma_x$ ,  $\sigma_y$  and  $\sigma_z$  and defined as [44]

$$\sigma_x = \begin{pmatrix} 0 & 1 \\ 1 & 0 \end{pmatrix},$$

$$\sigma_y = \begin{pmatrix} 0 & i \\ -i & 0 \end{pmatrix},$$

$$\sigma_z = \begin{pmatrix} 1 & 0 \\ 0 & -1 \end{pmatrix}.$$

The point here is to try perfectly interpreting and understanding the above operator. In Quantum Mechanics, this operator simply represents a rotational operator, which rotates a spin around the  $z$ -axis one half wave functions with an angle. However, from the optics point of view, the interpretation is quite different. To understand the issue, let us consider that a light beam propagates along the  $z$ -axis in anisotropic medium. Since the optical system is anisotropic, and has two propagation velocities, the medium will break the incoming light beam into two waves. One of the waves will propagate parallel to the director and the other one will propagate perpendicular to the director. As the waves start to propagate inside the optical system, and as we mentioned earlier that the medium has two velocities, one component of the decomposed light will be retarded when compared to the second component. This retardation will accumulate and eventually will introduce a change of the state of polarization, as the two components recombined again as they leave the medium. The phase difference between the

waves can be measured via the following formulae

$$\text{Phase difference} = \frac{-i\omega}{c}\Delta n z, \quad (3.15)$$

where  $\Delta n = n_e - n_0$  is the birefringence of the medium,  $c$  is the speed of light in vacuum,  $\omega$  is angular speed of the light beam and  $z$  is distance measured from the beginning of the medium. In addition, as mentioned before the scalar factor

$$F = \frac{i\omega}{2c}[n_e + n_0]z, \quad (3.16)$$

has no consequence and can be negated when the multiple reflections due to the propagation is small.

### 3.5 Relationship between the Jones vector and the Stokes parameters

In studying polarized light which propagates through an optical element in the direction of  $z$ -axis, there are two different methods to relate the output to the input electric field components of the light beam. The first method is the Jones matrix method which has been fully discussed in the previous sections. This method can be written as

$$\begin{pmatrix} E_x \\ E_y \end{pmatrix} = \begin{pmatrix} J_{11} & J_{12} \\ J_{21} & J_{22} \end{pmatrix} \begin{pmatrix} E_{0x} \\ E_{0y} \end{pmatrix},$$

where the  $2 \times 2$  square matrix is the Jones matrix of the optical device,  $E_{0x}$  and  $E_{0y}$  are the input electric field along the  $x$ -axis and  $y$ -axis respectively. The

second method is the Berreman  $4 \times 4$  matrix method which has been derived directly from Maxwell's equations. In fact, this method will be discussed in more details in the coming chapters. In the meantime, we will pay attention to the third method and its relationship with the Jones matrix method.

### 3.5.1 Stokes parameters

The third method uses the Stokes vector and Muller matrix to relate the output electric field components to the input ones

$$S(\omega) = \begin{pmatrix} s_0 \\ s_1 \\ s_2 \\ s_3 \end{pmatrix} = MS(\omega)_i.$$

The first element of the Stokes vector  $s_0$  gives us the total power of the light beam. The power difference between the orthogonal components is given by the second element of the Stokes vector  $s_1$ . The third element  $s_2$  gives us the component of the light polarized at  $45^\circ$  and  $-45^\circ$ , whereas the left and right polarized beam component is given by the fourth element  $s_3$ . In fact, a relationship between the elements of the Stokes parameters exists, and is given by the following equation

$$s_0^2 = s_1^2 + s_2^2 + s_3^2. \quad (3.17)$$

The previous paragraph can be mathematically written as [56], [26]

$$s_0 = E_x^2 + E_y^2, \quad (3.18)$$

$$s_1 = E_x^2 - E_y^2, \quad (3.19)$$

$$s_2 = 2E_x E_y \cos(\delta), \quad (3.20)$$

$$s_3 = 2E_x E_y \sin(\delta), \quad (3.21)$$

where  $\delta$  is the phase difference between the orthogonal components of the electric field. These equations show the exact relation between the Stokes vector and the Jones vector. From these relations, one might easily switch between Stokes and Jones to determine the Jones matrix or between Jones and Stokes to determine the Muller matrix.

Moreover, the above Stokes parameters can be used to determine light polarization. In practice, light polarization can be characterized by two elements. The first element is the azimuth angle which is the angle between the  $x$ -axis and the major axis of the polarized ellipse. The second element is the ellipticity of the ellipse which is defined as the square of the ratio of the major axis to the minor axis of the polarized ellipse

$$\varepsilon = \frac{\text{Major axis}}{\text{Minor axis}}. \quad (3.22)$$

The relationships between the Stokes parameters and these elements are given by [8]

$$\alpha = \frac{1}{2} \arctan\left(\frac{s_2}{s_1}\right), \quad (3.23)$$

$$\zeta = \frac{1}{2} \arcsin\left(\frac{s_3}{\sqrt{s_1^2 + s_2^2 + s_3^2}}\right) = \frac{1}{2} \arcsin\left(\frac{s_3}{s_0}\right), \quad (3.24)$$

$$\zeta = \frac{1}{\sqrt{\varepsilon}}. \quad (3.25)$$

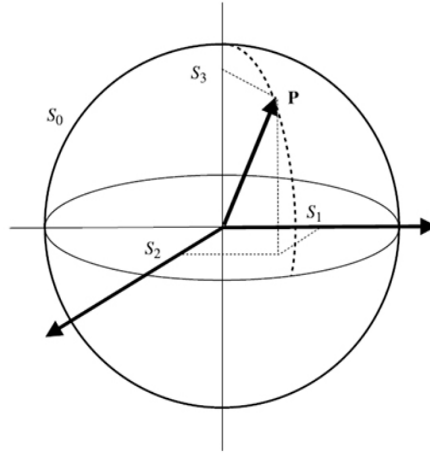


Figure 3.9: The representation of the state of polarization by the Poincaré sphere using the Stokes parameters.

### 3.5.2 Poincaré sphere

According to Stokes parameters, the total power of a monochromatic plane wave of a light beam is always constant and given by the following relationship [20], [59]

$$s_0^2 = s_1^2 + s_2^2 + s_3^2. \quad (3.26)$$

This relationship has a good geometric representation, which is a sphere if one regards  $s_1$ ,  $s_2$  and  $s_3$  as the Cartesian coordinates. For each fixed Stokes vector, there is only one point on the sphere corresponding to the Stokes vector with total power  $s_0$  as shown in the figure 3.9. This sphere is known as the Poincaré sphere and has the ability to represent all possible states of polarization. To clarify the last point, all points lying, for example, in the equatorial plane represent the linear polarization. However, the north and south poles of the sphere represent the right and left handed circular polarization respectively. The remaining points on the sphere represent the elliptic polarization which is the general type of polarization.

## 3.6 Conclusion

In this chapter some of the basic concepts needed to understand the propagation of light inside the materials has been reviewed. This includes the polarization, Jones treatments and Stokes treatment. These concepts will help us to understand some of the contents of the coming chapters and more details can be seen in the given references.

# Chapter 4

## Experiment and Berreman solution

### 4.1 The experimental setup

The starting point to describe the experimental setup is to begin with the formulation of the nematic cell. A thin cell of nematic liquid crystal is sandwiched between two parallel glass plates. To avoid a possible change in the direction of the director orientation at the boundaries, the outside glass plates are coated with certain chemicals. This coating is to set the boundary condition of the director.

A beam with known frequency  $\omega$  is directed to the nematic liquid crystal cell. After the beam passes through the polarizer, it will be polarized and the state of polarization will be recorded. Then, the polarized beam will penetrate the nematic liquid crystal sample. After that, the laser beam will pass through a polarimeter which again measures the polarization state and intensity of the laser beam. In fact, this polarimeter gives the normalized Stokes parameters. In order to change the angle of incidence, we rotate the cylindrical box that

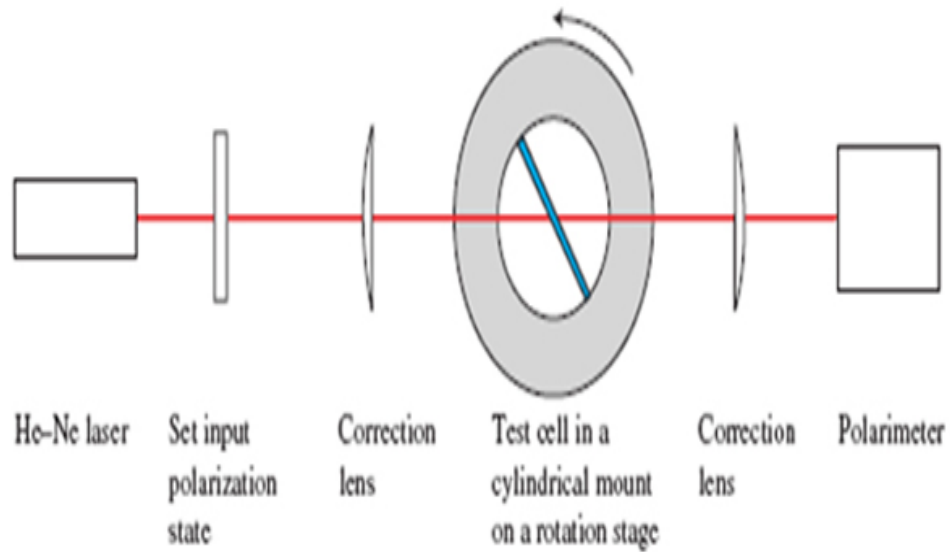


Figure 4.1: This figure shows the experiment setup used at Hewlett Packard Laboratories in Bristol(HPLB). The nematic liquid crystal sample is fixed inside the cylindrical mount and the incident angle can be changed by rotating the cylindrical mount.

contains the nematic liquid crystal sample as shown in figure 4.1. By measuring the polarization state and intensity of the outgoing laser beam, some information can be gathered about the director configuration inside the cell.

Moreover, it should be noted that the collected information is affected by some factors such as:

- The thickness of the nematic liquid crystal sample.
- The orientation of the director at the boundaries with the glass plates.
- The degree of polarization.
- The angle of incidence.
- The intensity of the laser beam.

## 4.2 The solution of the Berreman wave equation

The solution of the Berreman equation can be written by the use of the evolution matrix, which relates the tangential components of both electric and magnetic fields at the input  $z_1$  to those at the output  $z_2$  [55]

$$\psi[z_2] = F[z_1, z_2]\psi[z_1]. \quad (4.1)$$

The following two sections will explain how to obtain this fundamental matrix.

### 4.2.1 Fundamental matrix for single layer

The main challenge to the Berreman method is to find and calculate the fundamental matrix  $F[z_1, z_2]$  for a nematic liquid crystal sample. This matrix relates the output fields to the input fields. To overcome this difficulty, in practice, the nematic liquid crystal sample is divided into thin slabs with thickness  $h$  as it is shown in figure 4.2.

For a sufficiently thin layer of thickness  $h$ , the director orientation will be uniform and can be considered as constant. According to Berreman, if a monochromatic plane wave with known frequency  $\omega$  is incident on this thin layer, the output field is given by [7]

$$\psi[z_{out}] = F[h]\psi[z_{in}], \quad (4.2)$$

where  $F[h]$  is  $4 \times 4$  matrix known as the transfer matrix for the single layer of thickness  $h$  which is given by [40]

$$F[h] = \exp\left[\frac{ih\omega}{c}M(z)\right]. \quad (4.3)$$

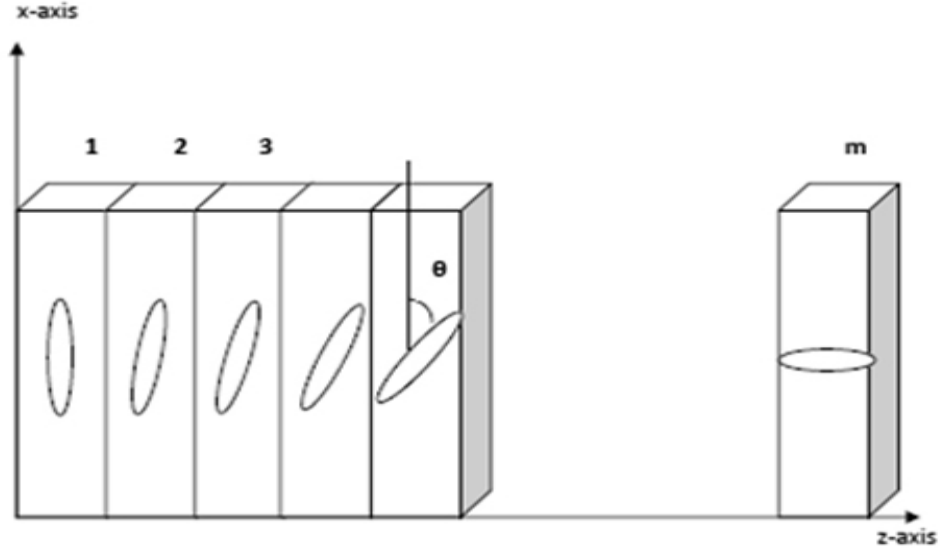


Figure 4.2: The nematic liquid crystal sample is divided into thin layers with thickness  $h$ . For each layer, the orientation of the director is considered to be constant.

The matrix  $M(z)$  is obtained during the derivation of the Berreman equation from Maxwell's equations. Also, as we will mention later in chapter seven in this thesis that the matrix  $M(z)$  depends mainly on

- The dielectric constants
- The extraordinary and ordinary refractive indices.
- The Euler angles of the local director  $n_o$  within the cell.

Since the director orientation is uniform within a single thin layer of thickness  $h$ , the transfer matrix for the layer is given by the following expression [19]

$$F[h] = \exp\left(\frac{i\omega h M}{c}\right) = I + \frac{i\omega h}{c} \frac{M}{1!} + \left(\frac{i\omega h}{c}\right)^2 \frac{M^2}{2!} + \dots \quad (4.4)$$

Also, since  $h \ll \lambda$ , the above Taylor series can be truncated by neglecting the higher order terms of  $h$ . As a result of this truncation, the fundamental matrix

$F[h]$  is obtained for each single layer.

### 4.2.2 Fundamental matrix for the sample

In order to calculate the overall transfer matrix for the nematic liquid crystal sample, we first have to label the layers as  $1, 2, \dots, m$  as it is shown in figure 4.2. Once the calculation for each layer has been done, the boundary conditions between the two dielectric media are needed to find the overall evolution matrix for  $m$  layers. More precisely, according to electromagnetic theory, the parallel components to the interface between two dielectric layers of both electric and magnetic fields have to be continuous with the condition that there is no charge or current at the interface between the two layers. As a result of this concept, the Berreman vector is continuous at the interface between the two layers, since it contains only the parallel components due to the derivation of the Berreman equation. In other words, the normal components of both electric and magnetic fields have been canceled. However, the parallel components remained and formed what is known as the Berreman vector field. The overall fundamental matrix for  $m$  layers is formed by multiplying the evolution matrix for each layer in the following sequences [34], [3]

$$F[z_2, z_1] = F_{z_2, z_1+mh}(h)F_{z_1+(m-1)h}(h) \dots F_{z_1+2h}(h)F_{z_1+h}(h). \quad (4.5)$$

Hence, the solution for the Berreman equation for  $m$  layers is given by equation 4.1.

### 4.3 Discussion for propagation matrix

In order to understand the issue behind the last section, we will address a simple example where we can calculate the exact propagation matrix. For simplicity, we will consider isotropic medium in which the dielectric tensor has the following form  $\epsilon_{ij} = n^2\delta_{ij}$  where  $n$  is the refractive index of the medium. Moreover, the Berreman matrix will have the following simple structure

$$M(z) = \begin{pmatrix} 0 & 1 - \frac{A^2}{\epsilon} & 0 & 0 \\ \epsilon & 0 & 0 & 0 \\ 0 & 0 & 0 & 1 \\ 0 & 0 & \epsilon - A^2 & 0 \end{pmatrix}.$$

According to Berreman, the plane wave will propagate inside the layer and a propagation matrix will be formed to connect the fields at the boundaries. In fact, the propagation matrix for this example will be calculated by two different methods as illustrated in the coming subsections.

#### 4.3.1 Exponential series expansion method

Since the medium is homogeneous, then the propagation matrix for the whole sample is given by

$$F[h] = \exp\left(\frac{i\omega h M}{c}\right). \quad (4.6)$$

The beauty behind the above example is  $M^2 = \lambda^2 I$  where  $\lambda$  is the eigenvalue of the Berreman wave matrix and  $I$  is  $4 \times 4$  identity matrix. This property of the above Berreman matrix allows us to calculate the exact propagation matrix

which connects the fields at the boundaries of the layer.

$$F[h] = \exp\left(\frac{i\omega h M}{c}\right) \quad (4.7)$$

$$= I + \frac{i\omega h M}{c} \frac{1}{1!} + \left(\frac{i\omega h}{c}\right)^2 \frac{M^2}{2!} + \dots \quad (4.8)$$

$$= \left[I + \left(\frac{i\omega h}{c}\right)^2 \frac{M^2}{2!} + \dots\right] + \left[\frac{i\omega h}{c} M + \left(\frac{i\omega h}{c}\right)^3 \frac{M^3}{3!} + \dots\right] \quad (4.9)$$

$$= \left[1 - \left(\frac{\omega h \lambda}{c}\right)^2 \frac{1}{2!} + \dots\right] I + \frac{i}{\lambda} \left[\frac{\omega h \lambda}{c} - \left(\frac{\omega h \lambda}{c}\right)^3 \frac{1}{3!} + \dots\right] M \quad (4.10)$$

$$= \left[\cos\left(\frac{\omega h \lambda}{c}\right)\right] I + \frac{i}{\lambda} \left[\sin\left(\frac{\omega h \lambda}{c}\right)\right] M. \quad (4.11)$$

and by writing down the identity and the matrix  $M$ , the propagation matrix will take the following form

$$F[h] = \left[\cos\left(\frac{\omega h \lambda}{c}\right)\right] \begin{pmatrix} 1 & 0 & 0 & 0 \\ 0 & 1 & 0 & 0 \\ 0 & 0 & 1 & 0 \\ 0 & 0 & 0 & 1 \end{pmatrix} + \frac{i}{\lambda} \left[\sin\left(\frac{\omega h \lambda}{c}\right)\right] \begin{pmatrix} 0 & 1 - \frac{A^2}{\epsilon} & 0 & 0 \\ \epsilon & 0 & 0 & 0 \\ 0 & 0 & 0 & 1 \\ 0 & 0 & \epsilon - A^2 & 0 \end{pmatrix}.$$

By adding up the above two matrices together, we obtain the final form for the propagation matrix

$$F[h] = \begin{pmatrix} \cos\left(\frac{\omega h \lambda}{c}\right) & \frac{i}{\lambda} \left[1 - \frac{A^2}{\epsilon}\right] \sin\left(\frac{\omega h \lambda}{c}\right) & 0 & 0 \\ \frac{i\epsilon}{\lambda} \sin\left(\frac{\omega h \lambda}{c}\right) & \cos\left(\frac{\omega h \lambda}{c}\right) & 0 & 0 \\ 0 & 0 & \cos\left(\frac{\omega h \lambda}{c}\right) & \frac{i}{\lambda} \sin\left(\frac{\omega h \lambda}{c}\right) \\ 0 & 0 & \frac{i}{\lambda} \left[\epsilon - A^2\right] \sin\left(\frac{\omega h \lambda}{c}\right) & \cos\left(\frac{\omega h \lambda}{c}\right) \end{pmatrix}.$$

### 4.3.2 Caylay- Hamilton method

It worths to mention that this exact propagation matrix can be obtained by another method. According to Caylay- Hamilton theorem, the following matrix

expansion

$$F[h] = \exp\left(\frac{i\omega h M}{c}\right) = I + \frac{i\omega h}{c} \frac{M}{1!} + \left(\frac{i\omega h}{c}\right)^2 \frac{M^2}{2!} + \dots, \quad (4.12)$$

can be obtained exactly by a finite series up to a power of  $n - 1$  where  $n$  is the order of the matrix  $M$ . In other words, the propagation matrix for the Berreman equation with a homogenous medium is given by the following expression [1], [38]

$$F[h] = \exp\left(\frac{i\omega h M}{c}\right) = a_0 I + a_1 M + a_2 M^2 + a_3 M^3. \quad (4.13)$$

The scalars  $a_i$ ,  $i = 0, 1, 2, 3$ , in the above equation are given via the following equations

$$\exp[i\omega h \lambda_i] = a_0 + a_1 \lambda_i + a_2 \lambda_i^2 + a_3 \lambda_i^3, \quad (4.14)$$

where  $\lambda_i$  and  $i = 1, 2, 3, 4$ . are the eigenvalues for the Berreman matrix. Moreover, nice formulas have been worked out for the above scalars and they are given in terms of the eigenvalues of the Berreman matrix.

$$a_0 = - \sum_{i=1}^{i=4} \lambda_j \lambda_k \lambda_l \frac{f_i}{\lambda_{ij} \lambda_{ik} \lambda_{il}}, \quad (4.15)$$

$$a_1 = - \sum_{i=1}^{i=4} [\lambda_i \lambda_k + \lambda_j \lambda_l + \lambda_k \lambda_l] \frac{f_i}{\lambda_{ij} \lambda_{ik} \lambda_{il}}, \quad (4.16)$$

$$a_2 = - \sum_{i=1}^{i=4} [\lambda_k + \lambda_j + \lambda_l] \frac{f_i}{\lambda_{ij} \lambda_{ik} \lambda_{il}}, \quad (4.17)$$

$$a_3 = - \sum_{i=1}^{i=4} \frac{f_i}{\lambda_{ij} \lambda_{ik} \lambda_{il}}, \quad (4.18)$$

where  $\lambda_{ij} = \lambda_i - \lambda_j$  and  $f_i = \exp[i\omega h \lambda_i]$  and all the indices  $i, j, k, l$  run between 1, 2, 3, 4. For the above example, these scalars had been worked out in [38]

$$a_0 = \frac{1}{2}[\cos(\omega h q) + \omega h q \sin(\omega h q)], \quad (4.19)$$

$$a_1 = \frac{i \sin(\omega h q)}{2q} [2 - \omega h q], \quad (4.20)$$

$$a_2 = \frac{1}{2q^2} [\cos(\omega h q) - \omega h q \sin(\omega h q)], \quad (4.21)$$

$$a_3 = \frac{i}{2q^2} \cos(\omega h q). \quad (4.22)$$

By using these scalars and according to the Cayley-Hamilton theorem, the propagation matrix is

$$F[h] = \exp\left(\frac{i\omega h M}{c}\right) = a_0 I + a_1 M + a_2 M^2 + a_3 M^3 \quad (4.23)$$

$$= a_0 I + a_1 M + a_2 q^2 I + a_3 q^3 M \quad (4.24)$$

$$= [a_0 + a_2 q^2] I + [a_1 + a_3 q^3] M. \quad (4.25)$$

By substituting the values of the above scalars and adding up the matrices we end up with the same matrix

$$F[h] = \begin{pmatrix} \cos\left(\frac{\omega h \lambda}{c}\right) & \frac{i\lambda}{\epsilon} \sin\left(\frac{\omega h \lambda}{c}\right) & 0 & 0 \\ \frac{i\epsilon}{\lambda} \sin\left(\frac{\omega h \lambda}{c}\right) & \cos\left(\frac{\omega h \lambda}{c}\right) & 0 & 0 \\ 0 & 0 & \cos\left(\frac{\omega h \lambda}{c}\right) & \frac{i}{\lambda} \sin\left(\frac{\omega h \lambda}{c}\right) \\ 0 & 0 & i\lambda \sin\left(\frac{\omega h \lambda}{c}\right) & \cos\left(\frac{\omega h \lambda}{c}\right) \end{pmatrix}.$$

One can notice that, this propagation matrix is exactly the same one which was obtained by the exponential series expansion.

## 4.4 Conclusion

In this chapter, the experiment used at HPLB was introduced and explained. Also, this chapter explains in detail the technique used to solve the forward problem. By employing isotropic medium, for the seek of understanding, we were able to calculate the exact propagation matrix for the Berreman equation. However, in most cases, the propagation can be found only numerically. The reason is that the Berreman is more general and is used for all media such as inhomogeneous anisotropic medium.

If the medium is inhomogeneous isotropic then the medium is sliced into sufficiently thin slices in which each slice can be treated as isotropic medium and the exact propagation matrix is given by  $F[h]$  for each layer. Since the tangential components of the Berreman field continuous, then the approximated solution is given by equation (4.5).

Equation (4.5) can also be extended to be used for an inhomogeneous anisotropic medium. This can be done by dividing the medium into sufficiently thin slices for which each slice is treated as homogenous anisotropic medium. Later we will use a new technique to find the propagation matrix for twisted nematic liquid crystals which is an inhomogeneous anisotropic medium without dividing the medium into slices.

# Chapter 5

## Maxwell's equations and dielectric tensor

We start this chapter by introducing the basic equations governing the propagation of electromagnetic waves in materials known as Maxwell's equations. The first section involves some discussion which shows how James Clerk Maxwell obtained his set of four partial differential equations. In the second section, the concept of dielectric tensor is explained in some details for both isotropic and anisotropic media. Particular attention is given in the final sections of this chapter to dielectric tensor for uniaxial materials, for both positive and negative birefringence.

### 5.1 Maxwell's equations

Maxwell's equations are a set of four partial differential equations which had been devised by James Clerk Maxwell (1831-1879). From Ampere's law, Faraday's law and the Gaussian theorem, Maxwell introduced the basic equations that govern

the electromagnetic fields.

The first equation of Maxwell has been totally derived from Ampere's law. According to Ampere's law, the electric current in the medium generates an induced magnetic field

$$\nabla \times \mathbf{H} = \mathbf{J}. \quad (5.1)$$

However, if the electric field in the medium varied with time, Maxwell noticed that there is another factor which will induce a magnetic field. This factor is called the displacement current  $\frac{\partial \mathbf{D}}{\partial t}$  which comes from the varying electric field in the medium. By combining these two factors, Maxwell introduced his first equation which briefly says that the induced magnetic field in the medium is coming from both the conductive current and the displacement current. Mathematically, this statement can be expressed as:

$$\nabla \times \mathbf{H} = \mathbf{J} + \frac{\partial \mathbf{D}}{\partial t}. \quad (5.2)$$

Maxwell derived his second equation from Faraday's principle. According to Faraday's principle, a moving magnet will generate an alternating current and Faraday formulates his principle as

$$\mathbf{E} = -\frac{\partial \psi}{\partial t}, \quad (5.3)$$

where  $\psi$  is the magnetic potential. By taking the cross product for both sides, Maxwell obtained his second equation

$$\nabla \times \mathbf{E} = -\frac{\partial \mathbf{B}}{\partial t}. \quad (5.4)$$

In short, this equation basically means that the magnetic variation induces electric

field into the medium.

The remaining two equations, one for the magnetic field and one for the electric field have been derived from the Gaussian theorem

$$\nabla \cdot \mathbf{D} = \rho, \quad (5.5)$$

$$\nabla \cdot \mathbf{B} = 0. \quad (5.6)$$

This theorem states that the integration of a vector field over an entire closed surface is equivalent to the integration of the divergence of a vector field over the volume containing the surface

$$\oint_S V \cdot ds = \int \int \int \nabla \cdot V dv. \quad (5.7)$$

For linear medium, the electric and magnetic fields are connected through the constitutive relations [2], [19]

$$\mathbf{B} = \mu \mathbf{H}, \quad (5.8)$$

$$\mathbf{D} = \epsilon \mathbf{E}, \quad (5.9)$$

where  $\mu$  is the permeability of the medium and  $\epsilon$  is the permittivity of the medium which will be discussed in more detail in the coming section.

## 5.2 Dielectric tensor

The starting point to describe the dielectric tensor which represents the material's properties is the Maxwell equations. The electric field, in Maxwell's equations, is related to the displacement by a relative electric primitivity  $\epsilon$ . If the medium

under investigation is an absorbing medium, then the electric primitivity will be complex. On the other hand, it will be real if the medium is non-absorbing [18].

For isotropic materials whose characteristics are independent of direction of propagation, the electric primitivity is a real scalar. In the other hand, the electrical primitivity is a real tensor for anisotropic materials whose characteristics depend on the direction of propagation. In our study, the medium is a source free interior. In such medium, the liquid crystal is known to be inhomogeneous and electrically anisotropic. Moreover, the electrical primitivity or dielectric tensor which is used to describe the electrical properties of the medium, is defined in term of  $3 \times 3$  symmetric positive definite tensor [18], [48]:

$$\varepsilon = \begin{pmatrix} \epsilon_{11} & \epsilon_{12} & \epsilon_{13} \\ \epsilon_{21} & \epsilon_{22} & \epsilon_{23} \\ \epsilon_{31} & \epsilon_{32} & \epsilon_{33} \end{pmatrix}.$$

With a certain rotation of axes, the above dielectric tensor can be always written in a diagonal form

$$\varepsilon = \begin{pmatrix} \epsilon_{11} & 0 & 0 \\ 0 & \epsilon_{22} & 0 \\ 0 & 0 & \epsilon_{33} \end{pmatrix}.$$

The new Cartesian system in which the dielectric tensor is diagonal, is known as the proper reference system of the material medium. The directions of axes in the proper system are called the eigen-axes or sometimes principal axes [13].

In order to understand the idea behind the proper system and eigen-axes, we will consider an example. Suppose that we have a twisted uniaxial sample with ordinary refractive index  $n_o = 1.400$  and extraordinary refractive index  $n_e = 1.550$ . For simplicity, we will assume that this sample has a vanishing tilt

angle and the extraordinary axis along the  $x$ -axis at the first boundary. Based on these data the dielectric tensors at  $z = 0.2$  and at  $z = 0.6$  are given respectively by

$$\varepsilon = \begin{pmatrix} \epsilon_{11} & \epsilon_{12} & \epsilon_{13} \\ \epsilon_{21} & \epsilon_{22} & \epsilon_{23} \\ \epsilon_{31} & \epsilon_{32} & \epsilon_{33} \end{pmatrix} = \begin{pmatrix} 2.3602 & 0.1300 & 0 \\ 0.1300 & 2.0023 & 0 \\ 0 & 0 & 1.9600 \end{pmatrix},$$

and

$$\varepsilon = \begin{pmatrix} \epsilon_{11} & \epsilon_{12} & \epsilon_{13} \\ \epsilon_{21} & \epsilon_{22} & \epsilon_{23} \\ \epsilon_{31} & \epsilon_{32} & \epsilon_{33} \end{pmatrix} = \begin{pmatrix} 2.1129 & 0.2104 & 0 \\ 0.2104 & 2.2496 & 0 \\ 0 & 0 & 1.9600 \end{pmatrix}.$$

In the proper system, the above dielectric tensors have the following values

$$\varepsilon = \begin{pmatrix} \epsilon_{11} & \epsilon_{12} & \epsilon_{13} \\ \epsilon_{21} & \epsilon_{22} & \epsilon_{23} \\ \epsilon_{31} & \epsilon_{32} & \epsilon_{33} \end{pmatrix} = \begin{pmatrix} 2.4025 & 0 & 0 \\ 0 & 1.9600 & 0 \\ 0 & 0 & 1.9600 \end{pmatrix}.$$

Since this sample has a vanishing tilt angle, one of the eigen-axes will not change throughout the sample. Figure 5.1 and figure 5.2 show the projection of the eigen-axes on the  $xy$ -plane. The directions of axes of the ellipse are the directions of the principal axes in which the dielectric tensor has a diagonal form.

### 5.3 Dielectric tensor for uniaxial materials

Two values of the diagonal elements for uniaxial materials are the same when the dielectric tensor is written in a diagonal form. These values are called the ordinary refractive index or ordinary principal value [12]. The third one is called the extraordinary refractive index or extraordinary principal value [12]. Moreover,

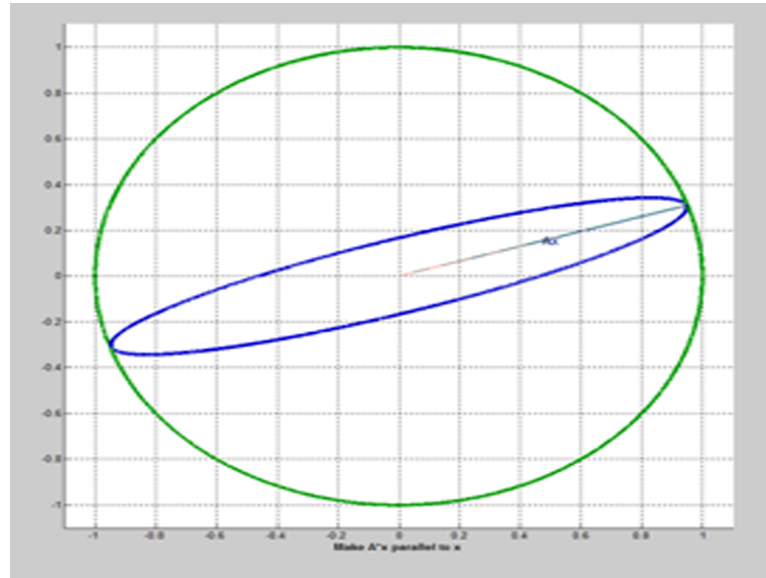


Figure 5.1: The axes of the ellipse give us the direction of the principal axes for  $z = 0.2$ , in which the dielectric tensor has a diagonal form.

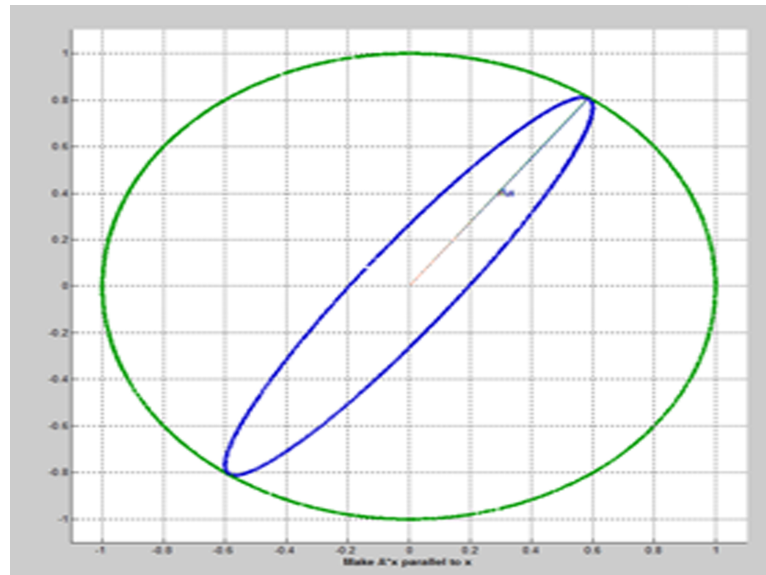


Figure 5.2: The axes of the ellipse give us the direction of the principal axes for  $z = 0.6$ , in which the dielectric tensor has a diagonal form.

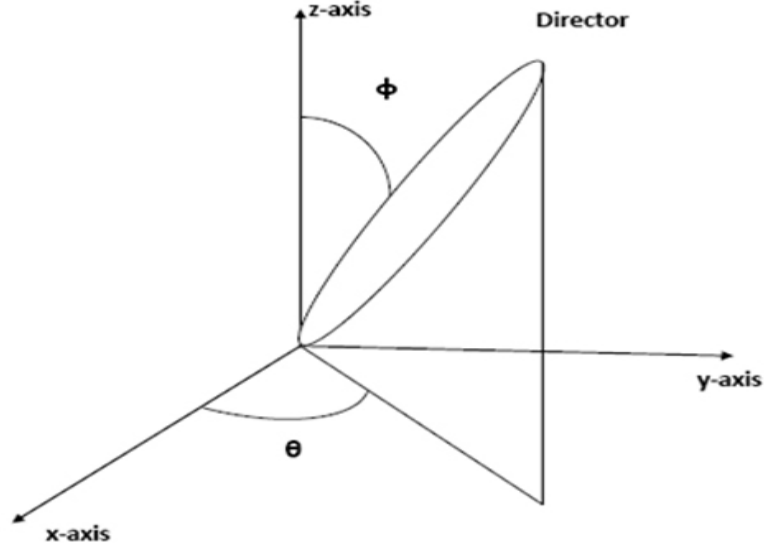


Figure 5.3: Director orientation inside the sample with tilt angle  $\theta$  and azimuthal angle  $\phi$ .

the direction of the extraordinary principal axis is known as the director.

In general, The dielectric tensor for uniaxial materials can be written in terms of the polar and azimuthal angles. In other words, if the director has tilt angle  $\theta$  and twist angle  $\phi$  as illustrated in figure 5.3, then the dielectric tensor elements are given by the following equations [13], [27], [29]:

$$\epsilon_{11} = n_0^2 + (n_e^2 - n_0^2) \cos^2(\theta) \cos^2(\phi), \quad (5.10)$$

$$\epsilon_{12} = (n_e^2 - n_0^2) \cos^2(\theta) \cos(\phi) \sin(\phi), \quad (5.11)$$

$$\epsilon_{13} = (n_e^2 - n_0^2) \sin(\theta) \cos(\theta) \cos(\phi), \quad (5.12)$$

$$\epsilon_{22} = n_0^2 + (n_e^2 - n_0^2) \cos^2(\theta) \sin^2(\phi), \quad (5.13)$$

$$\epsilon_{23} = (n_e^2 - n_0^2) \sin(\theta) \cos(\theta) \sin(\phi), \quad (5.14)$$

$$\epsilon_{33} = n_0^2 + (n_e^2 - n_0^2) \sin^2(\theta). \quad (5.15)$$

## 5.4 Discussion

In fact, there are four special cases in which the dielectric tensor reduces to a diagonal form. The first case is for the isotropic materials which have only one refractive index. As a result of that, the components of the dielectric tensor will be zeros except the diagonal elements. Also, all the diagonal elements are the same as mentioned in the beginning of this section and the dielectric tensor will take the following form

$$\varepsilon = \begin{pmatrix} n_0^2 & 0 & 0 \\ 0 & n_0^2 & 0 \\ 0 & 0 & n_0^2 \end{pmatrix},$$

where  $n_0$  is the refractive index of the medium.

The second case is for anisotropic materials with transmission axis along the  $x$ -axis throughout the sample, with vanishing tilt angle. In this case the orientation of the director is along the  $x$ -axis and the dielectric tensor is given by

$$\varepsilon = \begin{pmatrix} n_e^2 & 0 & 0 \\ 0 & n_0^2 & 0 \\ 0 & 0 & n_0^2 \end{pmatrix},$$

where  $n_0$  is the ordinary refractive index and  $n_e$  is the extraordinary refractive index for the medium.

The third and fourth cases are similar to the second case except that the orientation of the director, is either along the  $y$ -axis or  $z$ -axis throughout the sample and the tilt angle is zero. The dielectric tensor for transmission oriented along

the  $y$ -axis is given by

$$\varepsilon = \begin{pmatrix} n_0^2 & 0 & 0 \\ 0 & n_e^2 & 0 \\ 0 & 0 & n_0^2 \end{pmatrix},$$

and the dielectric tensor with transmission axis oriented along the  $z$ -axis is given by

$$\varepsilon = \begin{pmatrix} n_0^2 & 0 & 0 \\ 0 & n_0^2 & 0 \\ 0 & 0 & n_e^2 \end{pmatrix}.$$

In conclusion, if the director has a non-vanishing tilt and twist angles, then the dielectric tensor is given in general by [21]

$$\varepsilon = R(\varphi)^{-1}R(\theta)^{-1}\varepsilon_xR(\theta)R(\varphi), \quad (5.16)$$

where  $\varphi$  and  $\theta$  are the tilt and twist angles of the director respectively.  $R(\varphi)$  and  $R(\theta)$  are the rotational matrices,  $\varepsilon_x$  is the dielectric tensor where the orientation of the director is along the  $x$ -axis throughout the sample. Later in the coming chapter we will use an elegant way to diagonalize the dielectric tensor if the tilt angle is zero and the twist angle is either fixed or changing through the sample, such as twisted nematic liquid crystal. This idea will enable us to solve the wave equation analytically and the obtained solution will be compared with the solution obtained by the Jones matrix method.

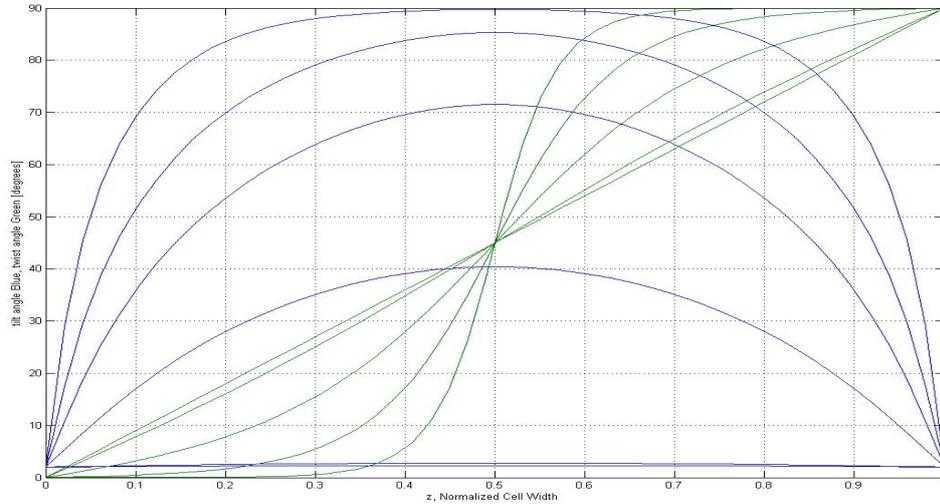


Figure 5.4: The twist(Green) and tilt(Blue) angles profiles for some voltages applied across the sample. The voltage in the above graph are 0.2, 0.4, 1.2, 1.9, 2.9, and high voltage 5

#### 5.4.1 Profiles of the elements of dielectric tensor for twisted nematic liquid crystal cell in the off state

One of the challenging problems in liquid crystal cells, is to deduce the dielectric tensor throughout the cell as an electrical field is applied through the cell. The main challenge is that the dielectric tensor depends on the director, which coincides with long optical axis of the molecules. Unfortunately, this optical axis in twisted nematic liquid crystal has a continuous change throughout the cell from one position to another and is affected by the applied electrical voltage. When a high enough voltage is applied, the twist will concentrate in the middle of the cell. Figure 5.4 shows the profiles for both twist and tilt angles for some different voltages applied across a twisted liquid crystal sample.

However, in the field-off-state this change is linear throughout the cell from one side to the other side. Mathematically, the optical axis, in field off state,

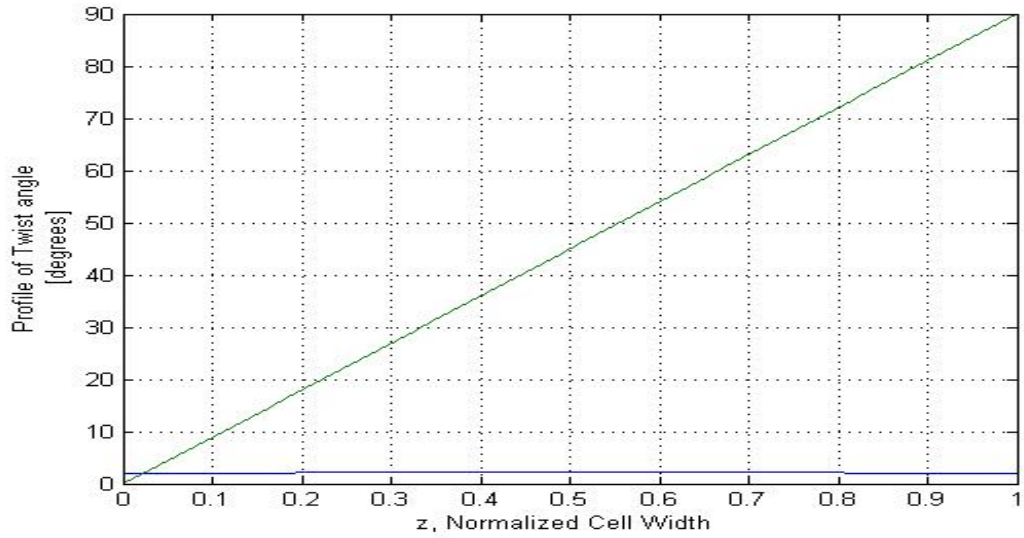


Figure 5.5: The profile of the optical axis which coincides with the director as a function of position.

inside the cell can be tracked with the following equation

$$\text{Twist angle} = \alpha x, \quad (5.17)$$

where  $\alpha$  is the total twist for the optical axis inside the cell. Figure 5.5 shows the profile of the optical axis which coincides with the director as a function of position. The knowledge of both the optical refractive indices of the cell and the director profile, allows us to obtain all six elements of the dielectric tensor of the cell.

### 5.4.2 Relationship between the diagonal elements of dielectric tensor

A closer look at the main diagonal elements of the dielectric tensor, shows that a relationship between these elements exists, as the optical axis twists through the

cell. By adding these elements, we obtain the following relation

$$\begin{aligned}
\epsilon_{11} + \epsilon_{22} + \epsilon_{33} &= n_0^2 + (n_e^2 - n_0^2) \cos^2(\theta) \cos^2(\phi) + n_0^2 \\
&\quad + (n_e^2 - n_0^2) \cos^2(\theta) \sin^2(\phi) + n_0^2 + (n_e^2 - n_0^2) \sin^2(\theta) \\
&= 3n_0^2 + (n_e^2 - n_0^2) \cos^2(\theta) [\cos^2(\phi) + \sin^2(\phi)] \\
&\quad + (n_e^2 - n_0^2) \sin^2(\theta) \\
&= 3n_0^2 + (n_e^2 - n_0^2) [\cos^2(\theta) + \sin^2(\theta)] \\
&= 2n_0^2 + n_e^2.
\end{aligned}$$

This relation shows independence of the twist and tilt angles of the sample in any position. In other words, no matter what the values of twist  $\theta$  and tilt  $\phi$  angles are or whether no field is applied to the sample or even a high voltage is applied, this relation between the diagonal elements has to be satisfied at any position inside the sample. In order to clarify the above concept, we have investigated this relationship in the field off state where the twist in the sample varies linearly throughout the cell as illustrated in figure 5.5. The liquid crystal sample is modeled as continuous layers and the twist is varied along the  $z$ -axis with the fast axis of anisotropy is oriented along the  $x$ -axis at the first boundary. This model allows us to calculate exactly all six elements of the dielectric tensor throughout the sample as we will show in the coming sections.

### 5.4.3 Positive birefringence

Figure 5.6 shows how the profile of first element  $\epsilon_{11}$  of the dielectric tensor is changing as we travel inside the cell. Figure 5.6 shows clearly that this element achieves its maximum value which is  $n_e$  at the first boundary, since it has been assumed that the fast axis of anisotropy lies on the  $x$ -axis at the first boundary,

and reaches its minimum value which is  $n_0$  at the second boundary, since the slow axis of anisotropy is oriented along the  $y$ -axis and the total twist of the director is 90 degrees.

Figure 5.7 shows the profile of the second diagonal element  $\epsilon_{22}$  for the dielectric tensor and shows the opposite story to the first element  $\epsilon_{11}$ . In other words, the second element  $\epsilon_{22}$  has its minimum value which is  $n_0$  at the first boundary since the slow axis of anisotropy is oriented along the  $y$ -axis. As we move across the sample and due to the twist in the sample, the fast axis of anisotropy will eventually become oriented along the  $y$ -axis and this element will achieve its maximum value which is  $n_e$ .

Figure 5.8 shows the profile of the third diagonal element  $\epsilon_{33}$  for the dielectric tensor, together with previous diagonal elements. From this profile, one may notice that this element has a constant value, which indeed equals to the ordinary refractive index  $n_o$ , as we travel across the sample. Finally, figure 5.9 shows the profiles of the off diagonal elements of the dielectric tensor. The blue profile belongs to  $\epsilon_{12} = \epsilon_{21}$  and the red profiles belong to the remaining off diagonal elements.

### Dielectric tensor profile of a positive birefringence

In order to see the profiles of all dielectric tensor elements in one figure, a simple trick has to be made to put the elements of the dielectric tensor on the same scale. This can be done by subtracting the value of the ordinary refractive index  $n_0$  from all diagonal elements only. Once we do that, it is possible to see the continuous change of all dielectric tensor elements as we travel across the entire sample. Figure 5.10 shows how the profiles of all six elements of the dielectric tensor in off-state, change across the sample.

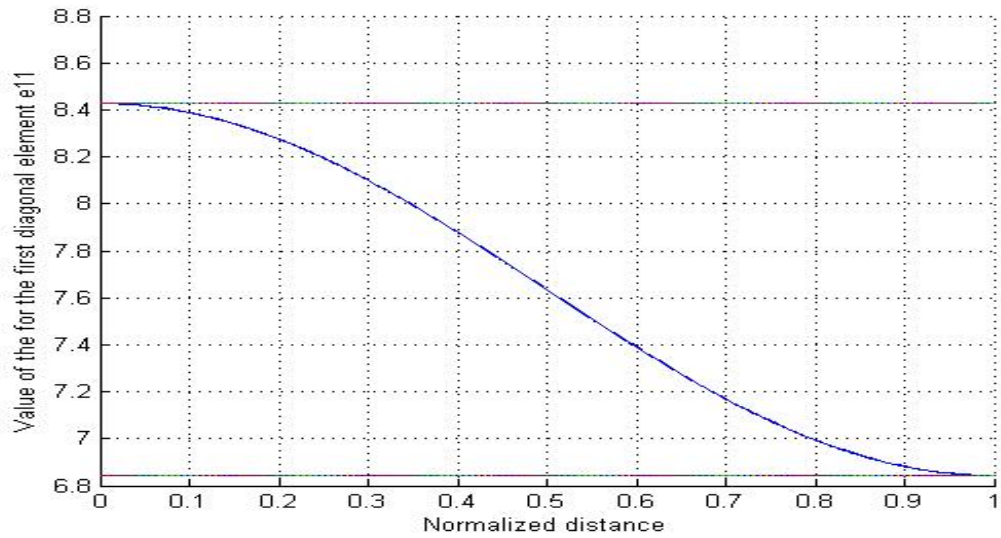


Figure 5.6: The profile of the first diagonal element of the dielectric tensor in the off state as we travel through the sample with a positive birefringence.

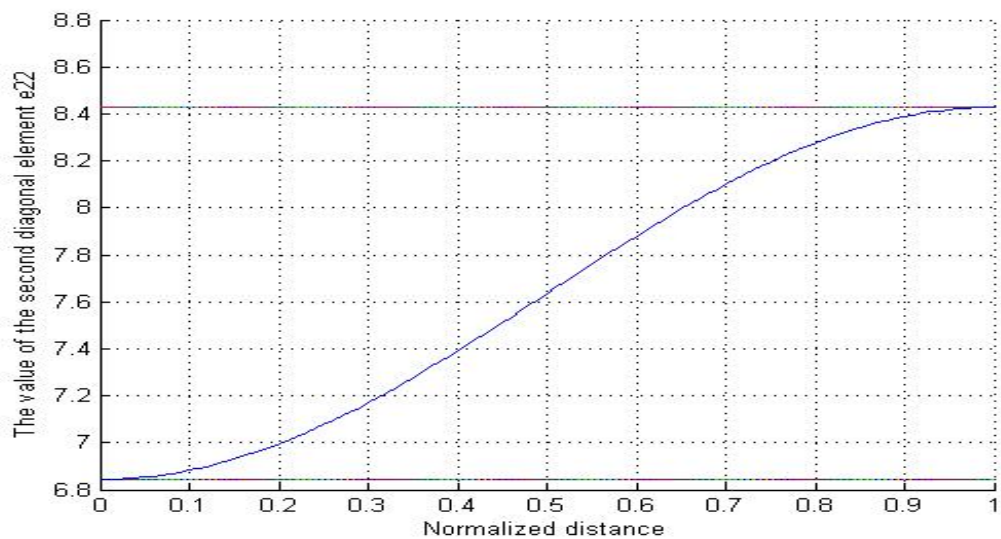


Figure 5.7: The profile of the second diagonal element of the dielectric tensor in the off state as we travel through the sample with a positive birefringence.

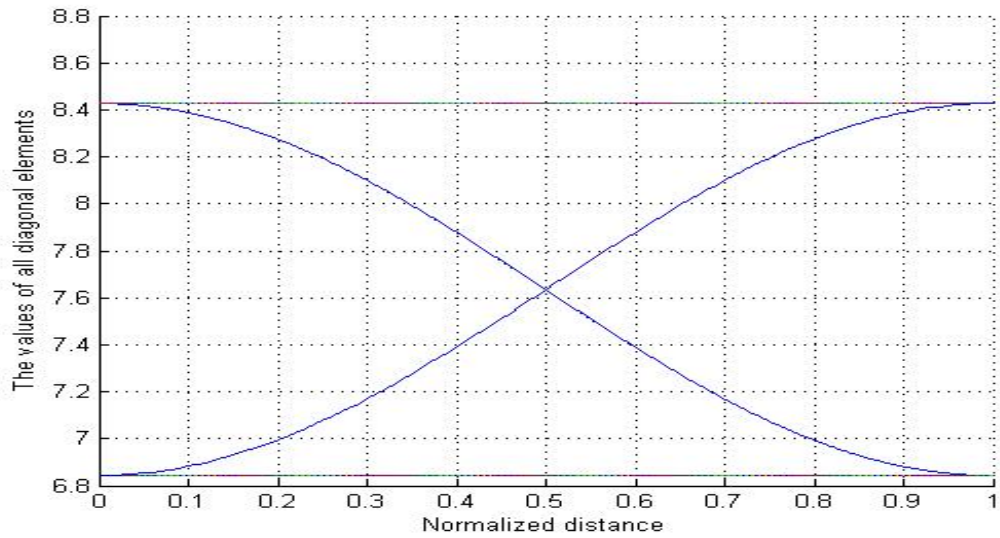


Figure 5.8: The profiles of all diagonal elements of the dielectric tensor in the off state as we travel through the sample with a positive birefringence.

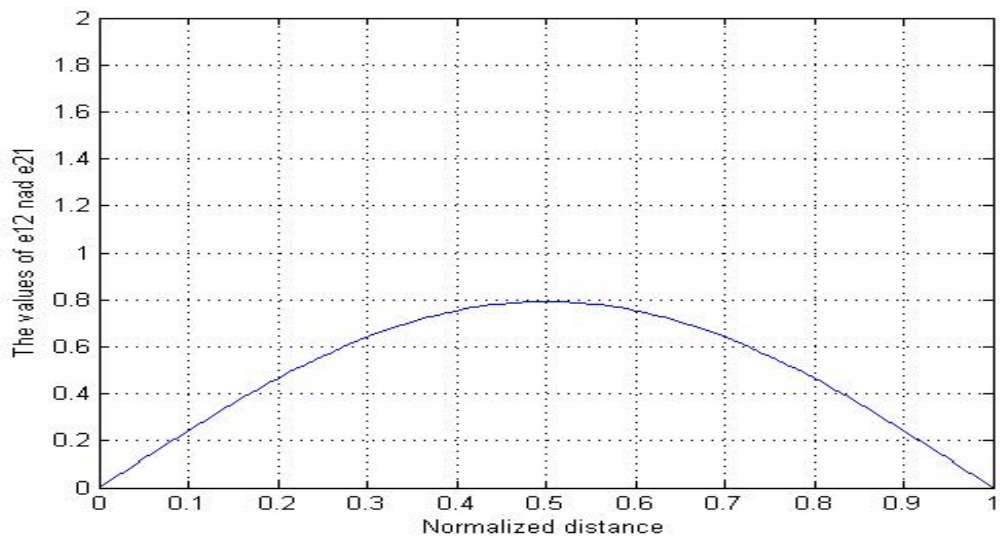


Figure 5.9: This graph shows the profiles of all remaining off-diagonal elements of the dielectric tensor in the off state for a sample with a positive birefringence.

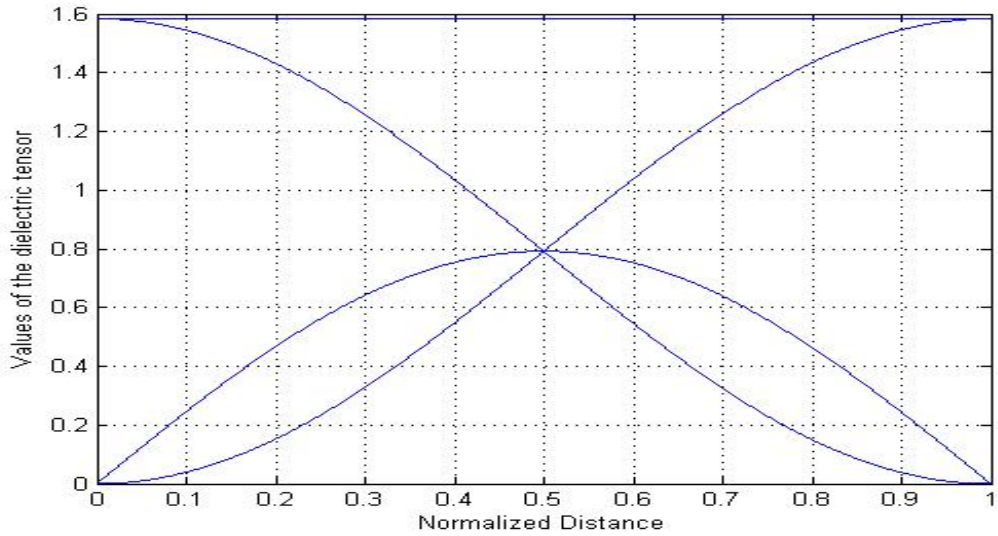


Figure 5.10: The profiles of all elements of a dielectric tensor in the off-state after re-scaling the diagonal elements.

#### 5.4.4 Negative birefringence

For a negative birefringence, where the refractive index along the director is lower than the refractive index perpendicular to the director, the first element  $\epsilon_{11}$  of the dielectric tensor achieves its minimum value, which is  $n_0$  at the beginning of the sample, since it is assumed that the fast axis of anisotropy is oriented perpendicular to the  $x$ -axis. Figure 5.11 shows that this element  $\epsilon_{11}$  will reach its maximum value which is the extraordinary refractive index  $n_e$  at the opposite boundary as we travel through the sample, since the director will twist and eventually become oriented along the  $y$ -axis.

Since the fast axis of anisotropy is oriented along the  $y$ -axis on the first boundary and linearly changes as we travel across the cell, figure 5.12 illustrates how the profile of the second diagonal element  $\epsilon_{22}$  for the dielectric tensor is changing inside the cell. Since the third diagonal element is constant in field off state, the amount of decay of the second diagonal element is gained by the first element to

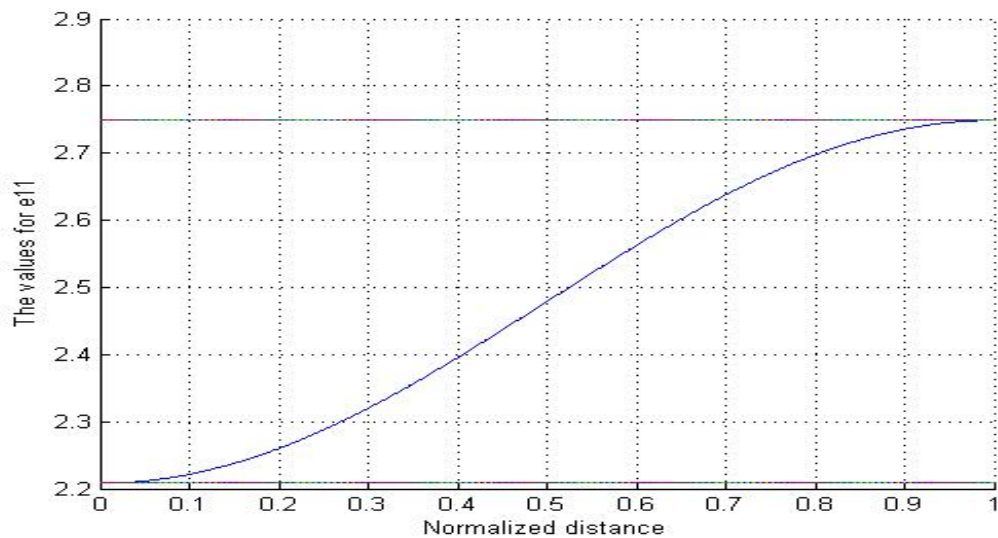


Figure 5.11: The profile of the first diagonal element of the dielectric tensor in the off state as we travel through the sample with a negative birefringence.

achieve the balance between the diagonal elements.

The profiles of the off diagonal elements of the dielectric tensor, are shown in figure 5.14. It should be noted that the values are non-positive for a negative birefringence. The blue curve shows the profile for both elements  $e_{12} = e_{21}$  and the red profiles belong to the other remaining off diagonal elements  $e_{13}, e_{31}, e_{23}$  and  $e_{32}$ .

### Dielectric tensor profile of a negative birefringence

In order to achieve this goal and to see the profiles of all elements in one figure, some adjustment has to be made to the diagonal elements. This adjustment is to remove the value of the ordinary refractive index  $n_0$  from all diagonal elements. Once this has been done the profiles can be seen in the figure 5.15.

Now let's try to calculate the dielectric tensor for a negative birefringence at four different locations, for calcite  $\text{CaCO}_3$  where the ordinary refractive index is

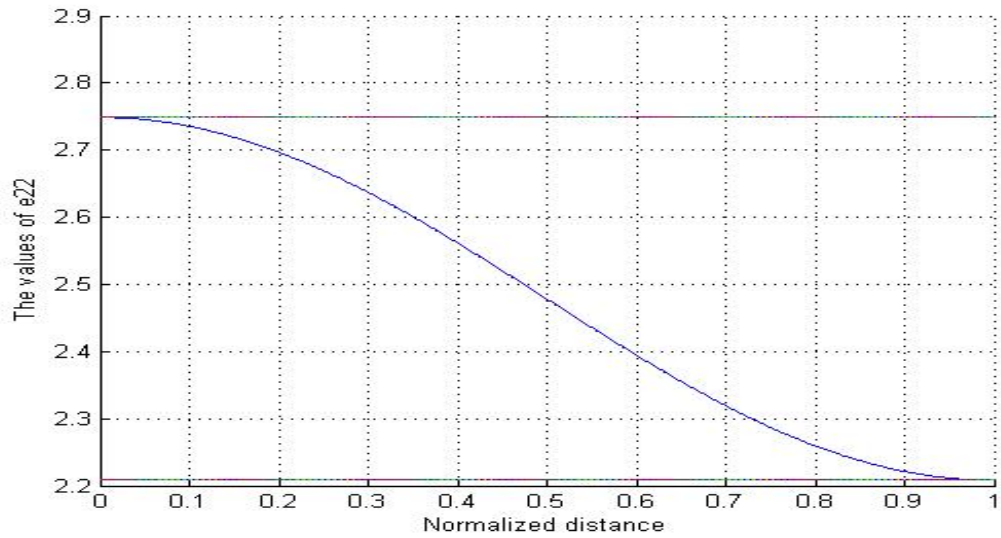


Figure 5.12: The profile of the second diagonal element of the dielectric tensor in the off state as we travel through the sample with a negative birefringence.

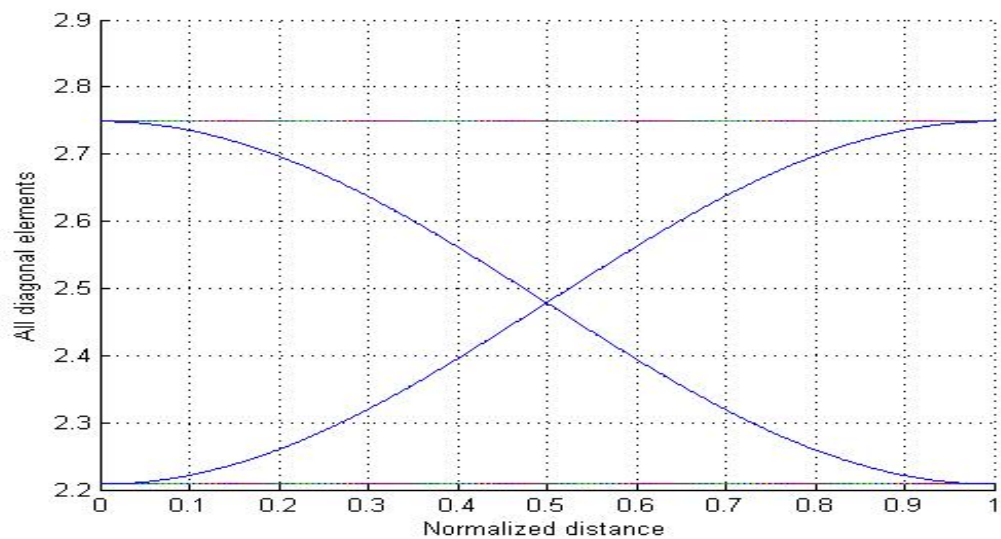


Figure 5.13: The profiles of all diagonal elements of the dielectric tensor in the off state as we travel through the sample with a negative birefringence.

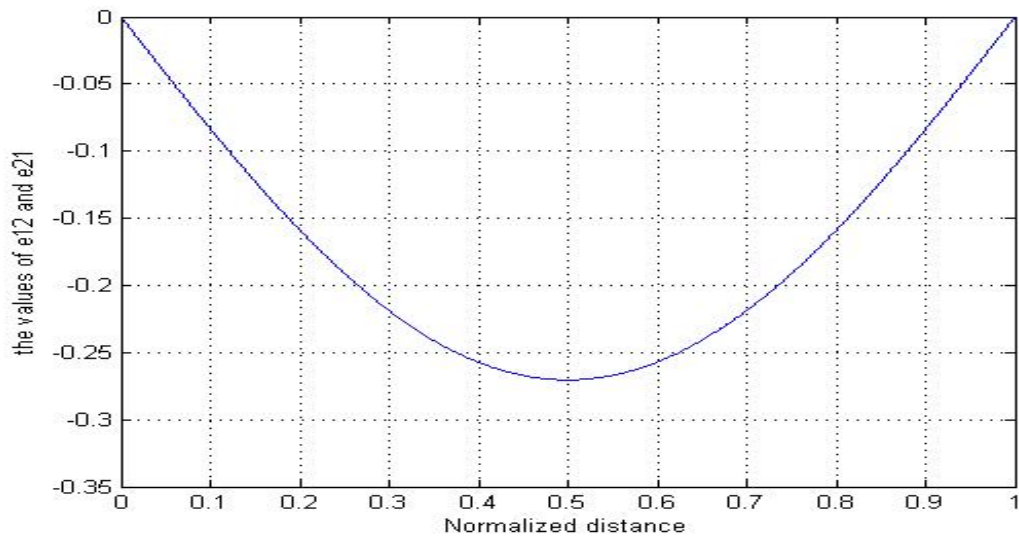


Figure 5.14: This graph shows the profiles of all remaining off diagonal elements of the dielectric tensor in the off state for a sample with a negative birefringence.

$n_0 = 1.658$  and the extraordinary refractive index is  $n_e = 1.486$ . The table 5.1 shows the values of all dielectric tensor elements at four different locations inside the sample.

<b>1.658</b> <b>1.486</b> <b>Calcite</b>	$\epsilon_{11}$	$\epsilon_{22}$	$\epsilon_{33}$	Sum of diagonal elements	$\epsilon_{12}$ = $\epsilon_{21}$	$\epsilon_{13}$ = $\epsilon_{31}$	$\epsilon_{23}$ = $\epsilon_{32}$
<b>Z=0</b>	<b>-0.5408+2.7490</b>	<b>+2.7490</b>	<b>+2.7490</b>	<b>7.7061</b>	<b>0.0</b>	<b>0.0</b>	<b>0.0</b>
<b>Z=0.3d</b>	<b>-0.4293+2.7490</b>	<b>-0.1115+2.7490</b>	<b>+2.7490</b>	<b>7.7061</b>	<b>-0.2187</b>	<b>0.0</b>	<b>0.0</b>
<b>Z=0.5d</b>	<b>-0.2704+2.7490</b>	<b>-0.2704+2.7490</b>	<b>+2.7490</b>	<b>7.7061</b>	<b>-0.2704</b>	<b>0.0</b>	<b>0.0</b>
<b>Z=1d</b>	<b>+2.7490</b>	<b>-0.5408+2.7490</b>	<b>+2.7490</b>	<b>7.7061</b>	<b>0.0</b>	<b>0.0</b>	<b>0.0</b>

Table 5.1: This table shows the values of the dielectric tensor elements at some different locations for calcite  $\text{CaCO}_3$  which has a negative birefringence.

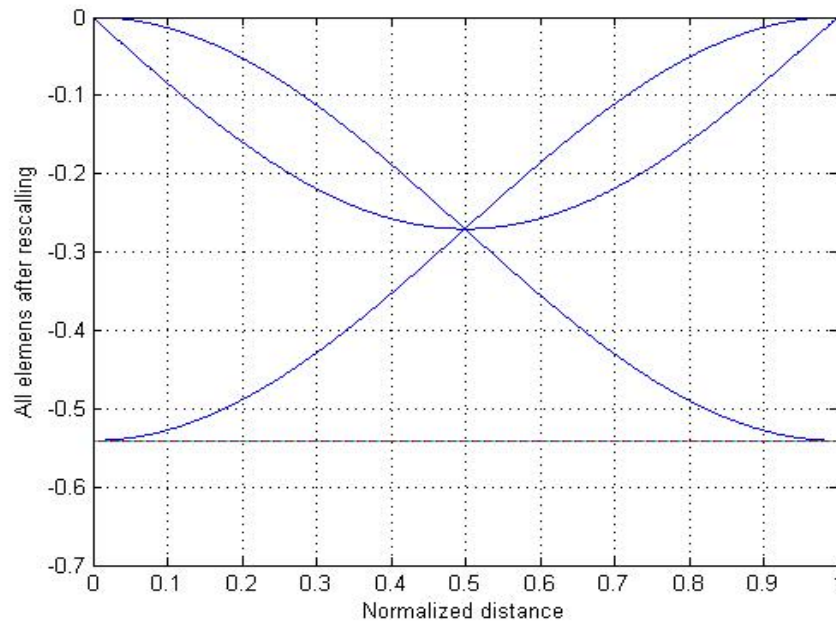


Figure 5.15: The profiles of all elements of a dielectric tensor in the off-state with a negative dielectric tensor after re-scaling.

## 5.5 Summary

In this chapter, we have studied the concept of the dielectric tensor which represents the material properties. For uniaxial materials with a vanishing tilt angle, we were able to project the eign-axes into the  $xy$ -plane since the third axis is not changing throughout the sample. This projection gives us the directions of the principal axes. In fact, these directions is the directions in which the extraordinary and ordinary waves propagate. Later in chapter seven, we will talk about these directions and the propagating modes.

A relationship between the diagonal elements obtained and this relationship shows independence of the tilt and twist angles of the sample. In other words, this relationship holds everywhere regardless the values of the tilt and twist angles. Two example, one for positive birefringence and one for negative birefringence, have been discussed to explain this independence.

# Chapter 6

## Matrix Schrödinger equation

### 6.1 Introduction

During the 1925, both Erwin Schrödinger and Werner Heisenberg made important contributions to the field of Quantum Mechanics by introducing their methods. Schrödinger derived his method on the bases of the partial differential equations, whereas Heisenberg derived his method on the idea of matrix Mechanics. One year later, it had been confirmed, that these two methods were indeed equivalent.

In fact, the Schrödinger equation is a partial differential equation which describes the dynamic of a system. This equation plays exactly the same role as Newton's law in classic Mechanics. In other words, the future of a dynamic system and its properties may be calculated from the Schrödinger equation [9].

There are actually two ODE forms of the Schrödinger equation. The first one is the time dependant and used to describe the evolution of the waves [42], [25]

$$ih \frac{d\Theta(z)}{dz} = H(z)\Theta(z), \quad (6.1)$$

where  $H(z)$  is a hamiltonian operator depending on the physical problem. The second form of the Schrödinger equation is the time independent which of the second order with respect coordinate and of the first order with respect to time. The second form takes the following form for standing waves [42], [50], [25]

$$a\Theta(z) = -\Theta\theta''(z) + V(z)\Theta(z), \quad (6.2)$$

where  $a$  is constant and  $V(z)$  is known as the potential Quantum Mechanics.

## 6.2 Our solution for the Schrödinger equation in matrix form

In order to put our analytical solution in perspective, we need first to formulate our problem of propagation of light and write it in the form of a Schrödinger equation. Mathematically, our problem can be formulated on the basis of the following problem. Suppose that a monochromatic plane light wave incident on an inhomogeneous slab with thickness  $d$  and refractive index  $n(z)$ . If the electric field is harmonic

$$E(z, \omega) = \tilde{E} \exp(i\omega z), \quad (6.3)$$

where

$$\tilde{E} = A \exp(i\frac{\omega}{c}n(z)z),$$

is the amplitude of the wave, then the amplitude inside the nonhomogeneous slab satisfies the Schrödinger equation with vanishing potential [49]

$$E'' + \frac{\omega}{c}n^2(z)E = 0. \quad (6.4)$$

From the optical point of view, obviously this equation is suitable for a medium with one constant refractive index, such as the isotropic medium or for a medium with one variable refractive index, such as a nonhomogeneous medium. It is clear that this equation is not suitable for uniaxial medium since there are two refractive indices. In fact, if the medium is homogenous and uniaxial then, we can extend the above equation to take the following matrix form, as we will see later in the coming chapters

$$\frac{d^2}{dz^2} \begin{pmatrix} E_x \\ E_y \end{pmatrix} + \frac{\omega}{c} n_0^2 \begin{pmatrix} E_x \\ E_y \end{pmatrix} = V(z) \begin{pmatrix} E_x \\ E_y \end{pmatrix}, \quad (6.5)$$

where  $n_0$  is the ordinary refractive index and  $\Delta n$  is the birefringence of the medium. One might notice that if the medium is isotropic then our Schrödinger equation in matrix form will reduce to the above one dimensional Schrödinger equation (6.4) with vanishing potential.

From the literature, one must distinguish between the methods used to solve direct and inverse problems for the Schrödinger equation. In general, there are two methods to solve the Schrödinger equation. The first method is the Green function method which is used to represent the solution of the Schrödinger equation

$$E(z) = E^i(z) + \int_0^d G(z, s) V(s) U(s) ds, \quad (6.6)$$

where  $E^i(z)$  is the field when the medium is homogenous. The second method is the Gel'fand-Levitan and Marchenko method, which is used to solve the inverse problem to recover the potential in the Schrödinger equation [52]

$$V(z) = -2 \frac{dA(z, z)}{dz}, \quad (6.7)$$

where  $A(z, z)$  is the solution of

$$A(z, s) = A_0(z + s) + \int_r^\infty A(z, s)A_0(z + s)ds. \quad (6.8)$$

Our approach is quite different from the Green function approach. In fact, our method to solve the Schrödinger equation is a rotational frame method. This method will be presented in some detail with application in the coming chapters. For twisted nematic liquid crystal, for example, the rotational frame method gives us the following analytical solution for the Schrödinger equation

$$U(z) = \begin{pmatrix} \cos(\theta) & -\sin(\theta) \\ \sin(\theta) & \cos(\theta) \end{pmatrix} \begin{pmatrix} \exp(-i\frac{\omega}{c}n_e z) & 0 \\ 0 & \exp(-i\frac{\omega}{c}n_o z) \end{pmatrix}.$$

In the rest of this section, two examples will be presented to compare the numerical and analytical solutions of the Schrödinger equation.

Using the Matlab software, we solve the Schrödinger equation numerically and the numerical solution is compared with the analytical solution which has been obtained by the rotational frame technique. In the first example, the following data is used,  $n_0 = 1.4$  as an ordinary refractive index,  $\Delta n = 0.550$  is the birefringence of the medium with a twist of ninety degrees across the sample. The  $x$ -component for both numerical and analytical solution of the Schrödinger equations is shown in figure 6.1 whereas numerical and analytical solutions for the second component, which is the  $y$ -component is shown in figure 6.2. The two components of the numerical solution of the Schrödinger equation as they propagate through the sample, is illustrated in figure 6.3. Finally, the analytical solution of the Schrödinger equation is presented in figure 6.4.

Our second example uses exactly the same data which has been used in the

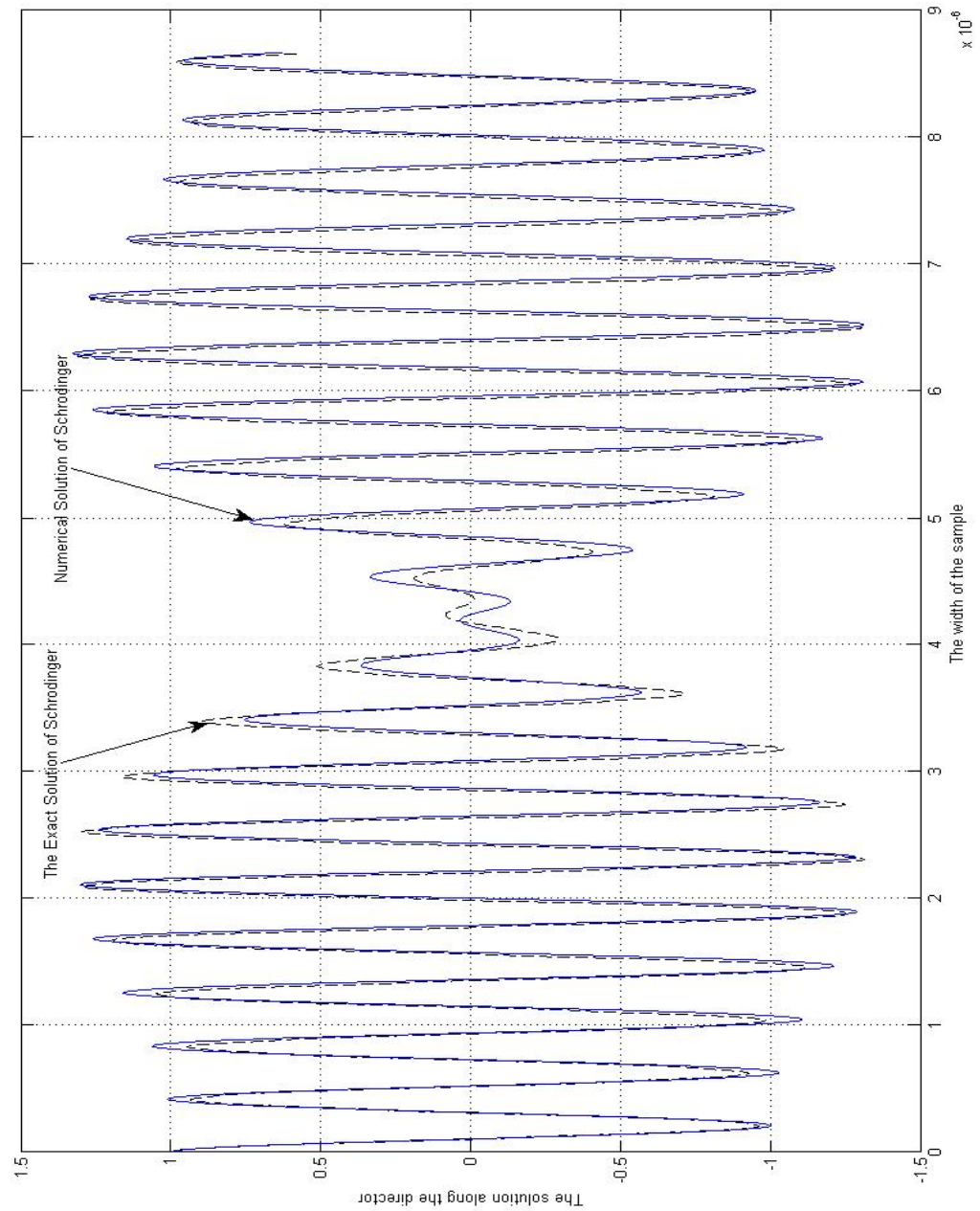


Figure 6.1: This graph shows the  $x$ -component for the exact and numerical solution of the Schrödinger equation.

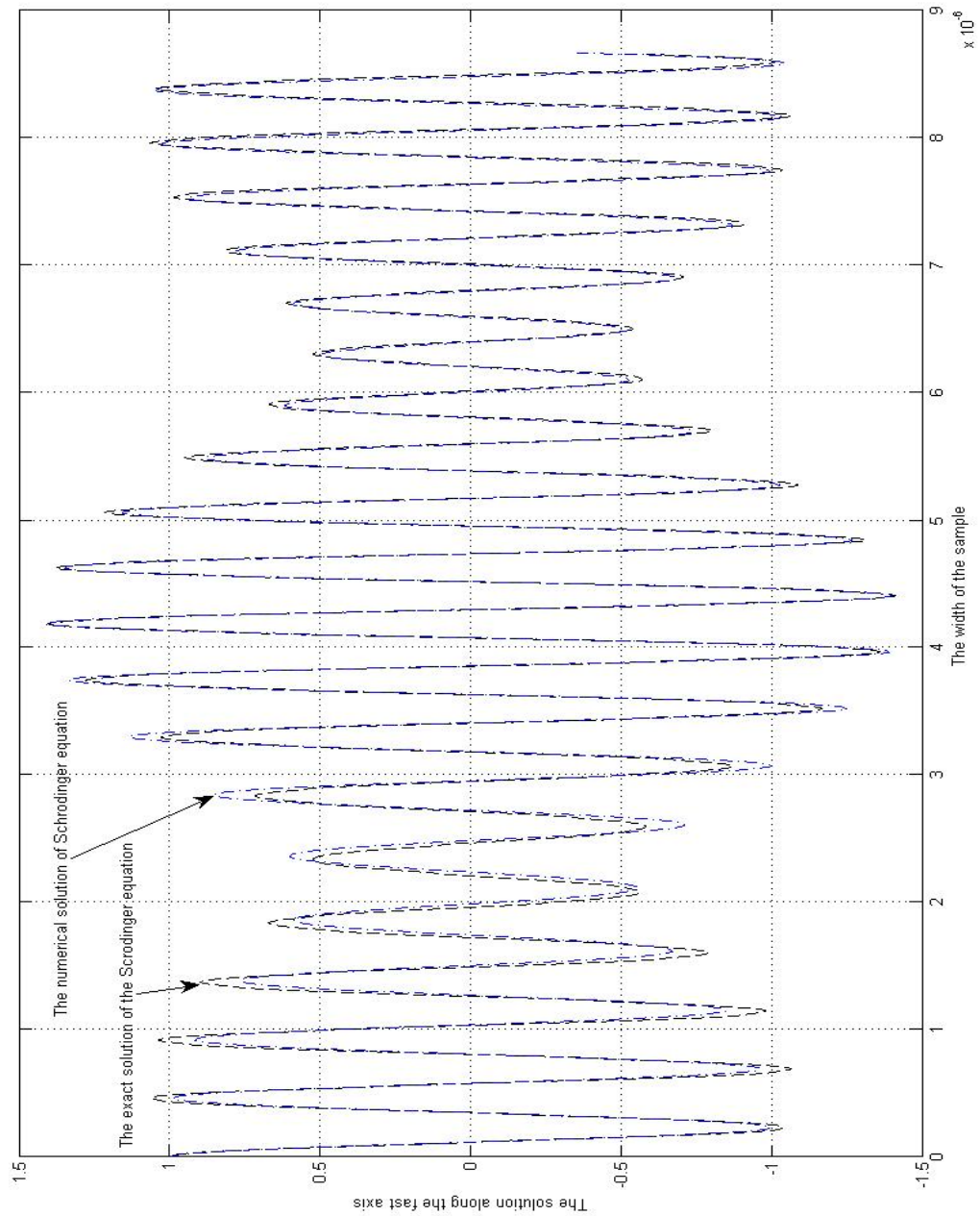


Figure 6.2: This graph shows the  $y$ -component for the exact and numerical solution of the Schrödinger equation.

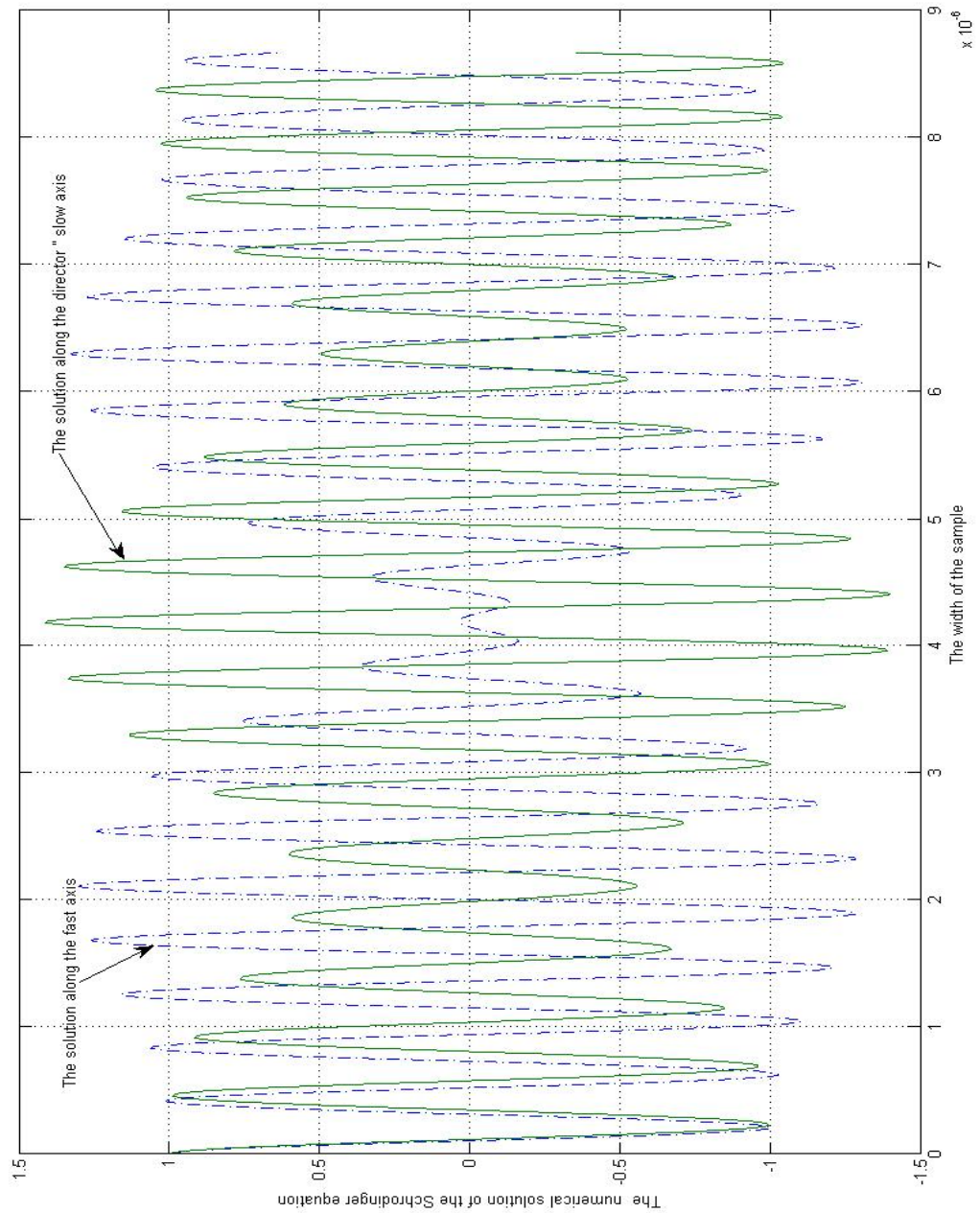


Figure 6.3: This graph shows both  $x$ -component and  $y$ -component for the numerical solution of the Schrödinger equation as they propagate through the medium.

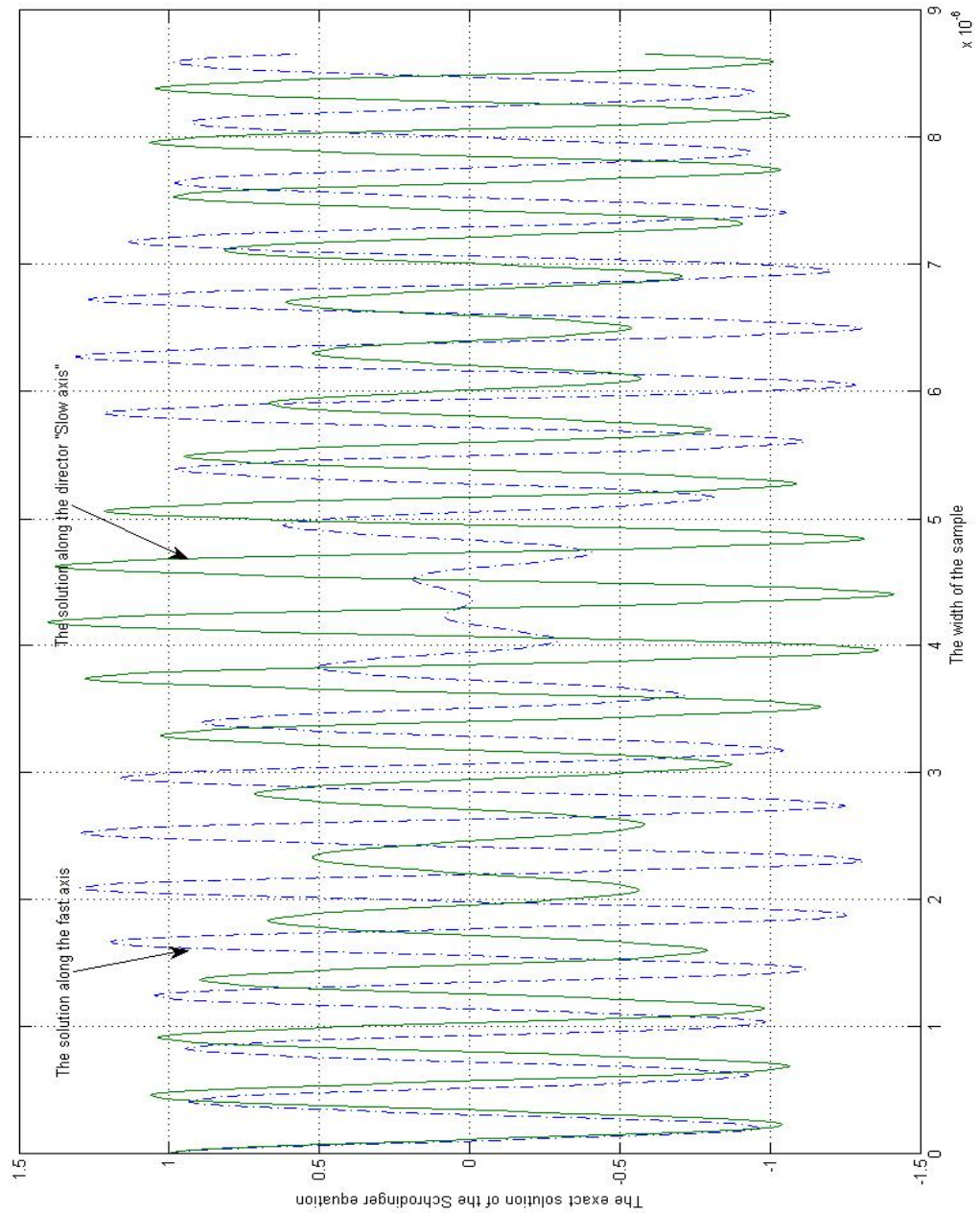


Figure 6.4: This graph shows both  $x$ -component and  $y$ -component for the exact solution of the Schrödinger equation as they propagate through the medium.

---

first example except that the domain has been increased from 8.66 nm to 13nm. Figure 6.5 shows the first component, which is  $x$ -component for numerical and analytical solution of the Schrödinger equation, whereas the numerical and analytical solution for the  $y$ -component is shown in figure 6.6. The two components for the numerical solution of the Schrödinger equation is illustrated in figure 6.7. Finally, the two components of the analytical solution of the Schrödinger equation as they propagate through the domain is presented in figure 6.8.

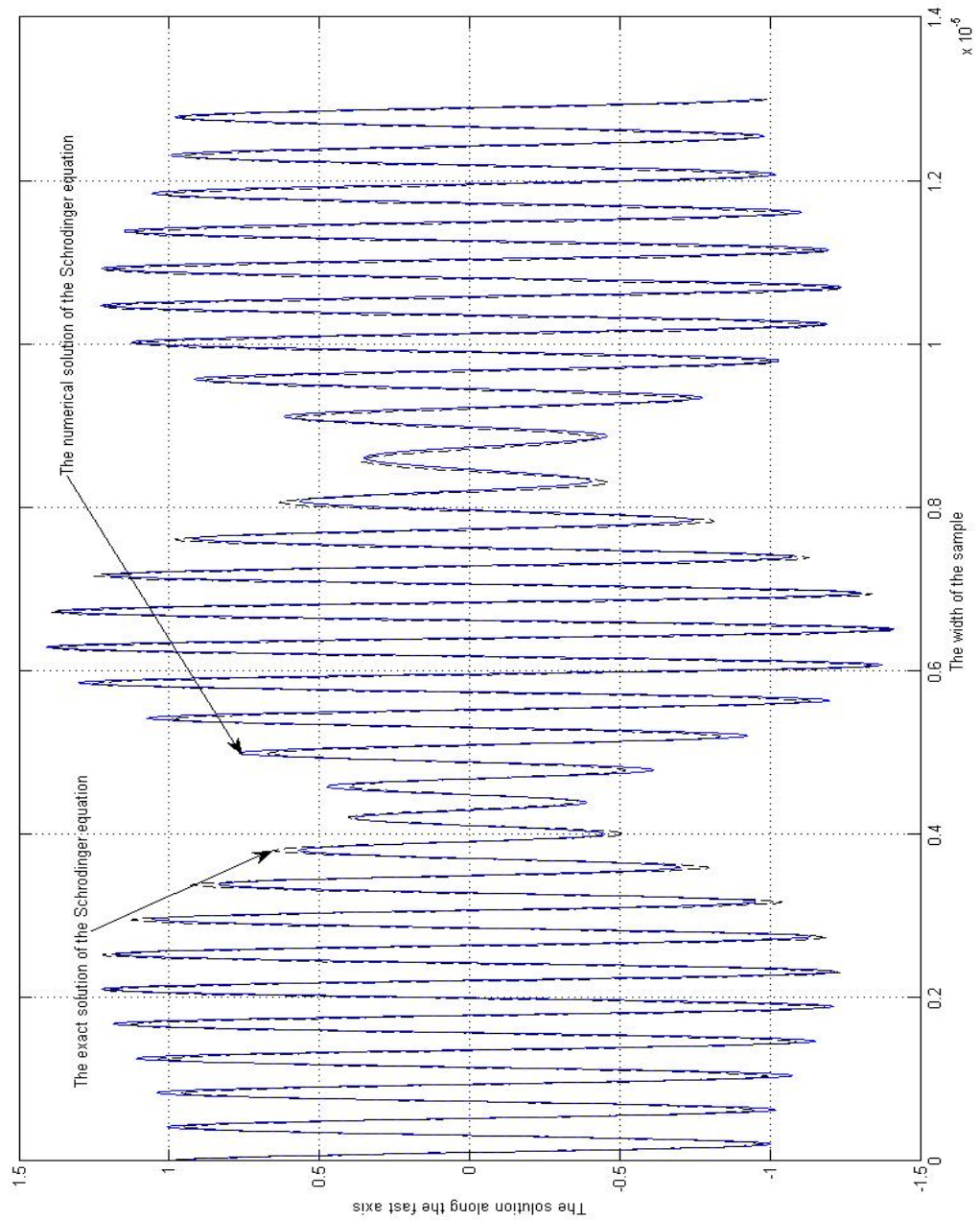


Figure 6.5: This graph shows the  $x$ -component for the exact and numerical solution of the Schrödinger equation.

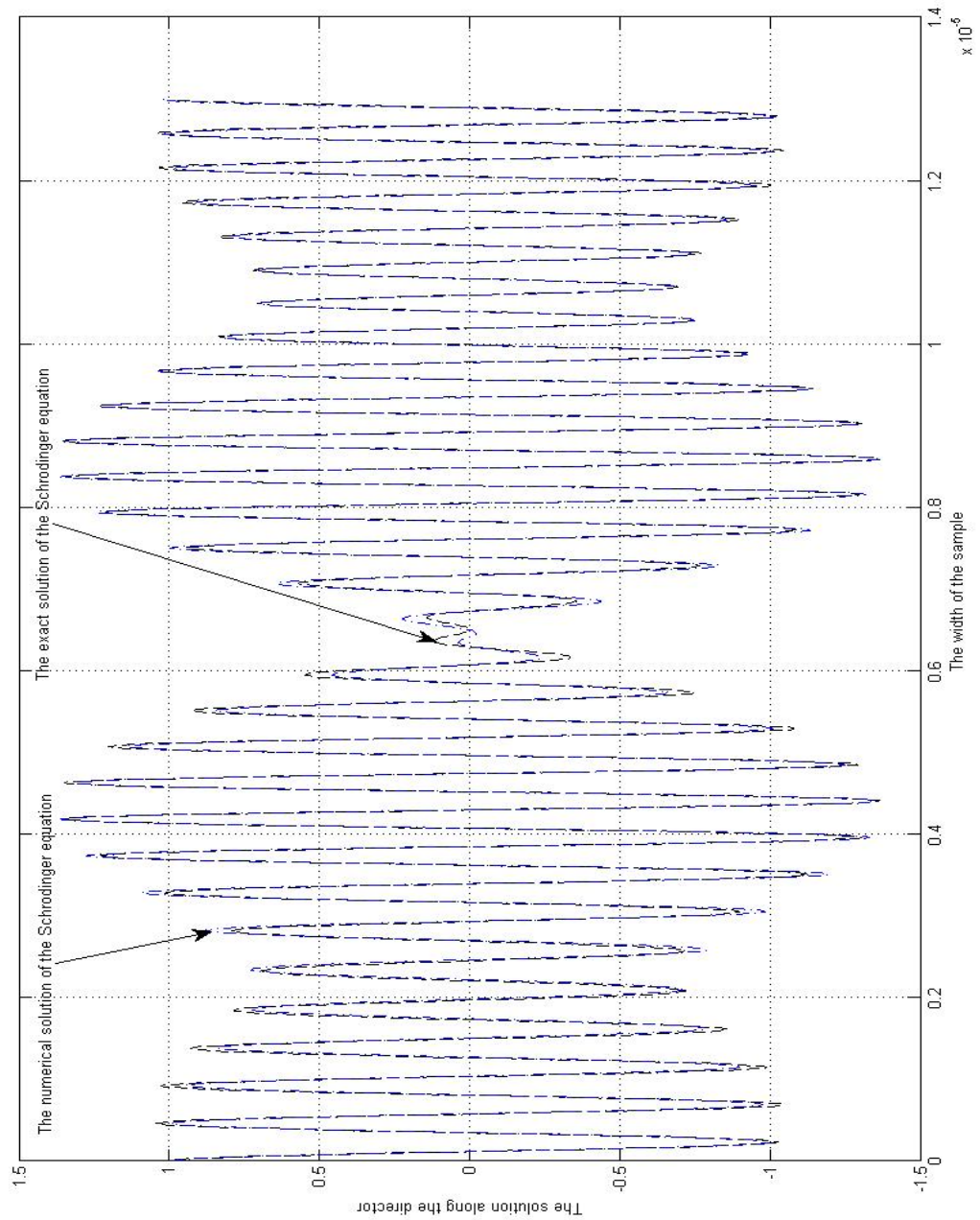


Figure 6.6: This graph shows the  $y$ -component for the exact and numerical solution of the Schrödinger equation.

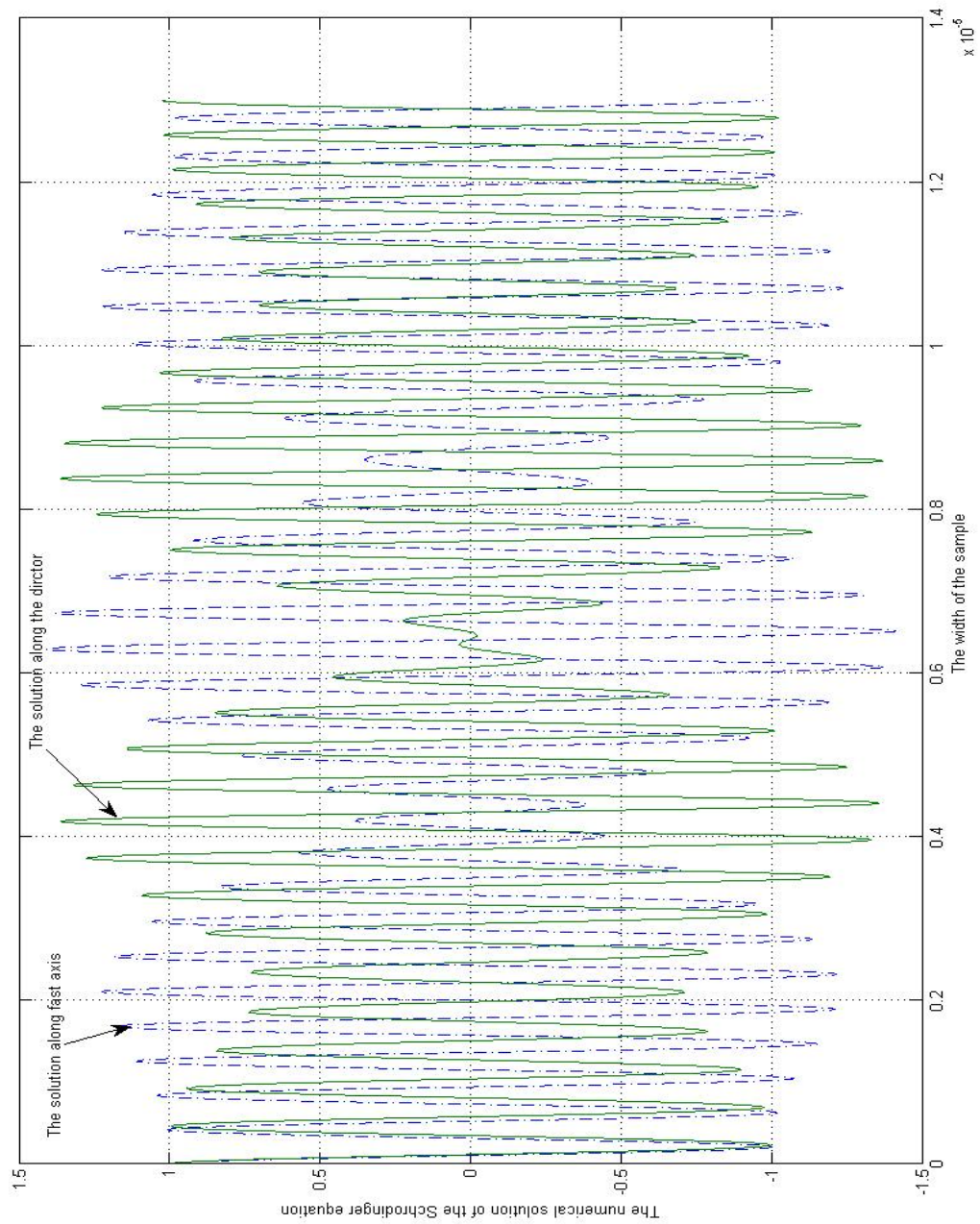


Figure 6.7: This graph shows both the  $x$ -component and  $y$ -component for the numerical solution of the Schrödinger equation as they propagate through the medium.

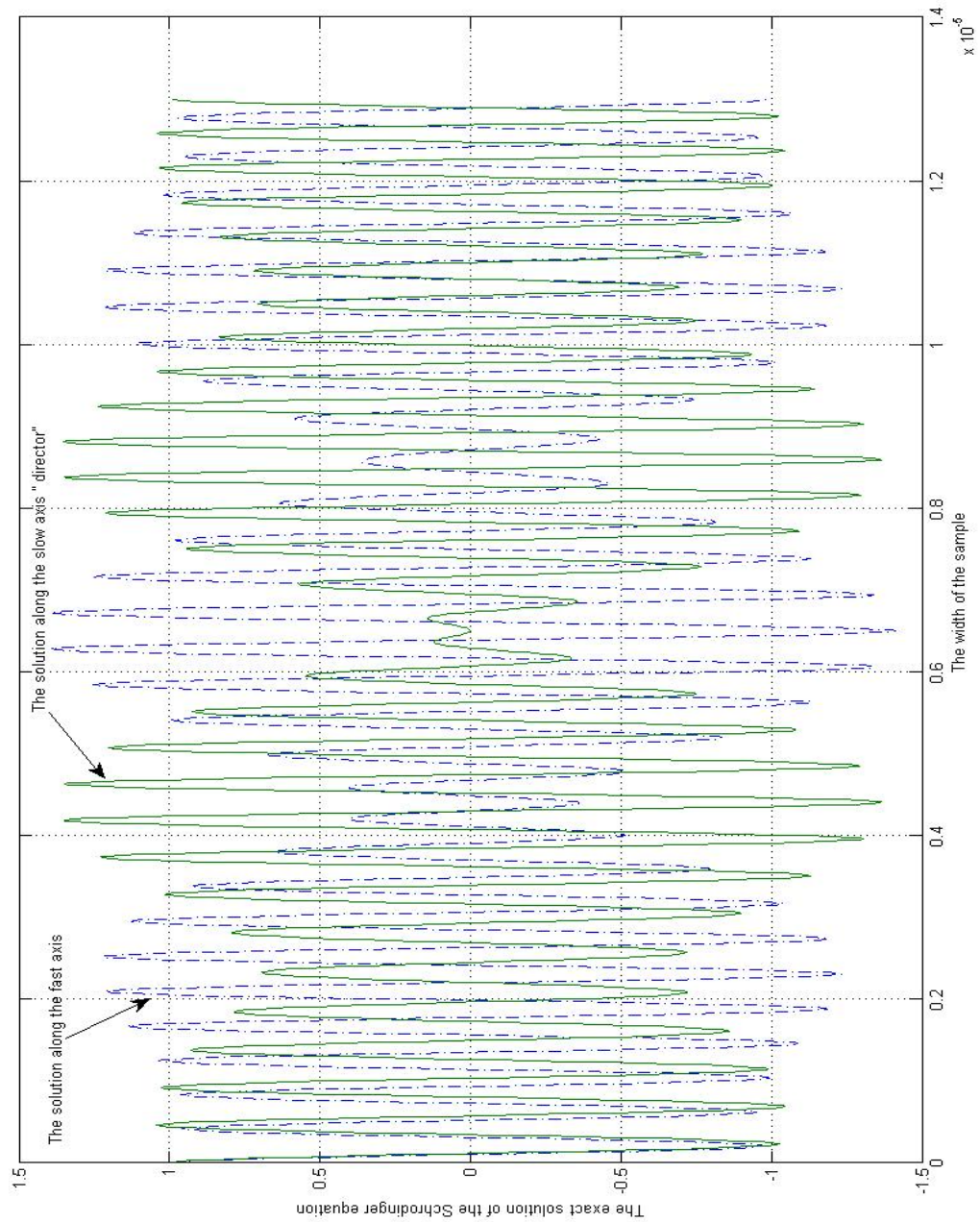


Figure 6.8: This graph shows both  $x$ -component and  $y$ -component for the exact solution of the Schrödinger equation as they propagate through the medium.

### 6.3 Relationship between the Schrödinger equation and the Jones matrix formalism

If waves enter a birefringent sample and propagate for some distance  $d$  inside it, then the relationship between the waves at the boundaries can be written in matrix form as:

$$\begin{aligned} \begin{pmatrix} E_x \\ E_y \end{pmatrix} &= \begin{pmatrix} v_{11} & v_{12} \\ v_{21} & v_{22} \end{pmatrix} \begin{pmatrix} \alpha_1^2 & 0 \\ 0 & \alpha_2^2 \end{pmatrix} \begin{pmatrix} v_{11} & v_{12} \\ v_{21} & v_{22} \end{pmatrix}^{-1} \begin{pmatrix} E_{ox} \\ E_{oy} \end{pmatrix} \\ &= V(z)P(z)V^{-1}(z)E(o), \end{aligned} \quad (6.9)$$

where  $v_{ij}$  are elements of the dynamical matrices, which are responsible for the direction of the waves inside the birefringent material and  $P(z)$  is the propagation matrix for the uniaxial sample, with a fixed transmission axis throughout the sample.

The mathematically differential equation that describes this dynamic system is the time dependent Schrödinger equation, which has been derived earlier from Maxwell's equations. The solution of the time dependent Schrödinger equation which is given by equation 6.5 can be written in a form exactly similar to Jones form

$$\begin{pmatrix} E_x \\ E_y \end{pmatrix} = T(z)P(z)T^{-1}(z) \begin{pmatrix} E_{ox} \\ E_{oy} \end{pmatrix},$$

where  $P(z)$ ,  $T(z)$  and  $T^{-1}(z)$  are given above.

## 6.4 Polarization in Quantum Mechanics

From the Quantum Mechanics point of view, this equation is known as the time dependent Schrödinger equation which has been derived from the original Schrödinger equation. In fact, the Schrödinger equation has been actively studied in the field of Quantum Mechanics and solutions for some special cases, and applications have been reported in the literature. The question to be answered at this stage: is it possible to identify the emerging polarization as the system evolves? This question implies that the problem to solve is the time-dependent Schrödinger equation with some initial input polarization. Before answering the above question, let's us first try to make some connections between our problem which has been developed from the field of optics with the time dependent Schrödinger equation which comes from the field of Quantum Mechanics.

Without losing the generality and for the sake of understanding our problem, we will consider a system that contains only two equations.

$$i \frac{d}{dz} \begin{pmatrix} E_x \\ E_y \end{pmatrix} = \begin{pmatrix} Energy_x & a_{xy} \\ b_{yx} & Energy_y \end{pmatrix} \begin{pmatrix} E_x \\ E_y \end{pmatrix}.$$

In Quantum Mechanics,  $x$  and  $y$  represent the two states of a quantum system and their corresponding amplitudes, as the system evolves with time, are  $E_x$  and  $E_y$ . Moreover,  $Energy_x$  and  $Energy_y$  represent the energy states of the quantum system and the difference between them is called the energy separation. However, in the field of optics, these two states represent the paths in which the ordinary and extraordinary waves follow, as the electric fields components propagate inside the birefringence materials. These paths need not to be straight as we will see later and the amplitudes of these two states will give us the polarization state.

The elements on the main diagonal of the dielectric tensor correspond to the energy states, and the difference between them is the separation energy as we have already mentioned.

## 6.5 Interpretation of our model with Schrödinger model

In this thesis one of our main interests is to pay some attention to the system which has been derived in the previous section. We mean the system of  $2 \times 2$  differential equation which is known in the literature as the time dependent Schrödinger equation.

$$\frac{d}{dz} \begin{pmatrix} E_x \\ E_y \end{pmatrix} = P(z) \begin{pmatrix} E_x \\ E_y \end{pmatrix}.$$

This equation, which first arises in the field of atomic research, in fact can be utilized as we will see later to make some clarifications in both our research and the field of optics.

By recalling some of the previous work, we see that the  $x$  and  $y$  represent the atomic states and  $E_x$  and  $E_y$  are their corresponding amplitudes. It should be clear that the potential of the Schrödinger equation is responsible for the interactions of these states as they progress in time. To see the connection between these states and our model which is the propagation of light through both isotropic and anisotropic media, we need to consider a specific example. Let us consider, for instance, the propagation of light in anisotropic medium. It is worth mentioning that the propagation of light in isotropic medium will be a special case.

Suppose that a light propagates through anisotropic medium in the  $z$ -direction and the axis of anisotropic of the medium makes an angle  $\theta$ , with the  $x$ -axis and perpendicular to the  $z$ -axis. As the light propagates through the medium the initial atomic states, that is the state of polarization, will be affected by the anisotropy of the medium. The result of this action will be clear on the final atomic states as they leave the medium. In fact, the potential in the Schrödinger equation is the responsible term of the interaction between the anisotropy of the medium and the atomic states.

## 6.6 Floquet's theory

In 1883, remarkable work was done by Floquet in developing the solution of a linear periodic system. This work is known today as Floquet's theory [45]. In fact, the Floquet's theory gives us useful information about the solution of a linear periodic system in terms of the state transition matrix. Before we state the basic idea behind this work, the following definitions are needed

**Definition:** A matrix function  $X(x)$  is said to be periodic with period  $T$  if there exists  $T > 0$  such that  $X(x + T) = X(x)$  for all  $x$  and  $X(x)$  is said to be  $T$ -periodic.

**Definition:** A matrix function  $X(x)$  is said to be antiperiodic with period  $T$  if there exists  $T > 0$  such that  $X(x + T) = -X(x)$  for all  $x$  and  $X(x)$  is said to be  $T$ -antiperiodic.

Now suppose that we have a linear  $T$ -periodic system

$$\frac{d\psi}{dz} = A(z)\psi, \quad (6.10)$$

where  $A(z)$  is a square complex matrix with  $n$ -dimension and  $\psi$  is a complex  $n$ -column vector. According to the classical Floquet's theory, the fundamental matrix solution of the above system has the following decomposition [51], [53]

$$U(z, z_o) = F(z) \exp(iQt) F^{-1}(z_o), \quad (6.11)$$

where  $F(z)$  is a periodical matrix with period  $T$  and  $Q$  is a diagonal matrix with constant elements [45].

## 6.7 Existence of the solution of the Schrödinger equation

Our goal is to recover and trace the director orientation inside birefringence materials. This can be done by studying the polarization state which results from the solution of the Schrödinger equation in the matrix form

$$i \frac{d}{dz} \begin{pmatrix} E_x \\ E_y \end{pmatrix} = \begin{pmatrix} n_0 + \Delta n a^2 & \Delta n a b \\ \Delta n a b & n_0 + \Delta n b^2 \end{pmatrix} \begin{pmatrix} E_x \\ E_y \end{pmatrix},$$

where  $\Delta n$  is the birefringence of the uniaxial material. Before doing this, we will first state the general form of the solution for the Schrödinger equation from the literature, and then we will introduce a novel idea to find the exact solution for the case of twisted uniaxial materials.

Now let us go back and investigate the solution of the Schrödinger equation. Floquet's theory guarantees the existence of the solution of the Schrödinger equation when the elements of the Hermitian matrix have periodical functions. The

general form of the solution according to Floquet's theory is

$$U(z) = \phi(z) \exp(-iAz),$$

where  $\phi(z)$  is a matrix which also has periodical coefficients.  $A$  is a diagonal matrix with constant elements and the elements are called the characteristic exponents. The evolution operator of the Schrödinger equation can be written as

$$E(z) = U(z, z_0)E(z_0). \quad (6.12)$$

Also, it can be shown from the solution of the Schrödinger equation that the solution satisfies this relation [45]

$$\det[U(z, z_0)] = \exp\left(-i \int_{z_0}^z \text{Tr}(M(z))dz\right). \quad (6.13)$$

## 6.8 Eigenvalues and the corresponding potential for the Schrödinger equation

This section will give us some information about the relationship between the potential and the eigenvalues of the Schrödinger equation and the direction of the director in the investigated sample. In order to do that, we need first to rewrite the time dependent Schrödinger equation in this matrix form

$$\frac{d}{dz} \begin{pmatrix} E_x \\ E_y \end{pmatrix} + i \frac{\omega}{c} n_o \begin{pmatrix} E_x \\ E_y \end{pmatrix} = -i \frac{\omega}{c} \Delta n \begin{pmatrix} \cos^2 \theta(z) & \cos \theta(z) \sin \theta(z) \\ \cos \theta(z) \sin \theta(z) & \sin^2 \theta(z) \end{pmatrix} \begin{pmatrix} E_x \\ E_y \end{pmatrix}, \quad (6.14)$$

which can be written as

$$\frac{d\mathbf{E}}{dz} + \lambda\mathbf{E} = \mathbf{V}(z)\mathbf{E}, \quad (6.15)$$

where  $\lambda$  is the eigenvalue and  $V(z)$  is the potential for the Schrödinger equation. As we will see later, the information for the director inside the sample is encoded inside the potential of the Schrödinger equation, as the light propagates through the material. The following sections will discuss the potential for isotropic sample, anisotropic sample with fixed transmission axis and anisotropic sample with a twisted transmission axis.

### 6.8.1 Potential for isotropic sample

Since the magnitude of the birefringence  $\Delta n$  is zero, the potential  $\mathbf{V}(z)$  in the above Schrödinger equation will reduce to zero. As a consequence of zero potential, the Schrödinger equation will reduce to two simple separable differential equations. One can easily solve the resulting system to obtain the corresponding electric field components  $E_x$  and  $E_y$ , and the obtained solution is exactly equivalent to that obtained by using the Jones matrix treatment for isotropic case. The corresponding eigenvalues for this case are

$$\lambda_1 = \lambda_2 = i\frac{\omega}{c}n_0. \quad (6.16)$$

Indeed this is what is expected from the Schrödinger equation in the case of isotropic. The reason behind this expectation is that the light has no preferred direction as it propagates inside isotropic samples. In other words, the isotropic sample has only one refractive index.

### 6.8.2 Potential for anisotropic sample with a fixed transmission axis

For anisotropic materials, the magnitude of the birefringence  $\Delta n$  is not equal to zero and as a consequence of that the potential of the Schrödinger equation will not vanish. This makes the system difficult to solve analytically since the differential equations in this system are not decoupled in most cases. We should point out that there are, in fact, two special cases where the system can be solved analytically to obtain the electric field components  $E_x$  and  $E_y$ . The first special case is when the transmission axis is along the  $x$ -axis and the second case is when the transmission axis is along the  $y$ -axis. In both cases, the obtained solutions are exactly the same solutions obtained by the Jones matrix treatment for anisotropic with a fixed transmission axis. Table 6.1 gives us the possible direction for the transmission axis, together with the corresponding potential and eigenvalues of the Schrödinger equation, for anisotropic sample with a fixed transmission axis.

<i>Transmission Axis</i>	<i>The Corresponding Potential for the Schrodinger Equation</i>	<i>Associated Eigenvalues</i>
<b>x-axis</b>	$V(z) = \begin{pmatrix} 1 & 0 \\ 0 & 0 \end{pmatrix}$	$\lambda_1 = i \frac{\omega}{c} n_e, \quad \lambda_2 = i \frac{\omega}{c} n_o$
<b>y-axis</b>	$V(z) = \begin{pmatrix} 0 & 0 \\ 0 & 1 \end{pmatrix}$	$\lambda_1 = i \frac{\omega}{c} n_o, \quad \lambda_2 = i \frac{\omega}{c} n_e$
<b>45 degree from the x-axis</b>	$V(z) = \frac{1}{2} \begin{pmatrix} 1 & 1 \\ 1 & 1 \end{pmatrix}$	$\lambda_1 = i \frac{\omega}{c} n_e, \quad \lambda_2 = i \frac{\omega}{c} n_o$
<b><math>\theta</math> - degree from the x-axis</b>	$V(z) = \begin{pmatrix} \cos^2 \theta & \cos \theta \sin \theta \\ \cos \theta \sin \theta & \sin^2 \theta \end{pmatrix}$	$\lambda_1 = i \frac{\omega}{c} n_e, \quad \lambda_2 = i \frac{\omega}{c} n_o$

Table 6.1: The possible direction for the transmission axis together with corresponding potential and eigenvalues of the Schrödinger equation for anisotropic sample with a fixed transmission axis.

### 6.8.3 Potential for anisotropic sample with a twisted transmission axis

In this case, which is the twisted nematic sample, the potential is location dependent. In other words, the potential of the Schrödinger equation is changing from one position to another. This did not surprise us, since the orientation of molecular director in a twisted nematic sample is changing from one position to another. It is really difficult to solve the wave equation, Schrödinger equation, analytically to obtain the electric field components since the potential of the Schrödinger equation is changing throughout the sample. The coming chapter, we will use an elegant idea to solve this Schrödinger equation analytically and the resulting solution will be tested via the numerical calculation.

It is worth mentioning that the previous two cases, isotropic sample and anisotropic sample with a fixed transmission axis, are just special cases of the twisted nematic sample. Solving Schrödinger equation at any location gives us these two eigenvalues

$$\lambda_1 = i\frac{\omega}{c}n_e, \quad (6.17)$$

$$\lambda_2 = i\frac{\omega}{c}n_o, \quad (6.18)$$

which are the same as the eigenvalues obtained in the case of anisotropic sample with a fixed transmission axis. Again this did not surprise us since the medium has only two refractive indices.

## 6.9 Conclusion

In this chapter, we studied the polarization states from the Quantum Mechanics point of view. In another words, we have showed that there is a strong relationship

between the Jones analysis in optics and the Schrödinger equation in Quantum Mechanics.

Also, in this chapter we showed that the corresponding differential equation for the Jones analysis is in fact the Schrödinger equation in matrix form. The last three sections explain in detail the information encoded in eigenvalues and their corresponding potentials of the Schrödinger equation from optics point of view.

# Chapter 7

## Equation of propagation

### 7.1 Introduction

The propagation of light in liquid crystal layers has been widely studied in literature. Jones first introduced the  $2 \times 2$  matrix technique which is useful to get some information about the amplitudes of the electric fields, and the emerging polarization of the light. Sometime later, more exact method which is known as the Berreman  $4 \times 4$  matrix technique had been introduced to study the propagation of light. This method had been derived directly from Maxwell's equations which describe the propagation of light, and as a consequence, it has the ability to produce the exact solution.

According to Berreman, if the medium is homogenous in the  $xy$ -plane and the optical axis varies in the direction of light propagation, then Maxwell's equations are easily transformed into a system of first order differential equations

$$\frac{d\psi}{dz} = \frac{-i\omega}{c}M(z)\psi, \quad (7.1)$$

where  $\omega$  and  $c$  are the angular frequency and the speed of light in space respectively. The matrix  $M(z)$  which depends completely on the dielectric tensor is given by

$$M = \begin{pmatrix} -\frac{\epsilon_{13}}{\epsilon_{33}}m & c\frac{\epsilon_{33}-m^2}{\epsilon_{33}} & -\frac{\epsilon_{23}}{\epsilon_{33}}m & 0 \\ \epsilon_0c[\epsilon_{11} - \frac{\epsilon_{13}^2}{\epsilon_{33}}] & -\frac{\epsilon_{13}}{\epsilon_{33}}m & \epsilon_0c[\epsilon_{12} - \frac{\epsilon_{12}\epsilon_{23}}{\epsilon_{33}}] & 0 \\ 0 & 0 & 0 & c \\ \epsilon_0c[\epsilon_{12} - \frac{\epsilon_{12}\epsilon_{23}}{\epsilon_{33}}] & -\frac{\epsilon_{23}}{\epsilon_{33}}m & \epsilon_0c[\epsilon_{22} - \frac{\epsilon_{23}^2}{\epsilon_{33}} - m^2] & 0 \end{pmatrix},$$

where  $m$  is related to the incident angle of the light via the relation  $m = n \sin \theta_i$  and  $\psi$  is known as the Berreman vector field which is given by

$$\psi = (E_x, H_y, E_y, -H_x)^T. \quad (7.2)$$

In general, the Berreman matrix method is used for the case of oblique incidence, whereas the Jones matrix method is used for normal incidences. A lot of research has been done to extend the Jones method to oblique incidence, since it is more easily understood than the Berreman method. In this chapter, we derive a first order differential equation, which based on the Maxwell equations and is equivalent to the Berreman equation. Our differential equation which is a  $2 \times 2$  matrix method contains only the electric fields components.

## 7.2 Detailed derivation for the Berreman equation from Maxwell's equations

In this section we will present a detailed derivation of the Berreman method which is used to study and compute the electromagnetic wave propagation in the

materials. The computation problem behind the propagation of electromagnetic waves in an anisotropic stratified medium, has been extensively studied in the literature. The Berreman matrix method is derived directly from the Maxwell equations. Although this method needs a lengthy calculation and is time consuming, it produces an exact solution. On the other hand, several approximations to the Berreman method have been proposed in the literature to overcome the problem of lengthy computation. One of them, for instance, is the fast  $4 \times 4$  method which gives reasonable accuracy for the exact Berreman method and reduces the computation time [54].

As we mentioned perviously, the propagation of light in stratified anisotropic media can be calculated by using the Berreman method. This method depends on the tangential components of the electric and magnetic fields. In order to derive the mathematical equations for this model, we will start from the following Maxwell equations for a dielectric medium

$$\nabla \cdot \mathbf{D} = 0, \quad (7.3)$$

$$\nabla \cdot \mathbf{B} = 0, \quad (7.4)$$

$$\nabla \times \mathbf{E} = -\frac{\partial \mathbf{B}}{\partial t}, \quad (7.5)$$

$$\nabla \times \mathbf{H} = \frac{\partial \mathbf{D}}{\partial t}. \quad (7.6)$$

At this stage, to proceed with the derivation, we have to specify the incident plane for the wave vector. Also to simplify the calculation, we shall assume that  $(E, H)$  is the medium satisfies frequency domain Maxwell's equations. In other

words, we will assume time harmonic waves.

$$\mathbf{E}(\mathbf{x}, \mathbf{t}) = \exp(i\omega t)\mathbf{E}(\mathbf{x}), \quad (7.7)$$

$$\mathbf{H}(\mathbf{x}, \mathbf{t}) = \exp(i\omega t)\mathbf{H}(\mathbf{x}), \quad (7.8)$$

Now, by differentiating these two equations with respect to time, we will get these relationships

$$\frac{\partial \mathbf{E}(\mathbf{x}, \mathbf{t})}{\partial t} = i\omega \exp(i\omega t)\mathbf{E}(\mathbf{x}) = i\omega \mathbf{E}(\mathbf{x}, \mathbf{t}), \quad (7.9)$$

$$\frac{\partial \mathbf{H}(\mathbf{x}, \mathbf{t})}{\partial t} = i\omega \exp(i\omega t)\mathbf{H}(\mathbf{x}) = i\omega \mathbf{H}(\mathbf{x}, \mathbf{t}). \quad (7.10)$$

As a result of that, the above Maxwell equations can further be simplified and written as:

$$\nabla \cdot \mathbf{D} = 0, \quad (7.11)$$

$$\nabla \cdot \mathbf{B} = 0, \quad (7.12)$$

$$\nabla \times \mathbf{E} = -i\omega \mathbf{B}, \quad (7.13)$$

$$\nabla \times \mathbf{H} = i\omega \mathbf{D}. \quad (7.14)$$

According to the experiment in HPLB, the wave vector had been chosen in the  $xz$ -plane. By this choice, the dielectric tensor will vary only along the  $z$ -direction and will be a constant along the  $xy$ -plane. Moreover, since the incidence plane was taken to be the  $xz$ -plane, the problem will be invariant in the  $y$ -direction, so that

$$k_y = 0, \quad (7.15)$$

$$\frac{\partial}{\partial y} = 0. \quad (7.16)$$

As a consequence of this choice, Ampere's law can be written as:

$$\begin{pmatrix} 0 & -\frac{\partial}{\partial z} & 0 \\ \frac{\partial}{\partial z} & 0 & -ik_x \\ 0 & ik_x & 0 \end{pmatrix} \begin{pmatrix} E_x \\ E_y \\ E_z \end{pmatrix} = i\omega\mu_0 \begin{pmatrix} H_x \\ H_y \\ H_z \end{pmatrix}.$$

Similarly Faraday's law can be written as:

$$\begin{pmatrix} 0 & -\frac{\partial}{\partial z} & 0 \\ \frac{\partial}{\partial z} & 0 & -ik_x \\ 0 & ik_x & 0 \end{pmatrix} \begin{pmatrix} H_x \\ H_y \\ H_z \end{pmatrix} = \begin{pmatrix} \epsilon_{xx}E_x + \epsilon_{xy}E_y + \epsilon_{xz}E_z \\ \epsilon_{yx}E_x + \epsilon_{yy}E_y + \epsilon_{yz}E_z \\ \epsilon_{zx}E_x + \epsilon_{zy}E_y + \epsilon_{zz}E_z \end{pmatrix}.$$

Before we go further in the derivation, we must mention to the reader that another orientation (i.e incident plane ) can be used by redefining the axis frame. Also, the derivation will be parallel to our derivation but there will be a slight change in both Ampere's and Faraday's laws. For our purpose, we will assume the permeability of the medium is unity and the constitutive relations are linear. In other words,

$$\mathbf{D} = \epsilon\mathbf{E}, \quad (7.17)$$

$$\mathbf{B} = \mu_0\mathbf{H}. \quad (7.18)$$

The above matrices, Ampere's and Faraday's laws, can be decomposed into six linear equations

$$-\frac{\partial E_y}{\partial z} = i\omega\mu_0 H_x, \quad (7.19)$$

$$-\frac{\partial E_x}{\partial z} - ik_x E_z = i\omega\mu_0 H_y, \quad (7.20)$$

$$ik_x E_y = i\omega\mu_0 H_z, \quad (7.21)$$

$$-\frac{\partial H_y}{\partial z} = \epsilon_{xx}E_x + \epsilon_{xy}E_y + \epsilon_{xz}E_z = \epsilon_{xk}E_k, \quad (7.22)$$

$$-\frac{\partial H_x}{\partial z} - ik_x H_z = \epsilon_{yx}E_x + \epsilon_{yy}E_y + \epsilon_{yz}E_z = \epsilon_{yk}E_k, \quad (7.23)$$

$$ik_x H_y = \epsilon_{zx}E_x + \epsilon_{zy}E_y + \epsilon_{zz}E_z = \epsilon_{zk}E_k. \quad (7.24)$$

Now if we take a close look at this system of equations, it can be noticed that this system of equations contains two types of equations. The first type of equations is the tangential components of both electric and magnetic fields

$$-\frac{\partial E_y}{\partial z} = i\omega\mu_0 H_x, \quad (7.25)$$

$$-\frac{\partial E_x}{\partial z} - ik_x E_z = i\omega\mu_0 H_y, \quad (7.26)$$

$$-\frac{\partial H_y}{\partial z} = \epsilon_{xx}E_x + \epsilon_{xy}E_y + \epsilon_{xz}E_z = \epsilon_{xk}E_k, \quad (7.27)$$

$$-\frac{\partial H_x}{\partial z} - ik_x H_z = \epsilon_{yx}E_x + \epsilon_{yy}E_y + \epsilon_{yz}E_z = \epsilon_{yk}E_k. \quad (7.28)$$

and the second type of equations is for normal components which are independent of the derivative

$$ik_x E_y = i\omega\mu_0 H_z, \quad (7.29)$$

$$ik_x H_y = \epsilon_{zx}E_x + \epsilon_{zy}E_y + \epsilon_{zz}E_z = \epsilon_{zk}E_k. \quad (7.30)$$

In fact, the latter type can be eliminated from the system by substituting the two equations that are independent of derivative. As a result of the elimination, the above system is reduced to a tangential field which is well known as the Berreman

field

$$\frac{d}{dz} \begin{pmatrix} E_x \\ H_y \\ E_y \\ -H_x \end{pmatrix} = \begin{pmatrix} -\frac{\epsilon_{13}}{\epsilon_{33}} A & c \frac{\epsilon_{33} - A^2}{\epsilon_{33}} & -\frac{\epsilon_{23}}{\epsilon_{33}} A & 0 \\ \epsilon_0 c [\epsilon_{11} - \frac{\epsilon_{13}^2}{\epsilon_{33}}] & -\frac{\epsilon_{13}}{\epsilon_{33}} A & \epsilon_0 c [\epsilon_{12} - \frac{\epsilon_{12}\epsilon_{23}}{\epsilon_{33}}] & 0 \\ 0 & 0 & 0 & c \\ \epsilon_0 c [\epsilon_{12} - \frac{\epsilon_{12}\epsilon_{23}}{\epsilon_{33}}] & -\frac{\epsilon_{23}}{\epsilon_{33}} A & \epsilon_0 c [\epsilon_{22} - \frac{\epsilon_{23}^2}{\epsilon_{33}} - A^2] & 0 \end{pmatrix} \begin{pmatrix} E_x \\ H_y \\ E_y \\ -H_x \end{pmatrix}.$$

By using linear algebra the above system can be written in matrix compact form and the resulting equation is well known in mathematics and optics as the Berreman equation.

$$\frac{d\psi}{dz} = \frac{-ik}{c} M(z)\psi, \quad (7.31)$$

and  $\psi = (E_x, H_y, E_y, -H_x)^T$  is known as the Berreman vector field.

### 7.2.1 Berreman in the presence of a source

The Berreman equation was derived on the basis that the medium is source free. However, in the presence of a source polarization in the medium, the Berreman equation will include an extra term. By adding this extra term, the Berreman equation will take the following form [23]

$$\frac{d\psi}{dz} = \frac{-ik}{c} [M(z)\psi + 4\pi\Omega(z)]. \quad (7.32)$$

The inhomogeneous term that is the extra term in the Berreman equation, will be responsible for the source polarization in the medium. The inhomogeneous term is a vector with dimension  $4 \times 1$  and the components of this vector are given

by [23]

$$\Omega(z) = \begin{pmatrix} -p_z \frac{ck_x}{w\epsilon_{33}} \\ p_x - p_z \frac{\epsilon_{13}}{\epsilon_{33}} \\ 0 \\ p_y - p_z \frac{\epsilon_{23}}{\epsilon_{33}} \end{pmatrix}.$$

### 7.2.2 Solution of Berreman in the presence of a source

The inhomogeneous Berreman equation is solved by first solving the homogeneous equation that is the source free equation. In general, as it will be explained later, the fields at the boundaries are related by a  $4 \times 4$  transfer matrix

$$\psi[z_2] = P(z_1, z_2)\psi[z_1], \quad (7.33)$$

which can be formally defined as [41]

$$P(z_1, z_2) = \exp\left(-i\frac{\omega}{c} \int_{z_1}^{z_2} M(z)dz\right). \quad (7.34)$$

After finding the propagation matrix which connects the fields at the boundaries, the inhomogeneous Berreman wave equation admits the following general solution [23]

$$\psi[z_2] = P(z_1, z_2)\psi[z_1] - 4\pi\frac{i\omega}{c} \int_{z_1}^{z_2} P(z_1, z)\Omega(z)dz, \quad (7.35)$$

where  $P(z_1, z_2)$  is the Green function of the problem [23].

### 7.3 Derivation of a $2 \times 2$ differential equation from Berreman

In a twisted nematic liquid crystal sample, the optical properties of the medium are described by a dielectric tensor which rotates around one axis. For the sake of simplicity, it will be assumed that the director rotates around the  $z$ -axis. As a result of this assumption, the principal axes of the director in this model are fully identified by two angles which are the tilt  $\theta(z)$  and twist  $\phi(z)$  angles. If the director stays in the  $xy$ - plane throughout the sample, the dielectric tensor will have two of its axes normal to the  $z$ -axis and the dielectric tensor is reduced to

$$\varepsilon = \begin{pmatrix} \varepsilon_{11} & \varepsilon_{12} & 0 \\ \varepsilon_{21} & \varepsilon_{22} & 0 \\ 0 & 0 & \varepsilon_{33} \end{pmatrix}.$$

Since the dielectric tensor has some elements off diagonal, the two linearly polarized local modes of the electric field will couple as they propagate inside the birefringence materials. This coupling is caused mainly by the variation in the director orientation. In other words, as the director twists inside the birefringence materials, the orientations of the two local birefringence axes which are parallel and perpendicular to the direction of the director change. According to the formulism [31], [33] and [61], the local modes of the electric field at position  $z + \Delta z$ , see figure 7.1, can be written in terms of the electric field at the position  $z$  as:

$$E_x(z + \Delta z) = [E_x(z) \cos \Delta\Omega + E_y(z) \sin \Delta\Omega] \exp(-iB_x \Delta z), \quad (7.36)$$

$$E_y(z + \Delta z) = [-E_x(z) \sin \Delta\Omega + E_y(z) \cos \Delta\Omega] \exp(-iB_y \Delta z). \quad (7.37)$$

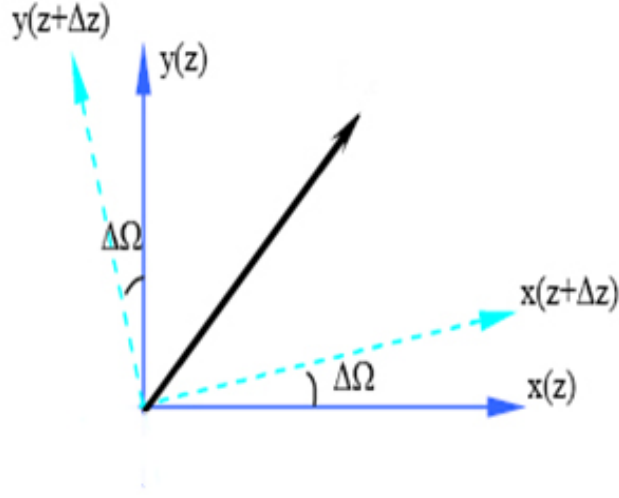


Figure 7.1: This figure illustrates the change in the orientation of the local birefringence axes from the initial input at the position  $z$  to the new position  $z + \Delta z$ .

When dividing both sides of the above equation by  $\Delta z$  and keeping the first order terms as the limit  $\Delta z$  approaches zero, then the coupling mode equations can be expressed as [61]

$$\frac{dE_x}{dz} = -iB_x E_x + \xi(z)E_y, \quad (7.38)$$

$$\frac{dE_y}{dz} = -iB_y E_y - \xi(z)E_x, \quad (7.39)$$

where  $B_x$  and  $B_y$  are the constants of propagation of the light polarized along the birefringence axes, and  $\xi(z)$  is the total twist of the medium. These coupling equations have two plane waves solution and the twist in the medium causes these plane waves to couple i.e interchange their energy as they propagate through the medium. In principle, these equations can be solved by introducing some constraints. For example, when the twist rate is constant through a slice of the medium, then the solution by the Laplace transform method is [31]

$$A_x = \left\{ p \cos\left(\frac{\xi z}{\sqrt{F}}\right) + \sqrt{F}(ipX + q) \sin\left(\frac{\xi z}{\sqrt{F}}\right) \right\} \exp(iB_s), \quad (7.40)$$

$$A_y = \left\{ q \cos\left(\frac{\xi z}{\sqrt{F}}\right) - \sqrt{F}(iqX + p) \sin\left(\frac{\xi z}{\sqrt{F}}\right) \right\} \exp(iB_s), \quad (7.41)$$

where  $B_s = \frac{1}{2}(B_x + B_y)$  and  $B_s = \frac{1}{2}(B_x - B_y)$  and the rest of the parameters can be found in [31].

When the twist is a function of position  $\xi = \xi(z)$ , there is no analytical solution to these coupling equations [31]. Of course, there are some exceptional cases. The first case is when the total twist is zero and the second case is when the propagation constants are the same. In both cases the above equation will be uncoupled and the solution is trivial as it was explained in this thesis.

### 7.3.1 Modes inside the infinitesimal layer

The above coupling modes equations are in fact a reformulation of Maxwell's equations as it can be seen in this section. To analyze the propagation of waves inside a twisted medium, an alternative method can be used, known as normal modes. These modes, which can be obtained by diagonalizing the coupled modes equations, propagate in medium without changing their shapes. The main difference between them is that they travel with different velocities. In order to obtain these modes, Maxwell's equations have to be solved exactly.

For any infinitesimal layer, there are four propagation modes in which two of them travel forward and the other two travel backward [28]. These traveling modes can be obtained by solving the following eigenvalue Berreman equation

$$MX = \alpha X. \quad (7.42)$$

Since the Berreman equation for a twisted nematic liquid crystal sample has special form, it is possible to reduce it from  $4 \times 4$  to  $2 \times 2$  without losing these

modes. This can be done as follows:

$$m_{12}H_y = \alpha E_x, \quad (7.43)$$

$$-m_{34}H_x = \alpha E_y, \quad (7.44)$$

$$m_{21}E_x + m_{23}E_y = \alpha H_y, \quad (7.45)$$

$$m_{41}E_x + m_{43}E_y = -\alpha H_x. \quad (7.46)$$

These equations can be combined together to eliminate the magnetic field components. After eliminating the magnetic field components, the resulting system is

$$m_{12}m_{21}E_x + m_{12}m_{23}E_y = \alpha^2 E_x, \quad (7.47)$$

$$m_{34}m_{41}E_x + m_{34}m_{43}E_y = \alpha^2 E_y. \quad (7.48)$$

This system can be written as

$$S(z)\mathbf{E} = \alpha^2\mathbf{E}. \quad (7.49)$$

A direct calculation shows that the elements of the matrix  $S(z)$  are

$$s_{11}(\phi, m) = \mu_o\epsilon_o c^2 \epsilon_{xx} \left(1 - \frac{m^2}{\epsilon_{zz}}\right) = \epsilon_{xx} \left(1 - \frac{m^2}{\epsilon_{zz}}\right), \quad (7.50)$$

$$s_{12}(\phi, m) = \mu_o\epsilon_o c^2 \epsilon_{xy} \left(1 - \frac{m^2}{\epsilon_{zz}}\right) = \epsilon_{xy} \left(1 - \frac{m^2}{\epsilon_{zz}}\right), \quad (7.51)$$

$$s_{21}(\phi, m) = \mu_o\epsilon_o c^2 \epsilon_{yx} = \epsilon_{xy}, \quad (7.52)$$

$$s_{22}(\phi, m) = \mu_o\epsilon_o c^2 (\epsilon_{yy} - m^2) = (\epsilon_{yy} - m^2). \quad (7.53)$$

For uniaxial anisotropic sample, as it is known, there are only two eigenvalues

which are along the principal axes of the director. As  $S(z)$  is symmetric and positive definite, it can always be written as

$$S(z) = \begin{pmatrix} s_{11} & s_{12} \\ s_{21} & s_{22} \end{pmatrix} = \begin{pmatrix} v_{11} & v_{12} \\ v_{21} & v_{22} \end{pmatrix} \begin{pmatrix} \alpha_1^2 & 0 \\ 0 & \alpha_2^2 \end{pmatrix} \begin{pmatrix} v_{11} & v_{12} \\ v_{21} & v_{22} \end{pmatrix}^{-1}.$$

Here,  $v_{ij}$  are the elements of the dynamic matrix that follows the rotation of the director inside the sample. By taking the square root of the eigenvalues, we obtain the new matrix

$$H(z) = \begin{pmatrix} v_{11} & v_{12} \\ v_{21} & v_{22} \end{pmatrix} \begin{pmatrix} \alpha_1 & 0 \\ 0 & \alpha_2 \end{pmatrix} \begin{pmatrix} v_{11} & v_{12} \\ v_{21} & v_{22} \end{pmatrix}^{-1},$$

and the new eigen-system with the above matrix is

$$H(z)\mathbf{E} = \alpha\mathbf{E}. \quad (7.54)$$

### 7.3.2 Elements of $2 \times 2$ system

The elements of the matrix  $H(z)$  can be obtained by performing the above multiplication

$$h_{11}(\phi, m) = \alpha_1 + \Delta\alpha \cos^2 \phi, \quad (7.55)$$

$$h_{12}(\phi, m) = h_{21}(\phi, m) = \Delta\alpha \cos \phi \sin \phi, \quad (7.56)$$

$$h_{22}(\phi, m) = \alpha_2 + \Delta\alpha \sin^2 \phi, \quad (7.57)$$

where  $\Delta\alpha = \alpha_1 - \alpha_2$ . In the case of normal incidence the above elements will reduce to

$$h_{11}(\phi, 0) = n_o + \Delta n \cos^2 \phi, \quad (7.58)$$

$$h_{12}(\phi, 0) = h_{21}(\phi, m) = \Delta n \cos \phi \sin \phi, \quad (7.59)$$

$$h_{22}(\phi, 0) = n_o + \Delta n \sin^2 \phi. \quad (7.60)$$

where  $\Delta n = n_e - n_o$  is the real birefringence of the material.

Surprisingly, this system is equivalent in some sense to the Berreman eigenvalue equation, since it gives exactly the same local traveling modes in any infinitesimal layer of the medium. In fact, the differential equation that can be used instead of Berreman's equation to study the emerging polarization is

$$\frac{dE}{dz} = \frac{-i\omega}{c} H(z) E. \quad (7.61)$$

The electric field vector is called the Jones vector of the propagating light, and the solution of this differential equation as we will see later is a transfer matrix, which relates the electric fields at the input to the output ones.

In practice, there are two kinds of media that affect the plane of polarization of a polarized wave. In the first one, the medium will keep the plane of polarization fixed as long as the waves propagate through the medium. As a result of that, the transfer matrix will either maintain the phase shift between the two orthogonal components of the electric fields and the medium will not change the type of polarization, and this medium is called isotropic medium, Or it will introduce a phase shift between the two orthogonal components as they propagate inside the medium, and eventually will change the type of polarization. This medium is called anisotropic medium. The other kind continuously rotates the plane of polarization of the polarized wave, as the waves propagate inside the medium. In this case, the medium will introduce a phase shift between the orthogonal components and a rotation of the plane of polarization through some angle.

## 7.4 Modes of propagation

The solution of the  $2 \times 2$  differential equation which has been derived from the Maxwell equations for the case of normal incident, is exactly the same solution introduced by Jones. As it is known that his method relates the electric field components at the boundaries and involve no derivatives

$$\mathbf{E}(out) = J(z)\mathbf{E}(i) = \begin{pmatrix} j_{11} & j_{12} \\ j_{21} & j_{22} \end{pmatrix} \mathbf{E}(i).$$

According to Berreman's paper [6], if  $H(z)$  is independent of  $z$  for a short interval, then there are modes propagating in the medium and these modes can be defined in terms of the eigenvalues equation

$$E_j(z) = \exp(-i\frac{\omega}{c}\lambda_j z)E_j(z_0),$$

where  $\lambda_j$  are the eigenvalues of the  $2 \times 2$  matrix  $H(z)$  which appears in the differential equation,  $E_j$  are the eigen-direction multiplied by amplitudes of the electric fields components in the  $x$ -direction and  $y$ -direction respectively.

### 7.4.1 Modes of propagation when $H(x)$ is constant

Fortunately, for isotropic medium or even anisotropic medium with a fixed transmission axis of anisotropy, these modes can be obtained exactly, since the  $2 \times 2$  matrix is constant in both cases. It is possible to plot these modes in one graph by using the Matlab software. However, it should be clear that these modes are perpendicular to each other inside the medium and the direction of propagation is the eigen-direction. Figure 7.2 shows these modes inside isotropic medium with

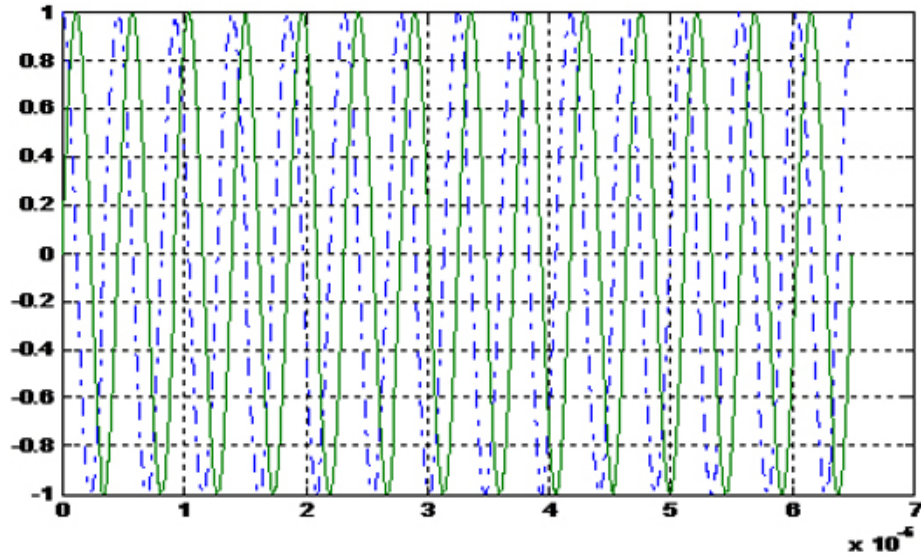


Figure 7.2: This figure shows the modes that propagate in isotropic medium with a circular polarization input. These modes propagate in the eigen-direction that is along the molecular axes.

amplitudes equal to one. By paying a closer look to the figure 7.2 , it can be noticed that these modes travel with the same velocity, and as a result of that, they retain the input polarization state.

On the other hand, this is not the case for anisotropic medium. As it can be seen from the figure 7.3. For anisotropic medium with axis of anisotropy along the  $x$ -axis, these modes travel with two different velocities. As a consequence of that, the input polarization state is changing as it progresses through the medium.

#### 7.4.2 Modes of propagation when $H(z)$ is a function of $z$

When  $H(z)$  is not a constant, then the exact propagation matrix which connects the boundaries maybe hard to obtain. In such situations, the medium is divided into intervals of length  $h$ , in which the difference between  $H(z+h)$  and  $H(z)$  is negligible [14]. As a consequence of this,  $H(z)$  will be constant and local modes can be obtained as we explained in the previous section. The overall modes for the

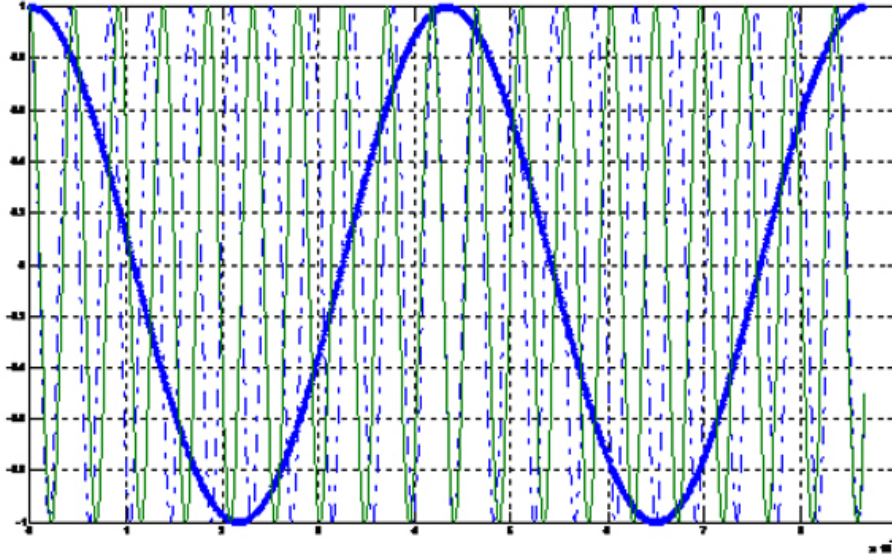


Figure 7.3: This figure shows the local modes for a sample with a fixed axis of anisotropy.

entire medium can be obtained by performing the correct order of multiplications

$$\begin{aligned}
 P[z_1, z_2] &= F(z_1 + (m-1)h, z_2)F(z_1 + (m-2)h, z_1 + (m-1)h) \\
 &+ \dots F(z_1 + h, z_1 + 2h)F(z_1, z_1 + h).
 \end{aligned}$$

It should be clear that the local propagation matrix can be obtained by integrating the  $2 \times 2$  differential equation directly and the solution is

$$\begin{aligned}
 \psi[z + mh] &= F[h]\psi[z + (m-1)h] \\
 &= \exp\left(\frac{i\omega h}{c}M_{z+mh}\right)\psi[z + (m-1)h] \\
 &= \left[I + \frac{i\omega h}{c}\frac{M_{z+mh}}{1!} + \left(\frac{i\omega h}{c}\right)^2\frac{M_{z+mh}^2}{2!} + \dots\right]\psi[z + (m-1)h]
 \end{aligned}$$

If a closed form of the matrix  $H(z)$  does not exist, the numerical analysis tells us that the series provides a sufficient accuracy, when the first few terms are considered, since the  $\frac{\omega h}{c}$  is small enough.

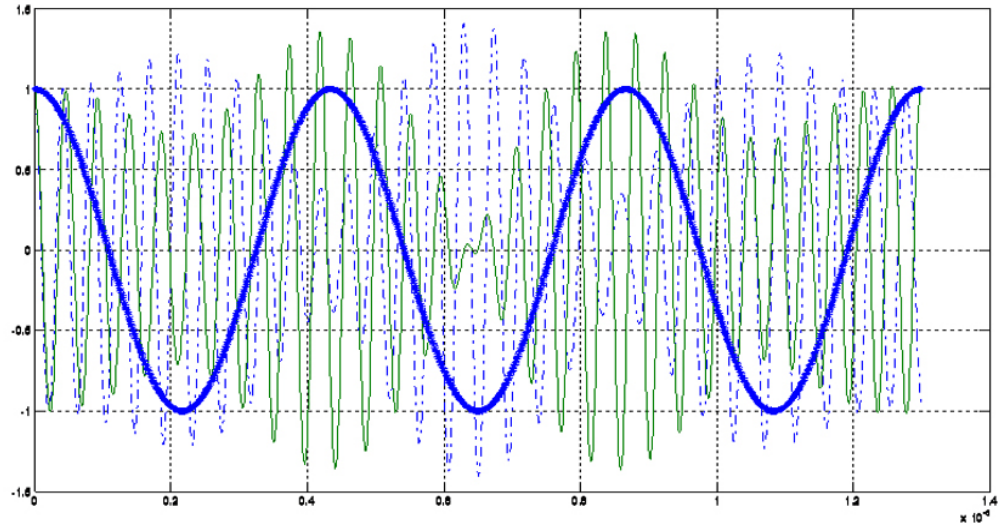


Figure 7.4: This figure shows the local modes for a sample with a twisted axis of anisotropy.

In short, it is clear from the above discussion that the modes which propagate in the medium, depend entirely on the propagation matrix. In other words, when the  $H(z)$  is constant, then the exact transfer matrix obtainable and when the  $H(z)$  is a function of  $z$  then the modes can be approximated. In the coming section, our technique will allow us to obtain the exact propagating modes for twisted axis of anisotropy in which  $H(z)$  is a continuous function of  $z$ . The basic idea behind the technique is to travel within the frame of anisotropy, which can be called anisotropy frame of reference. Figure 7.4 shows the modes that travel in a twisted medium which will be obtained in the coming sections.

## 7.5 Propagation matrix

Equation (7.61) is analogous to the time independent Schrödinger equation. In other words, the solution of this first order differential equation is determined completely for any location  $z$  inside the sample once it is specified at the input  $z_0$  [9]. The solution of the system can be written in terms of a propagating matrix, that relates the input components of the electric fields to the emerging fields as [9]

$$E(z) = P(z, z_0)E(z_0), \quad (7.62)$$

with initial condition

$$P(z_0, z_0) = \begin{pmatrix} 1 & 0 \\ 0 & 1 \end{pmatrix}.$$

If this solution, which subject to the initial condition, is substituted into the differential equation, the propagation matrix  $P(z, z_0)$  satisfies exactly the same differential equation

$$\frac{dP(z, z_0)}{dz} = \frac{-i\omega}{c}H(z)P(z, z_0). \quad (7.63)$$

In addition to that, this differential equation with above initial condition can be replaced by the integral equation

$$P(z, z_0) = I - \frac{i\omega}{c} \int_{z_0}^z H(x)P(x, z_0)dx. \quad (7.64)$$

A formal solution of this integral equation can be obtained by iteratively replacing the transfer matrix under the integral sign by its value from the left hand side.

The right hand side will eventually lead to the Born-Neumann series [15]

$$P(z, z_0) = I + \left(\frac{-i\omega}{c}\right) \int_{z_0}^z H(x_1) dx_1 + \left(\frac{-i\omega}{c}\right)^2 \int_{z_0}^z H(x_1) dx_1 \int_{z_0}^{x_1} H(x_2) dx_2 + \dots \quad (7.65)$$

Later at the end of this thesis, we will use the Calderón [11] argument to discuss the convergence of the Born-Neumann series.

## 7.6 Application to isotropic medium

For isotropic medium, there will be only one refractive index and the matrix  $H(z)$  will be a diagonal matrix

$$H(z) = \begin{pmatrix} \alpha & 0 \\ 0 & \alpha \end{pmatrix} = \alpha I.$$

The elements on the main diagonal depend on the incident angle. The analytical solution can be obtained easily by solving equation 7.61. This solution agrees with the Berreman solution. For normal incident, for example, the eigenvalues equal exactly to the refractive index  $n_o$  of the medium and the solution is

$$\mathbf{E}(z) = (E_x, E_y)^T = \left(\exp\left(\frac{-i\omega}{c}n_o z\right), \exp\left(\frac{-i\omega}{c}n_o z\right)\right)^T. \quad (7.66)$$

The propagation matrix that relates the incident electric field to the emerging electric field is

$$\mathbf{E}(out) = P(z)\mathbf{E}(i) = \begin{pmatrix} \exp\left(\frac{-i\omega}{c}n_o z\right) & 0 \\ 0 & \exp\left(\frac{-i\omega}{c}n_o z\right) \end{pmatrix} \mathbf{E}(i).$$

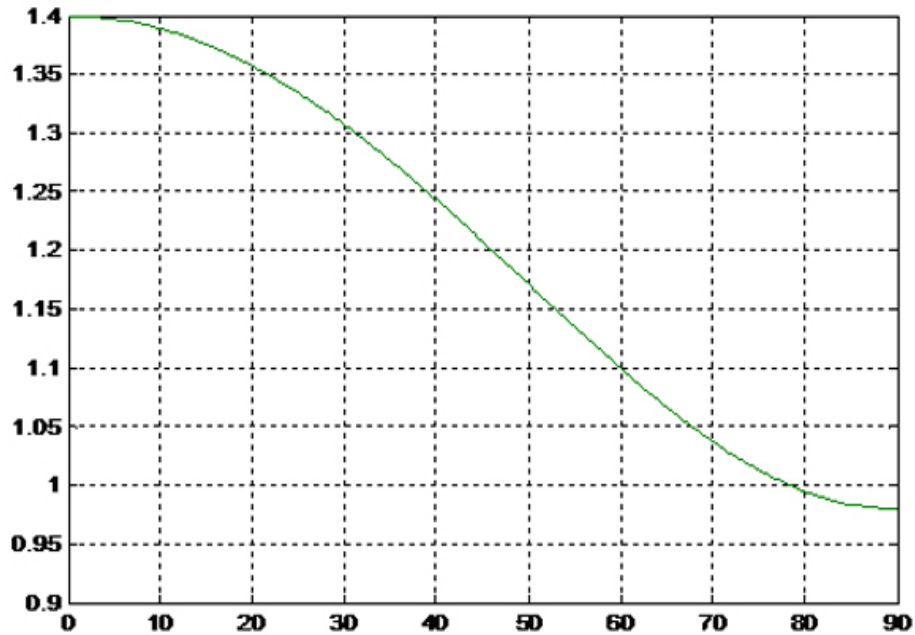


Figure 7.5: Dependence of the eigenvalue on the incident angle of a sample with refractive index  $n_o = 1.400$ .

It should be clear that the propagation matrix  $P(z)$  is exactly the same as the Jones propagation matrix for normal incident. As it can be seen, the propagation matrix will maintain the plane of polarization, and will not introduce any shift in the phase between the orthogonal components as they propagate inside the medium. Furthermore, the ratio of the electric field components

$$R = \frac{\exp\left(\frac{-i\omega}{c}n_o z\right)}{\exp\left(\frac{-i\omega}{c}n_o z\right)} = 1. \quad (7.67)$$

at any location is constant and this is exactly the same as the Rytov [43] law for isotropic medium. Figure 7.5 shows the dependence of the eigenvalue on the incident angle of a sample with refractive index  $n_o = 1.400$ . In fact, the propagation matrix which can be easily worked out for any incident angle  $\theta_i$  is

given by

$$H(z) = \begin{pmatrix} p_{11} & 0 \\ 0 & p_{22} \end{pmatrix} = \alpha I,$$

where

$$p_{11} = p_{22} = \exp\left(\frac{-i\omega}{c}[\sqrt{n_0^2 - m^2}]z\right). \quad (7.68)$$

As we mentioned before, the isotropic medium has the ability to maintain the phase shift between the waves, that propagate inside it, without any delay. This concept will be illustrated in the following two cases.

### 7.6.1 Two waves with phase shift zero

Figure 7.6 shows two plane waves which propagate according to the above solution inside isotropic medium. These waves have the same amplitude with phase shift zero between them and they, in fact, propagate perpendicular to each other which can be seen easily in figure 7.7. Since there is no change in the phase between them as long as they propagate inside the medium, they leave the medium with exactly the same incoming polarization which is the linear polarization in this case. Figures 7.7 and 7.8 illustrate the type of polarization at any location inside the medium

### 7.6.2 Two waves with phase shift ninety

In this example the waves begin to propagate inside the medium with phase shift ninety. Figure 7.9 shows again two plane waves inside isotropic medium with phase shift 90 degrees between them. Figure 7.10 illustrates how these waves propagate inside the medium. Since the phase between them stays fixed as long as they propagate inside the medium, they leave the medium with the same

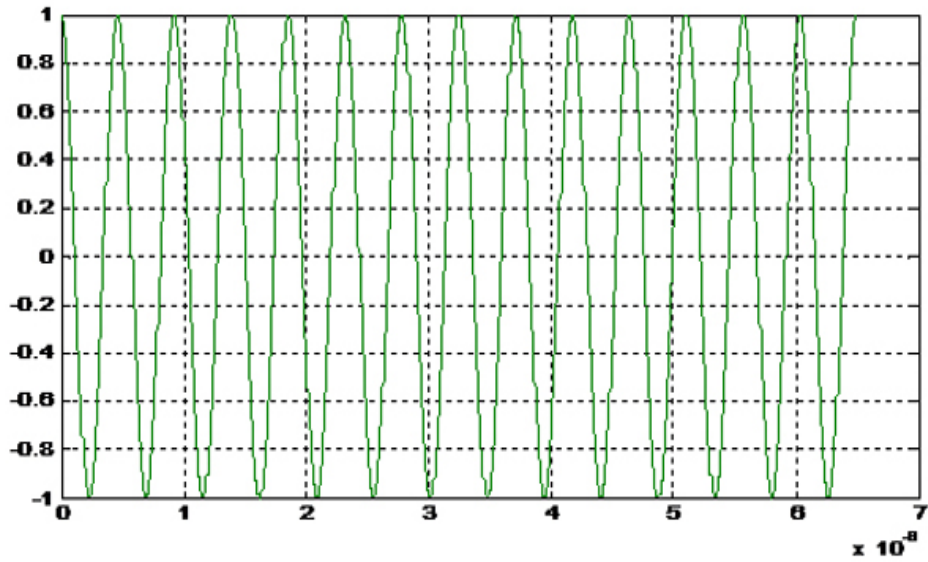


Figure 7.6: The propagation of the plan waves inside isotropic medium with phase shift zero according the above solution.

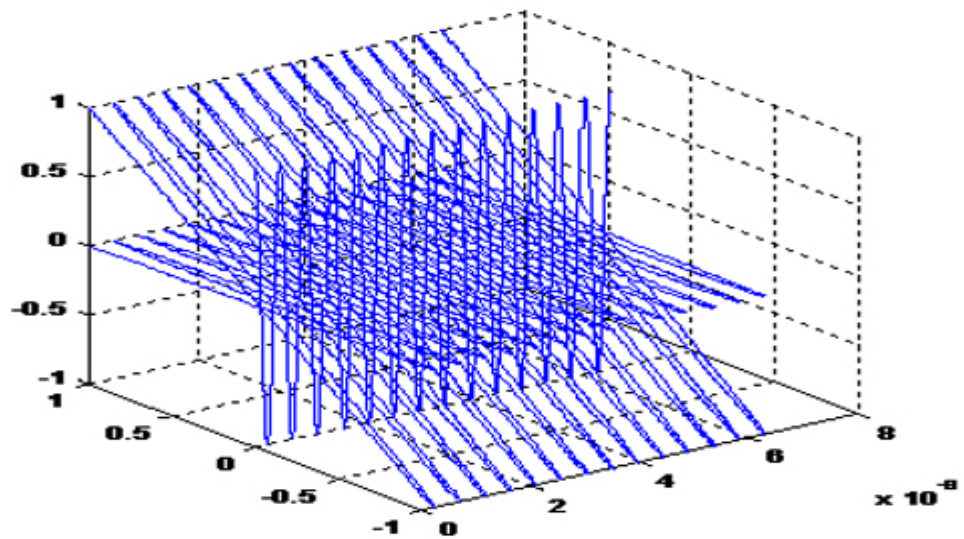


Figure 7.7: The directions of propagation of the waves inside the medium.

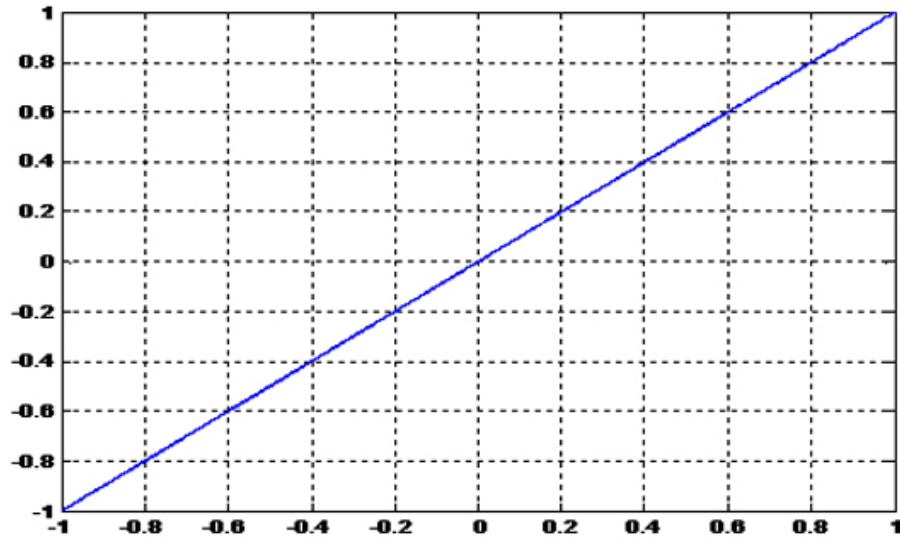


Figure 7.8: The resulting type of polarization at any location inside the medium with input phase shift zero.

polarization which is a circular polarization, as illustrated in figures 7.10 and 7.11.

## 7.7 Application to a non-twisted medium

Again in this case, the non-diagonal elements are zeros and the analytical solution can be obtained by solving equation (7.61). For simplicity, it will be assumed that the axis of anisotropic is along the  $x$ -axis. As a consequence, the matrix  $H(z)$  can be written as

$$H(z) = \begin{pmatrix} \sqrt{\frac{\epsilon_{xx}}{\epsilon_{zz}}} \sqrt{\epsilon_{zz} - m^2} & 0 \\ 0 & \sqrt{\epsilon_{yy} - m^2} \end{pmatrix}.$$

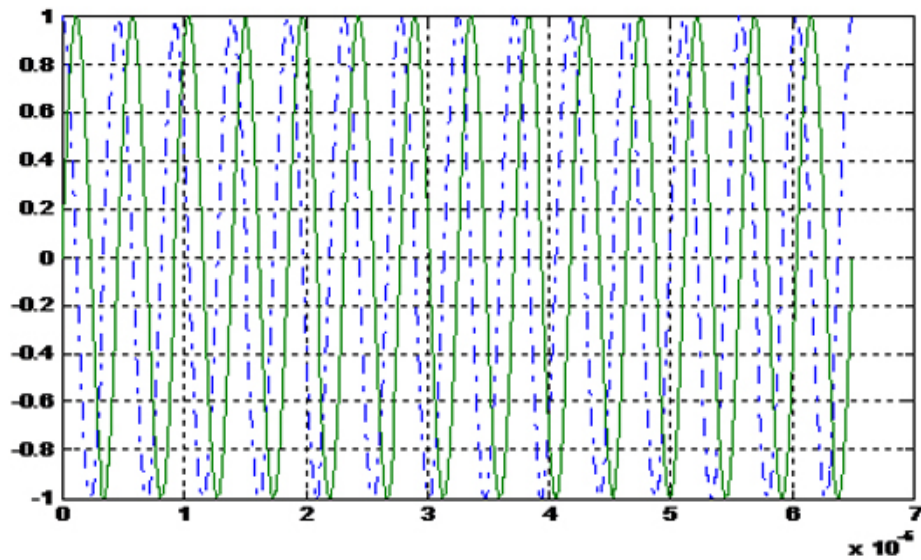


Figure 7.9: The propagation of the plan waves inside the isotropic medium with phase shift ninety.

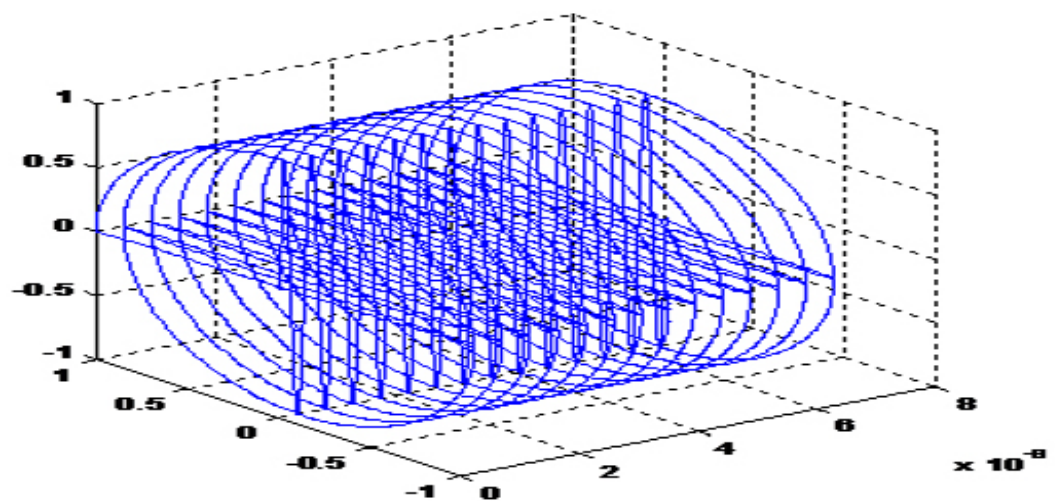


Figure 7.10: The directions of propagation of the waves inside the medium with input phase shift ninety.

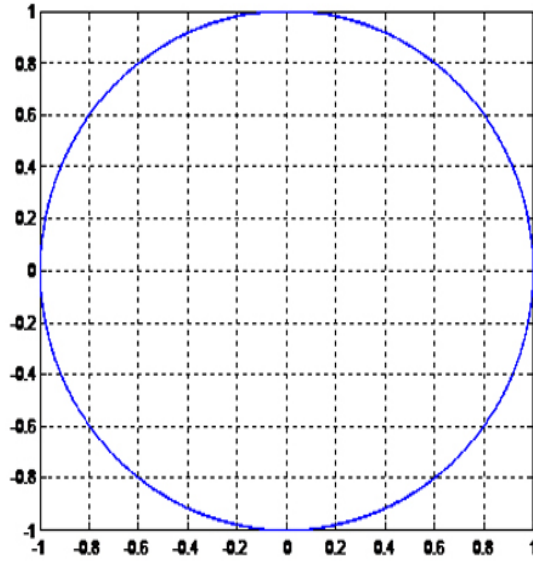


Figure 7.11: The resulting type of polarization at any location inside the medium with input phase shift ninety.

For normal incidence ( $m$ ) equals to zero and the matrix  $H(z)$  will take the following form

$$H(z) = \begin{pmatrix} \sqrt{\varepsilon_{xx}} & 0 \\ 0 & \sqrt{\varepsilon_{yy}} \end{pmatrix} = \begin{pmatrix} n_e & 0 \\ 0 & n_o \end{pmatrix},$$

and the analytic solution for this case is

$$\mathbf{E}(z) = (E_x, E_y)^T = \left( \exp\left(\frac{-i\omega}{c}n_e z\right), \exp\left(\frac{-i\omega}{c}n_o z\right) \right)^T. \quad (7.69)$$

The associated propagation matrix for uniaxial anisotropic medium with director along the  $x$ -axis is

$$\mathbf{E}(z) = P(z)\mathbf{E}(i) = \begin{pmatrix} \exp\left(\frac{-i\omega}{c}n_e z\right) & 0 \\ 0 & \exp\left(\frac{-i\omega}{c}n_o z\right) \end{pmatrix} \mathbf{E}(i),$$

where  $\mathbf{E}(i)$  is the input polarization and  $\mathbf{E}(z)$  is the polarization at the location  $z$ .

### 7.7.1 Discussion

Our calculations showed that the phase difference between the waves as they propagate inside the sample is given by

$$R(z) = \frac{\exp\left(\frac{-i\omega}{c}n_e z + \theta_i\right)}{\exp\left(\frac{-i\omega}{c}n_o z\right)} = \exp\left(\frac{-i\omega}{c}\Delta n z + \theta_i\right), \quad (7.70)$$

where  $\Delta n$  and  $\theta_i$  are the difference between the refractive indices of the medium and the initial phase difference between the waves respectively. Figure 7.12 illustrates how the ratio function  $R(z)$  works. The ones indicate that the waves are in phase, the zeros indicate that the waves are out of phase by 90 degrees and the minimums, which are the minus ones indicate that the waves are out of phase by 180 degrees. In fact, the linear polarization is obtained at the minimums and the maximums of the ratio function. The circular polarization is achieved at the zeros and the elliptical polarization is obtained otherwise. The accumulated relative phase difference between the waves is given by

$$\text{Relative phase} = \frac{\omega}{c}\Delta n z. \quad (7.71)$$

Figure 7.13 and figure 7.14 show the behavior of the eigenvalues with incident angle. As the incident angle increases, the eigenvalues decrease and the difference between them is getting closer. In the case of a positive birefringence, the difference between the eigenvalues is a decreasing function as illustrated in figure 7.15. Figure 7.16 shows that the difference between the eigenvalues is an increasing function for the case of a negative birefringence.

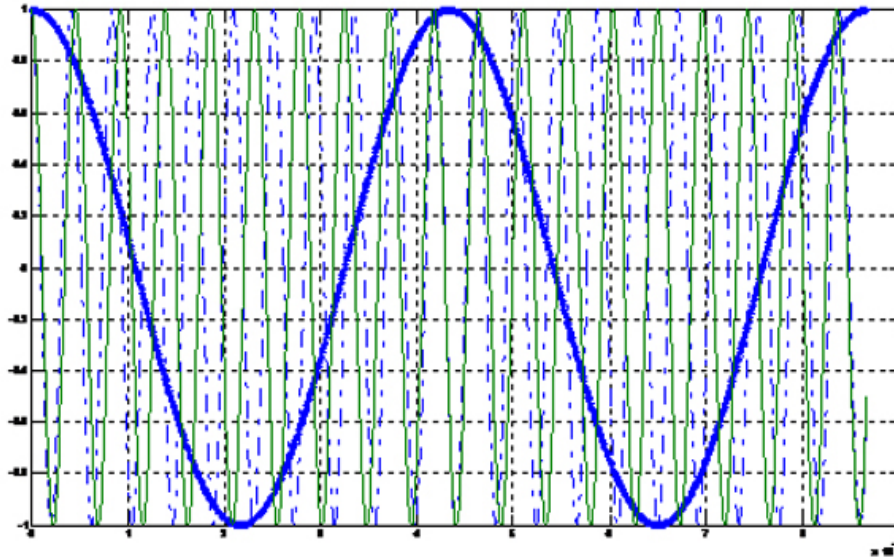


Figure 7.12: Illustration of the polarization in terms of the ratio of electric field components inside a medium with a fixed transmission axis of anisotropy.

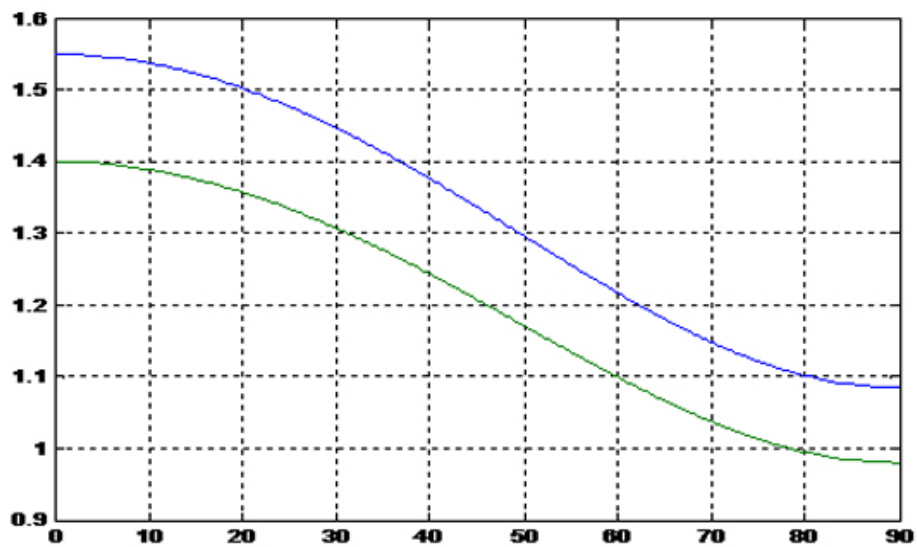


Figure 7.13: This figure shows the behavior of the eigenvalues with incident angle for a positive birefringence.

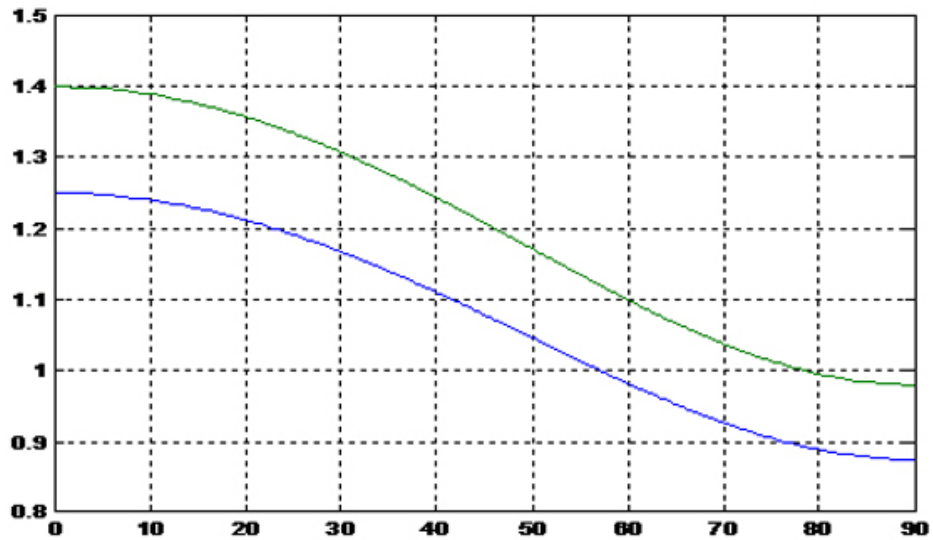


Figure 7.14: This figure shows the behavior of the eigenvalues with incident angle for a negative birefringence.

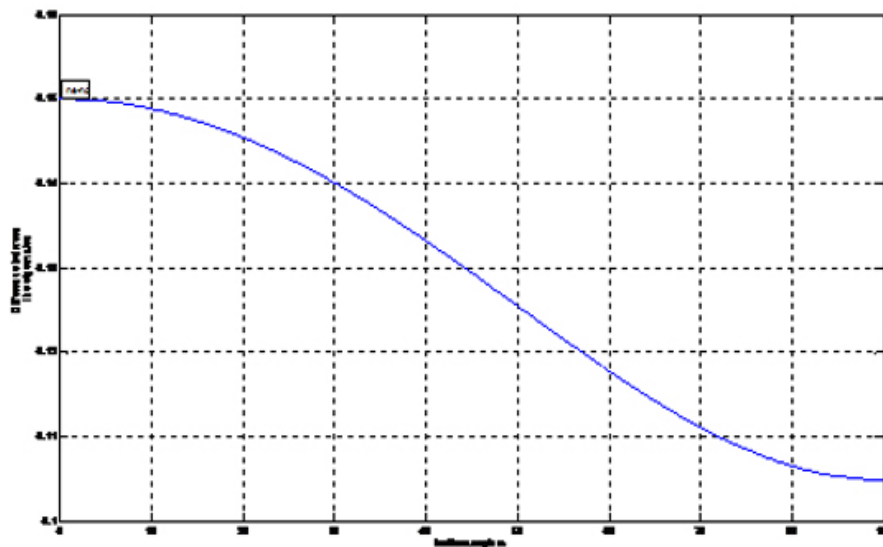


Figure 7.15: This figure shows the difference between the eigenvalues as the incident angle increases for a positive birefringence.

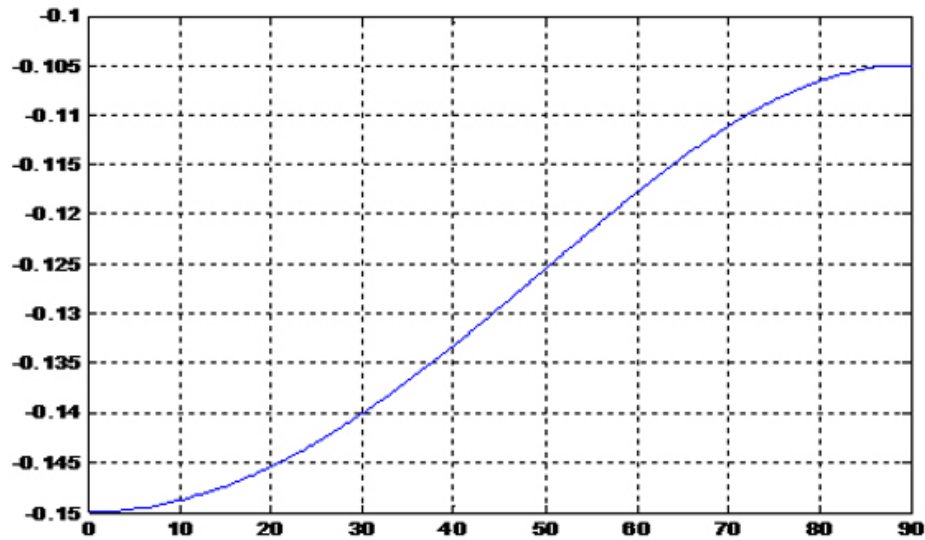


Figure 7.16: This figure shows the difference between the eigenvalues as the incident angle increases for a negative birefringence.

### 7.7.2 linear polarization with phase shift zero

To illustrate the propagation of the solution inside anisotropic medium, we will discuss two different input polarizations. First a linear polarization with phase shift zero between the input waves will be considered in some detail. Figure 7.17 shows that the waves started with a phase shift zero between them, and as they propagate inside the medium the phase shift between them accumulate. The length of the sample has been chosen such that the wave which propagates along the fast axis will be ahead by one period and a half. Figure 7.17 shows that the wave entered the medium with linear polarization  $+45$  degrees and it emerged from the medium with linear polarization  $-45$  degrees. The state of polarization at any location inside the medium can be easily seen from figures 7.18 and 7.19.

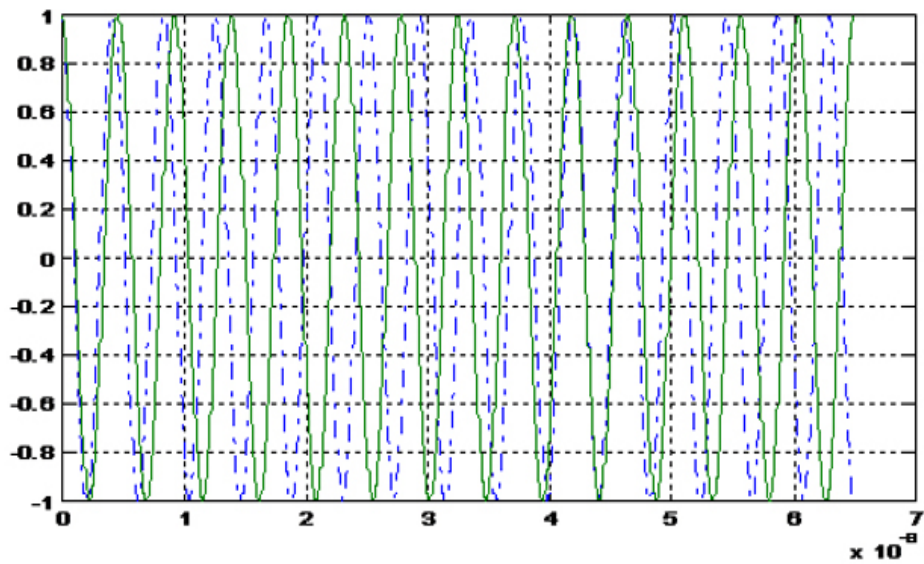


Figure 7.17: This figure shows the propagation of the wave inside anisotropic medium with a fixed transmission axis of anisotropy and a linear polarization input.

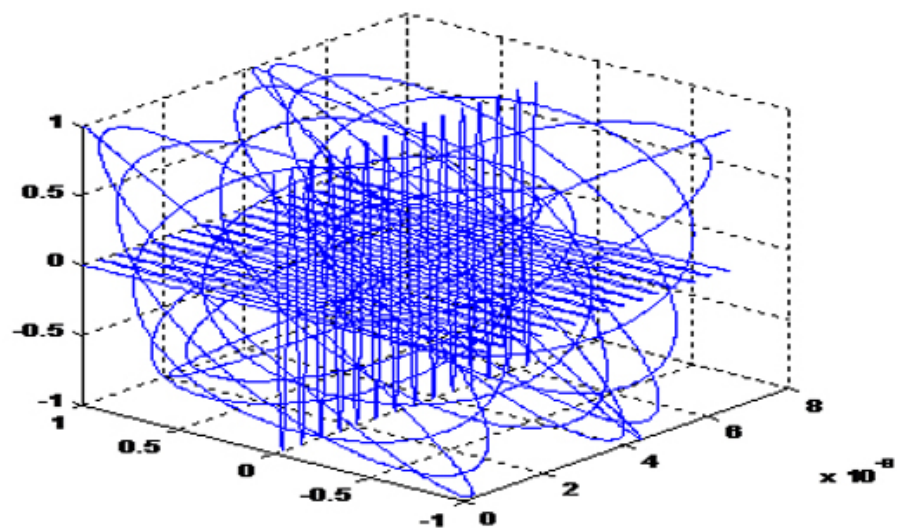


Figure 7.18: This figure illustrates the state of polarization at any location inside the medium together with the orthogonal waves.

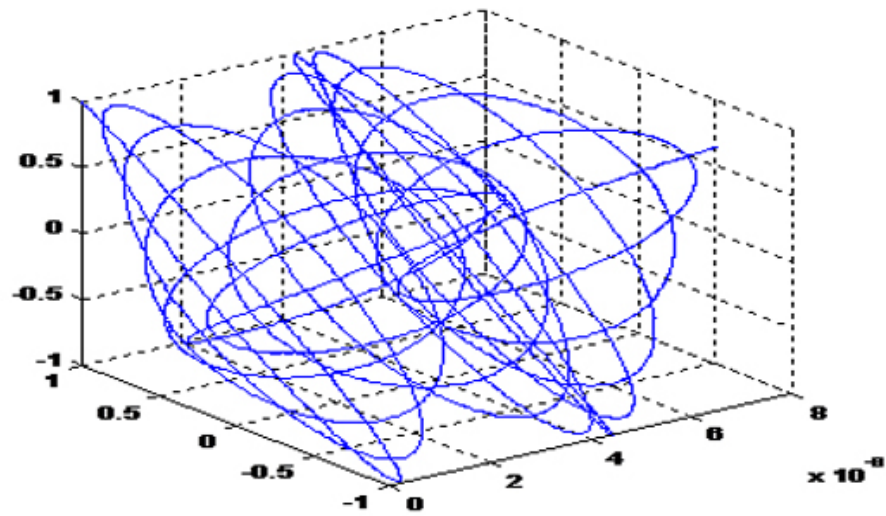


Figure 7.19: The state of polarization at any location inside the medium.

### 7.7.3 a circular polarization

On the Second example, we consider a circular polarization input. Figure 7.20 shows that the waves started with a phase shift ninety between them, and as they propagate inside the medium the phase shift between them accumulate. Again the length of the sample, has been chosen such that the wave which propagates along the fast axis will be ahead by one period and a half. Figure 7.20 shows that the wave entered the medium with a circular polarization and it emerged from the medium with a circular polarization. The state of polarization at any location inside the medium is changing, and can be deduced from figures 7.21 and 7.22.

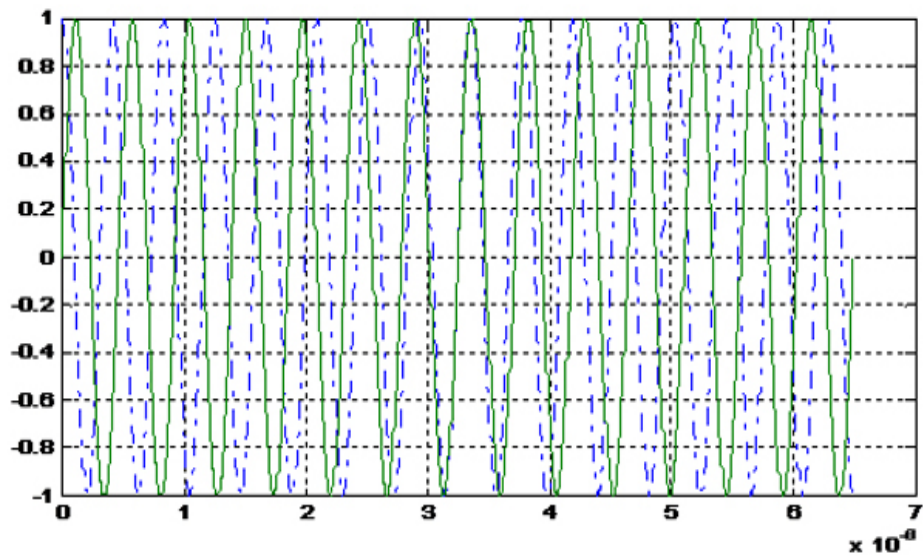


Figure 7.20: This figure shows the propagation of the wave inside anisotropic medium with a fixed transmission axis of anisotropy and a circular polarization input.

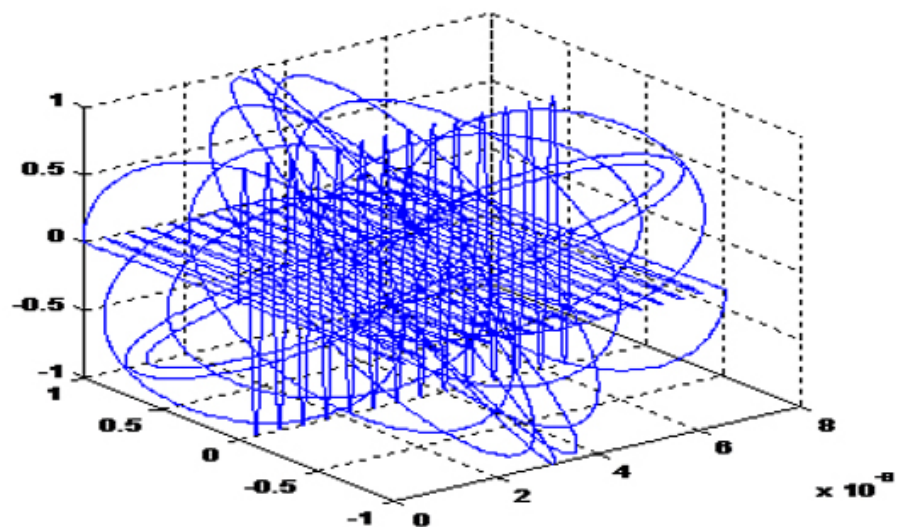


Figure 7.21: This figure illustrates the state of polarization at any location inside the medium together with the orthogonal waves.

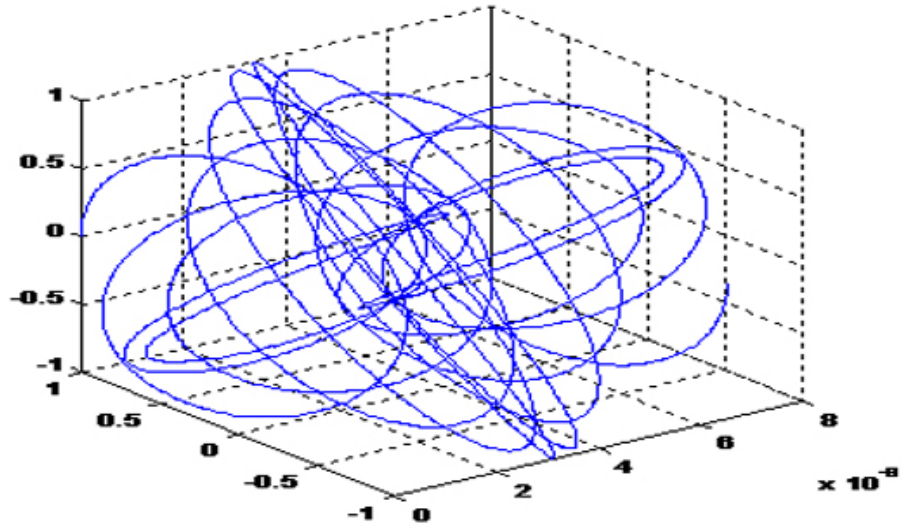


Figure 7.22: The state of polarization at any location inside the medium.

## 7.8 Application to a medium with a twisted transmission axis

In this section, we will introduce the main result of this thesis. First, the solution of equation (7.61) will be addressed for the case of normal incidence where the elements of the matrix are given by equations (7.58), (7.59) and (7.60). Then, the general case for oblique incident will be addressed in some detail.

### 7.8.1 Normal incident

In the case of normal incidence, the differential equation which is equivalent to the Maxwell equations can be rewritten as

$$\frac{d}{dz} \begin{pmatrix} E_x \\ E_y \end{pmatrix} + i \frac{\omega}{c} n_o \begin{pmatrix} E_x \\ E_y \end{pmatrix} = -i \frac{\omega}{c} \Delta n \begin{pmatrix} a^2 & ab \\ ab & b^2 \end{pmatrix} \begin{pmatrix} E_x \\ E_y \end{pmatrix}, \quad (7.72)$$

where  $a = \cos(\phi(z))$  and  $b = \sin(\phi(z))$ . Also, a second order differential equation, which is equivalent to this first order can be derived from the Berreman equation by eliminating the magnetic field

$$\frac{d^2}{dz^2} \begin{pmatrix} E_x \\ E_y \end{pmatrix} + \left[\frac{\omega}{c} n_o\right]^2 \begin{pmatrix} E_x \\ E_y \end{pmatrix} = -\left[\frac{\omega}{c}\right]^2 \Delta n \begin{pmatrix} a^2 & ab \\ ab & b^2 \end{pmatrix} \begin{pmatrix} E_x \\ E_y \end{pmatrix}. \quad (7.73)$$

This equation can be rewritten as

$$\frac{d^2 \mathbf{E}}{dz^2} + \lambda^2 \mathbf{E} = \mathbf{V}(z) \mathbf{E}, \quad (7.74)$$

where  $V(z)$  is called the potential. Both of these equations are equivalent and they have the same solution. Equation (7.74) is known as the Schrödinger equation in Quantum Mechanics and it can be solved only for special cases where the potential decay as  $z$  goes to infinity [50]. although our potential does not decay, but we will manage to solve the Schrödinger equation for these classes of potential as we will see later. Experiments showed that the components of the electric fields follow the twist of the director inside the sample. In order to solve the first order differential equation, we have to transform the differential equation into a frame that continuously rotates with rotation of the director. This can be done by rearranging equation (7.74)

$$\frac{d}{dz} \begin{pmatrix} E_x \\ E_y \end{pmatrix} = -i \frac{\omega}{c} \begin{pmatrix} n_o + \Delta n a^2 & \Delta n ab \\ \Delta n ab & n_o + \Delta n b^2 \end{pmatrix} \begin{pmatrix} E_x \\ E_y \end{pmatrix}, \quad (7.75)$$

$$\frac{d}{dz} \begin{pmatrix} E_x \\ E_y \end{pmatrix} = -i \frac{\omega}{c} \begin{pmatrix} a & -b \\ b & a \end{pmatrix} \begin{pmatrix} n_e & 0 \\ 0 & n_o \end{pmatrix} \begin{pmatrix} a & b \\ -b & a \end{pmatrix} \begin{pmatrix} E_x \\ E_y \end{pmatrix}. \quad (7.76)$$

By multiplying both sides, by the inverse of the first matrix in the left we obtain the following equation

$$\begin{pmatrix} a & b \\ -b & a \end{pmatrix} \frac{d}{dz} \begin{pmatrix} E_x \\ E_y \end{pmatrix} = -i \frac{\omega}{c} \begin{pmatrix} n_e & 0 \\ 0 & n_0 \end{pmatrix} \begin{pmatrix} a & b \\ -b & a \end{pmatrix} \begin{pmatrix} E_x \\ E_y \end{pmatrix}. \quad (7.77)$$

In this rotational frame, the differential equation can be written as

$$\frac{d}{dz} \begin{pmatrix} E_{Rx} \\ E_{Ry} \end{pmatrix} = -i \frac{\omega}{c} \begin{pmatrix} n_e & 0 \\ 0 & n_0 \end{pmatrix} \begin{pmatrix} E_{Rx} \\ E_{Ry} \end{pmatrix}. \quad (7.78)$$

This equation, which is in continuous rotational frame, is equivalent to the case of a non-twisted anisotropic case, where the fast axis of the anisotropy is along the  $x$ -axis. The solution has been found in the previous section, and the associated Jones matrix is

$$\begin{pmatrix} E_{Rx} \\ E_{Ry} \end{pmatrix} = P_R(z) \begin{pmatrix} E_x \\ E_y \end{pmatrix}_i = \begin{pmatrix} \exp(-i \frac{\omega}{c} n_e z) & 0 \\ 0 & \exp(-i \frac{\omega}{c} n_0 z) \end{pmatrix} \begin{pmatrix} E_x \\ E_y \end{pmatrix}_i. \quad (7.79)$$

Now, in order to find the solution in the original frame, we have to transform the solution back  $E_{R_j} \rightarrow E_j$

$$\begin{pmatrix} E_x \\ E_y \end{pmatrix} = \begin{pmatrix} \cos(\phi) & -\sin(\phi) \\ \sin(\phi) & \cos(\phi) \end{pmatrix} \begin{pmatrix} \exp(-i \frac{\omega}{c} n_e z) & 0 \\ 0 & \exp(-i \frac{\omega}{c} n_0 z) \end{pmatrix} \begin{pmatrix} E_x \\ E_y \end{pmatrix}_i, \quad (7.80)$$

which can be simplified to

$$\begin{pmatrix} E_x \\ E_y \end{pmatrix} = \begin{pmatrix} \cos(\phi)A & -\sin(\phi)B \\ \sin(\phi)A & \cos(\phi)B \end{pmatrix} \begin{pmatrix} E_x \\ E_y \end{pmatrix}_i, \quad (7.81)$$

where  $A = \exp(-i\frac{\omega}{c}n_e z)$  and  $B = \exp(-i\frac{\omega}{c}n_o z)$ . Figure 7.23 shows the solution for the differential equation inside the twisted nematic liquid crystal. As we mentioned earlier, the solid blue curve gives us the state of polarization inside the sample at any location. The parameters used to obtain this solution are: the twist angle 90 degrees, wavelength  $0.65\mu\text{m}$ , thickness of the sample  $13\mu\text{m}$  and the birefringence  $\Delta n = 0.15$ . One can notice that the solution achieved absolute maximum when the twist is 45. Also, at the location of the linear polarization the twist angle can be recovered from the solution. The absolute maximum, for example, is always  $\sqrt{2}$  which is attained at the 45 degrees twist.

### 7.8.2 Oblique incident

For the case of oblique incident, the elements of the matrix  $H(z)$  are given by equations(7.55), (7.56)and (7.57). By carrying out exactly the same procedure of the last section, we obtain similar equations except that the birefringence is given by  $\Delta\alpha = \alpha_1 - \alpha_2$  which depends on the incident angle as we explained before.

## 7.9 Berreman approximation

In this section, we will discuss the convergence of the Berreman approximation. As mentioned earlier in this thesis that Berreman equation

$$\frac{d\psi}{dz} = \frac{-ik}{c}M(z)\psi. \quad (7.82)$$

has four periodic solutions when the Berreman matrix is approximately independent of  $z$ . In other words, when the berreman matrix is homogenous then Berreman method solves the Maxwell equations exactly. However, when the

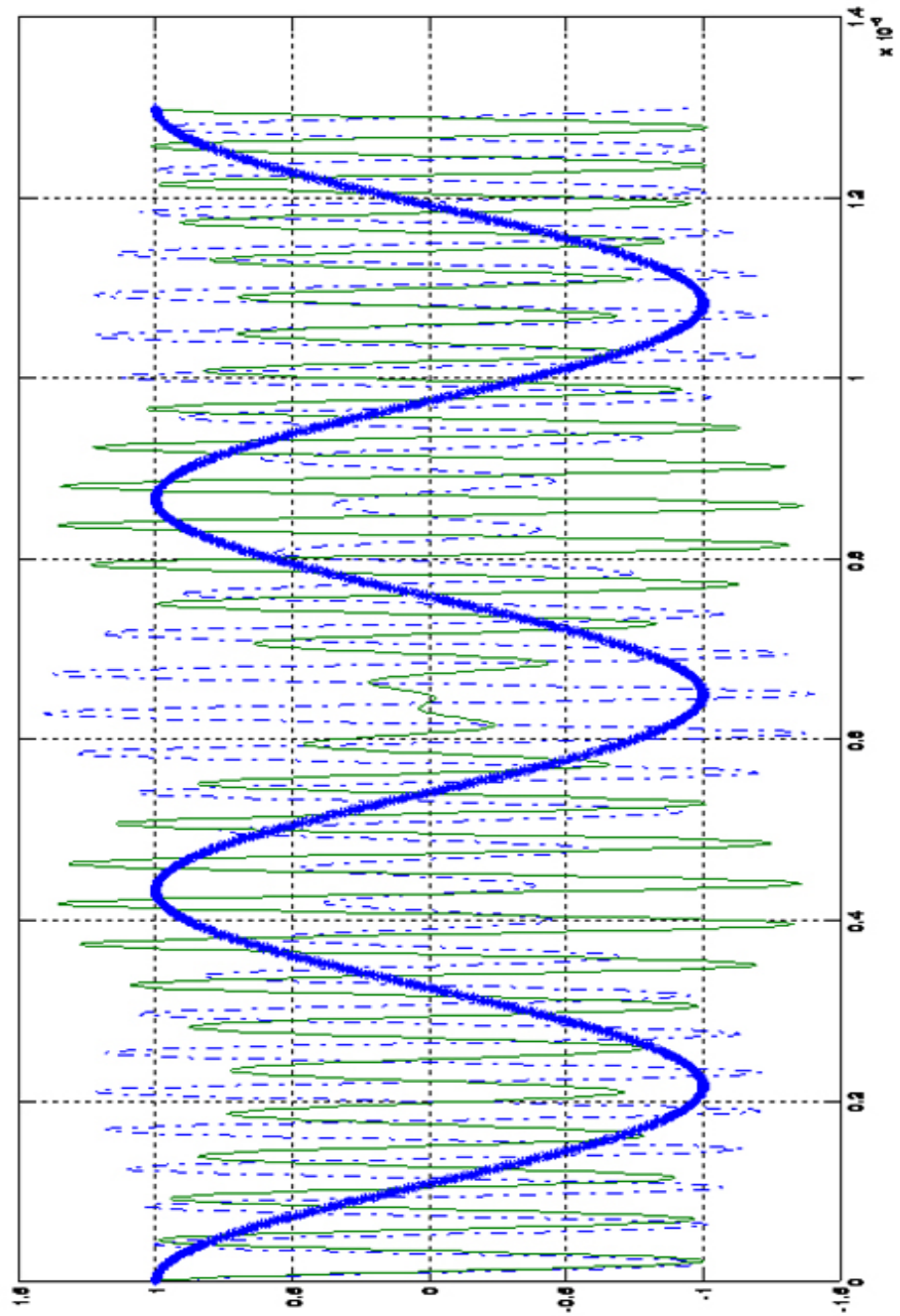


Figure 7.23: This figure shows how the waves propagate inside a sample with a twisted axis of anisotropy.

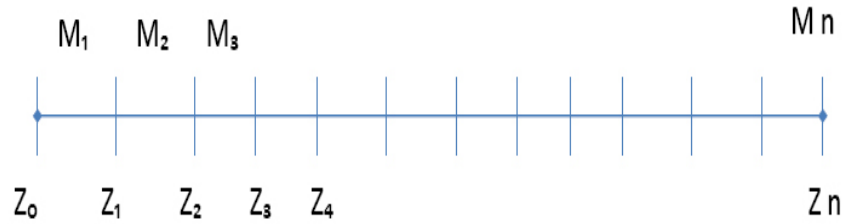


Figure 7.24: Berreman approaches to solve the Maxwell equations for inhomogeneous medium anisotropic medium.

medium is not homogenous, Berreman suggests that the solution can be approximated by partitioning the medium as illustrated in figure 7.24 and replacing the matrix  $M(z)$  by a piecewise continuous function on each interval. Berreman then solves the Maxwell equations and matches the boundary conditions since there is no source inside the medium. The question is, does Berreman approximation convergence to a solution with  $M(z)$  smooth as  $\Delta z \rightarrow 0$ ?

Let us consider a twisted anisotropic medium. In such medium, the Berreman matrix is inhomogeneous for any choices of partitions. As we stated in the last section, that the analytical solution of Berreman equation is given by equation (7.80). Our numerical analysis shows that the Berreman approximated solution will not converge to the exact solution when the numbers of partitions are not enough. Figure 7.25 and figure 7.26, for example, show that the Berreman approximated solution for a sample with twist  $22.5^\circ$ , ordinary refractive index 1.4 and birefringence 0.15 is not convergent to the analytical solution everywhere.

When number of partitions is increased, then the Berreman approximation solution will start to converge to the analytical solution everywhere as illustrated in figure 7.27. However, after some number of partitions, the error will not improve. Further investigation showed that the error in the Berreman approximated

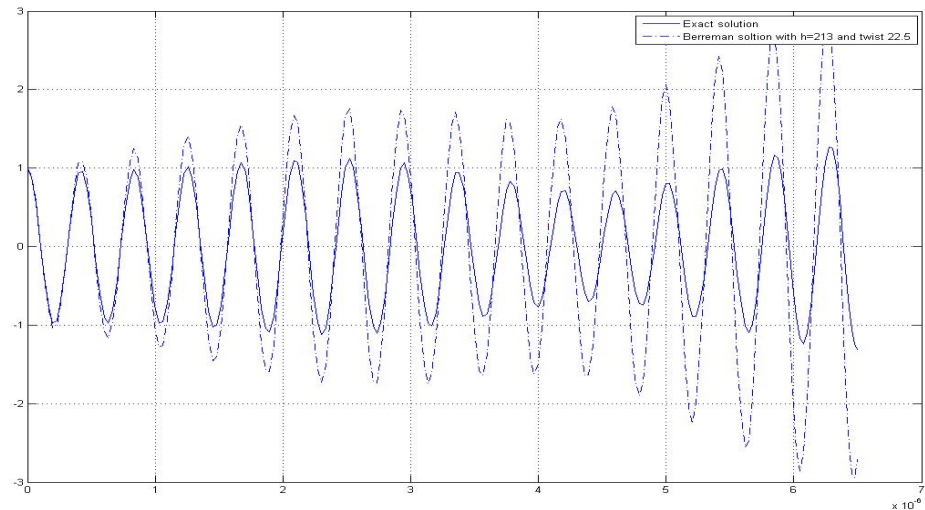


Figure 7.25: The first electric field component of Berreman approximated solution is not converging to the analytical solution for inhomogeneous sample with twist  $22.5^\circ$ .

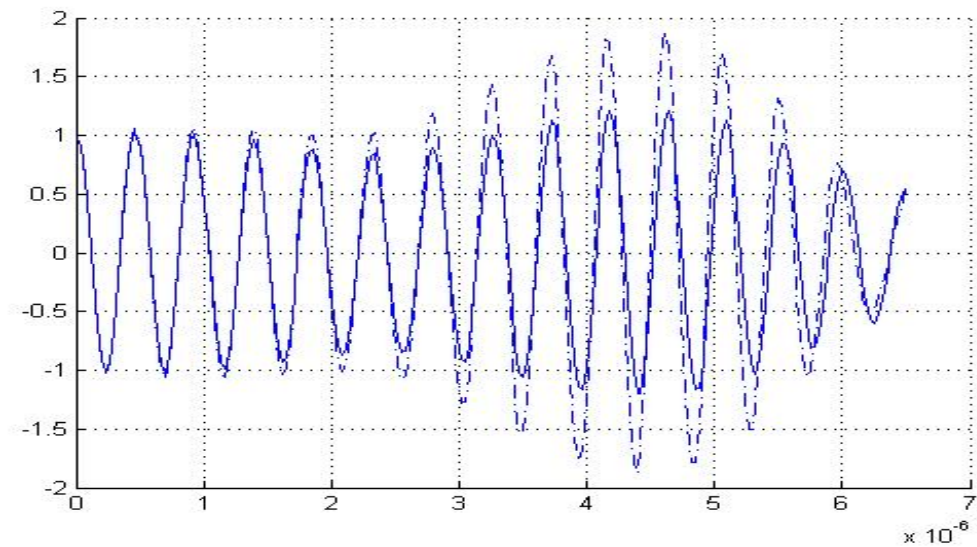


Figure 7.26: The second electric field component of Berreman approximated solution is not converging to the analytical solution for inhomogeneous sample with twist  $22.5^\circ$ .

solution depends on two factors. These factors are the length of the medium and the frequency of the used light beam.

Numerical calculation showed that the error between the Berreman approximated solution and the analytical solution can be improved by increasing the frequency of the used light beam. Figure 7.28 shows the error of the first component of the electric field for a fixed medium with seven different wavelengths. This figure tells us that the Berreman approximated solution converges linearly to the analytical solution. On the other hand, the error in the second component with the same frequencies is shown in figure 7.29. This figure tells that the solution in this components convergence linearly as well.

Figure 7.30 shows the error in the electric field with the same frequencies. In order to find the error in the electric field, we utilize the logarithmic scale. Figure 7.31 shows the log-log plot of the error for these frequencies. The corresponding equation for this figure is

$$\ln y = m \ln x + b \quad (7.83)$$

where the slope is  $m = 1.50$  and the intersection is  $b = 4.52$  for the log-log plot. This figure tells us that the error decreases as the wavelengths decreased.

## 7.10 Conclusion

This chapter contains some detailed derivation of the Berreman model from the Maxwell equations. By putting extra constraints on the Berreman model we were able to derive a system of  $2 \times 2$  differential equations which contains only electric fields components. It should be noticed that this system works for both normal and inclined incident angles.

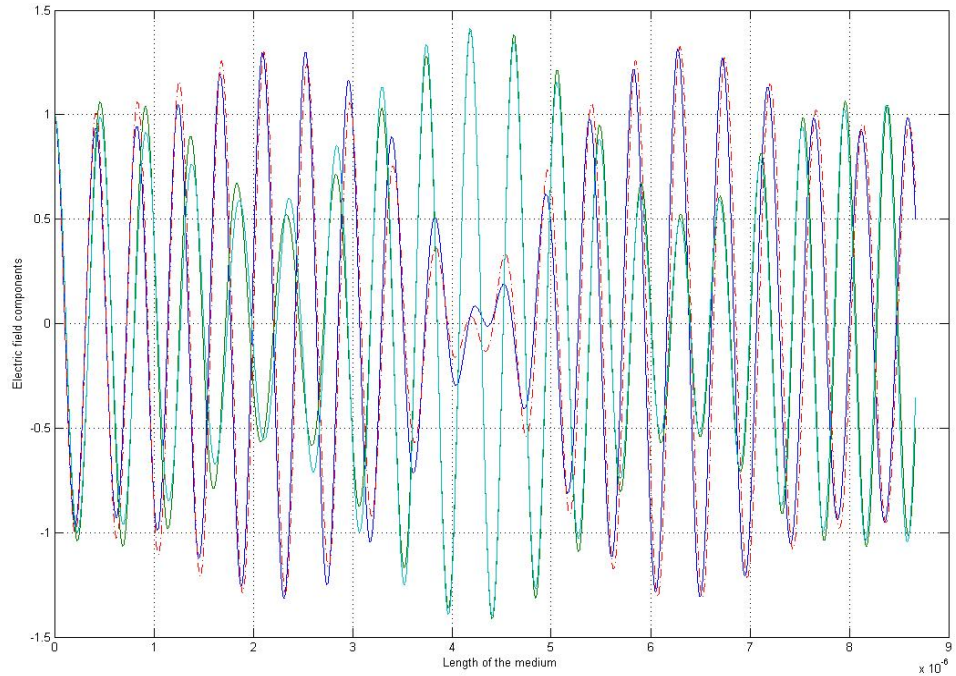


Figure 7.27: This figure shows the convergence of Berreman approximated solution to the exact solution of an inhomogeneous sample of length  $8.666\mu\text{m}$ . In this figure, the number of partition is 83557

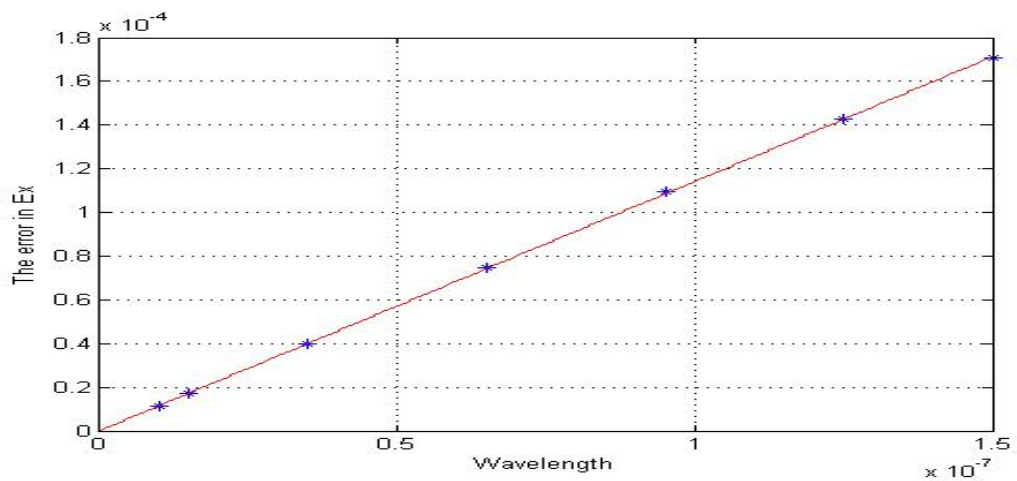


Figure 7.28: The error of the first component of the electric field  $E_x$  for a fixed medium with seven different wavelengths.

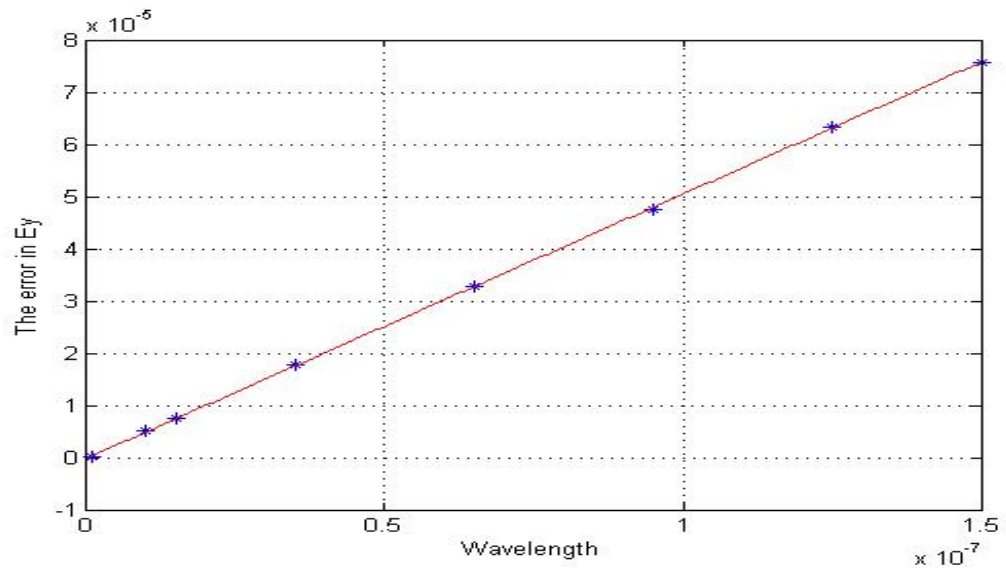


Figure 7.29: The error of the first component of the electric field  $E_y$  for a fixed medium with seven different wavelengths.

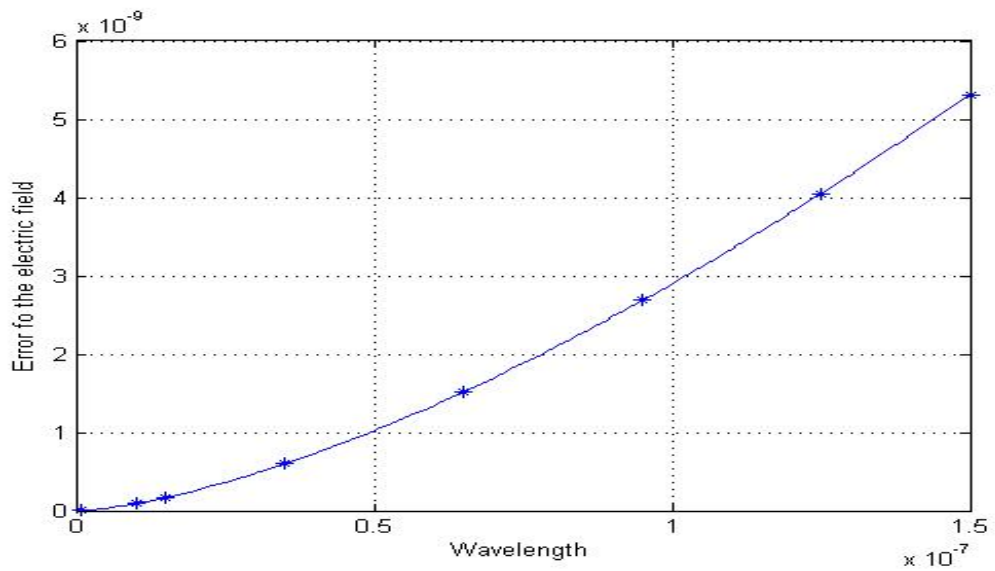


Figure 7.30: The error of the electric field for a fixed medium with the same seven different wavelengths.

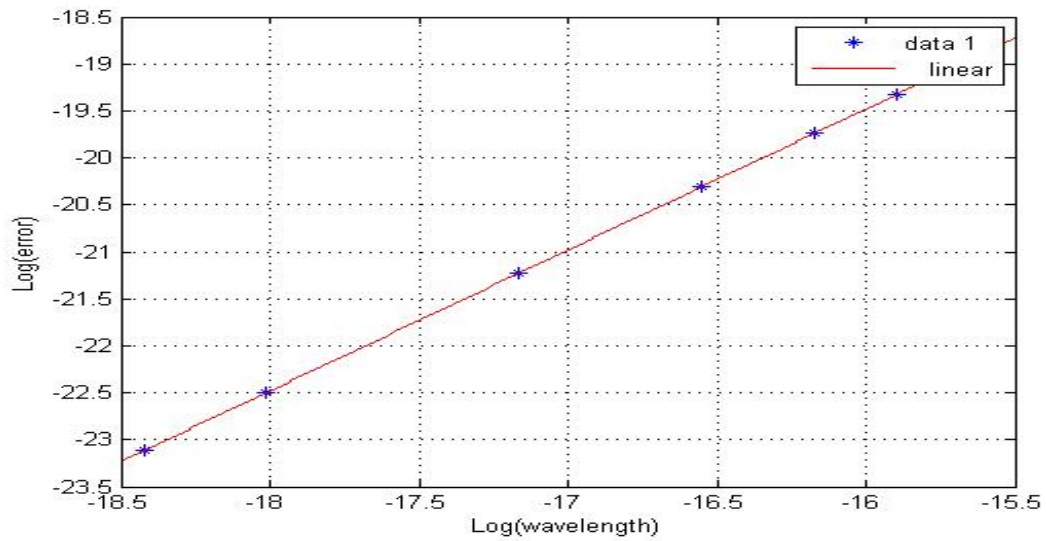


Figure 7.31: The log-log plot for the error of the electric field the same seven different wavelengths.

This system of differential equations has exactly the same form of the Schrödinger equation in Quantum Mechanics. One of the main advantage of this system is the visualization of the propagating modes inside the medium. In other words, it hard to visualize the propagating modes when there is a coupling between the differential equations such as twisted anisotropic medium.

In this chapter, a novel idea presented to solve these differential equations when there is a coupling between them. This idea has been called a rotational frame method. The obtained solution sketched in both rotational and original frames. The sketched in the original frame shows clearly the coupling between the waves and some other valuable information.

Furthermore, the analytical solution gives us a tool to test the accuracy of the Berreman approximated solution for inhomogeneous anisotropic medium. When Maugin condition is just satisfied, then the Berreman approximated solution will converge towards the analytical solution. However, the accuracy of the Berreman solution will not improve after some number of partitions. Further investigation

showed that the accuracy of the Berreman approximated solution depends on both wavelength of the used light beam and the length of the medium. In conclusion, for a fixed medium, there is a direct relation between the error and the wavelength.

# Chapter 8

## Forward and inverse problem

### 8.1 Derivation from Maxwell's equations

From Maxwell's equations for dielectric materials and harmonic field solution, we can derive the following equation [24]

$$\frac{d^2}{dz^2} \begin{pmatrix} E_x \\ E_y \end{pmatrix} = -\frac{k_0}{\epsilon_{33}} M \begin{pmatrix} E_x \\ E_y \end{pmatrix}, \quad (8.1)$$

where  $k_0$  is the wave number in the vacuum and  $M$  is a  $2 \times 2$  symmetric matrix. This matrix has components that depend on the dielectric tensor which appears in the Maxwell equations. This tensor also depends on the dielectric permittivity which is given by the following equation

$$\epsilon_{ij} = \epsilon_{\perp} \delta_{33} + \epsilon_a n_i n_j, \quad (8.2)$$

where  $\epsilon_{II}$  and  $\epsilon_{\perp}$  are the parallel and perpendicular dielectric permittivity respectively and  $\epsilon_a = \epsilon_{II} - \epsilon_{\perp}$ . Also, the matrix for the above system is given

by

$$M = \begin{pmatrix} \epsilon_{13}\epsilon_{33} - \epsilon_{13}^2 & \epsilon_{12}\epsilon_{33} - \epsilon_{13}\epsilon_{23} \\ \epsilon_{12}\epsilon_{33} - \epsilon_{13}\epsilon_{23} & \epsilon_{22}\epsilon_{33} - \epsilon_{23}^2 \end{pmatrix}.$$

As we mentioned previously, this equation has been derived on the basis that the medium varies in one direction, namely the  $z$ -direction. Moreover, the matrix has been derived for the case of normal incidence. The component of the electric field in the  $z$ -direction is given by [24]

$$E_z = \frac{\epsilon_{13}E_x + \epsilon_{23}E_y}{\epsilon_{33}}. \quad (8.3)$$

### 8.1.1 Ordinary and extraordinary matrices

In this section, we will try to rewrite the above matrix into ordinary and extraordinary matrices. This can be done as follows

$$\begin{aligned} \frac{1}{\epsilon_{33}}M &= \frac{1}{\epsilon_{33}} \begin{pmatrix} \epsilon_{13}\epsilon_{33} - \epsilon_{13}^2 & \epsilon_{12}\epsilon_{33} - \epsilon_{13}\epsilon_{23} \\ \epsilon_{12}\epsilon_{33} - \epsilon_{13}\epsilon_{23} & \epsilon_{22}\epsilon_{33} - \epsilon_{23}^2 \end{pmatrix} \\ &= \begin{pmatrix} \epsilon_{11} & 0 \\ 0 & \epsilon_{22} \end{pmatrix} - \frac{1}{\epsilon_{33}} \begin{pmatrix} \epsilon_{13}^2 & \epsilon_{13}\epsilon_{23} - \epsilon_{12}\epsilon_{33} \\ \epsilon_{13}\epsilon_{23} - \epsilon_{12}\epsilon_{33} & \epsilon_{23}^2 \end{pmatrix}. \end{aligned}$$

By assuming uniaxial medium and using the equations of dielectric tensor components which depend on the refractive indices of the medium, we can further simplify the above matrices.

$$\frac{1}{\epsilon_{33}}M = \begin{pmatrix} n_o^2 & 0 \\ 0 & n_o^2 \end{pmatrix} - \frac{1}{\epsilon_{33}} \begin{pmatrix} a_{11} & a_{12} \\ a_{21} & a_{22} \end{pmatrix} = M_o + M_e.$$

where the elements of the second matrix are given by the following equations

$$a_{11} = (n_e^2 - n_0^2) \cos^2(\theta) \cos^2(\phi) \epsilon_{33} - \epsilon_{13}^2, \quad (8.4)$$

$$a_{22} = (n_e^2 - n_0^2) \cos^2(\theta) \sin^2(\phi) \epsilon_{33} - \epsilon_{23}^2, \quad (8.5)$$

$$a_{12} = a_{21} = \epsilon_{13}\epsilon_{23} - \epsilon_{33}\epsilon_{12}. \quad (8.6)$$

By substituting the values of the dielectric tensor components into the above equation and by using straight forward calculations, the elements of the second matrix are given by

$$a_{11} = n_0^2 \Delta n \cos^2(\theta) \cos^2(\phi), \quad (8.7)$$

$$a_{22} = n_0^2 \Delta n \cos^2(\theta) \sin^2(\phi), \quad (8.8)$$

$$a_{12} = a_{21} = \Delta n \cos(\theta) \cos(\phi) \sin(\phi) (\Delta n \sin^2(\theta) \cos(\theta) + n_0^2 - \Delta n \sin^2(\theta)). \quad (8.9)$$

A quick look at the above decomposition of the  $M$  matrix, we notice that the first matrix  $M_o$  depends only on the ordinary refractive index. The second matrix  $M_e$  depends on both ordinary and extraordinary refractive indices of the medium. Also, the second matrix depends on the Euler angles of the director inside the sample.

### 8.1.2 Derivation of the Schrödinger Equation

The above equation (8.1) can be rewritten in a form similar to the Schrödinger equation. This can be achieved by replacing the matrix  $M$  by the two matrices

which have been derived in the previous section.

$$\frac{d^2}{dz^2} \begin{pmatrix} E_x \\ E_y \end{pmatrix} = -\frac{k_0^2}{\epsilon_{33}} M \begin{pmatrix} E_x \\ E_y \end{pmatrix} \quad (8.10)$$

$$= -k_0^2 \left( \begin{pmatrix} n_o^2 & 0 \\ 0 & n_o^2 \end{pmatrix} - \frac{1}{\epsilon_{33}} \begin{pmatrix} a_{11} & a_{12} \\ a_{21} & a_{22} \end{pmatrix} \right) \begin{pmatrix} E_x \\ E_y \end{pmatrix}, \quad (8.11)$$

$$\frac{d^2}{dz^2} \begin{pmatrix} E_x \\ E_y \end{pmatrix} + k_0^2 \begin{pmatrix} n_o^2 & 0 \\ 0 & n_o^2 \end{pmatrix} \begin{pmatrix} E_x \\ E_y \end{pmatrix} = \frac{k_0^2}{\epsilon_{33}} \begin{pmatrix} a_{11} & a_{12} \\ a_{21} & a_{22} \end{pmatrix} \begin{pmatrix} E_x \\ E_y \end{pmatrix}, \quad (8.12)$$

$$\frac{d^2}{dz^2} \begin{pmatrix} E_x \\ E_y \end{pmatrix} + (k_0 n_o)^2 \begin{pmatrix} E_x \\ E_y \end{pmatrix} = \frac{k_0^2}{\epsilon_{33}} \begin{pmatrix} a_{11} & a_{12} \\ a_{21} & a_{22} \end{pmatrix} \begin{pmatrix} E_x \\ E_y \end{pmatrix}. \quad (8.13)$$

By using linear algebra, the above equation can be written in matrix compact form as:

$$\frac{d^2}{dz^2} \mathbf{E}(z) + \lambda^2 \mathbf{E}(z) = \mathbf{V}(z) \mathbf{E}(z), \quad (8.14)$$

where

$$\mathbf{E}(z) = \begin{pmatrix} E_x \\ E_y \end{pmatrix},$$

and

$$\lambda = k_0 n_o.$$

This is a well known equation in Quantum Mechanics and is known as the Schrödinger equation. The potential for this Schrödinger equation is given by

$$\mathbf{V}(z) = \frac{k_0^2}{\epsilon_{33}} \begin{pmatrix} n_o^2 \Delta n \cos^2(\theta) \cos^2(\phi) & a_{12} \\ a_{21} & n_o^2 \Delta n \cos^2(\theta) \sin^2(\phi) \end{pmatrix}. \quad (8.15)$$

As it can be seen that the potential depends on Euler angles.

## 8.2 Discussion

The spectral equation

$$\frac{d^2}{dz^2} \begin{pmatrix} E_x \\ E_y \end{pmatrix} + (k_0 n_o)^2 \begin{pmatrix} E_x \\ E_y \end{pmatrix} = \frac{k_0^2}{\epsilon_{33}} \begin{pmatrix} a_{11} & a_{12} \\ a_{21} & a_{22} \end{pmatrix} \begin{pmatrix} E_x \\ E_y \end{pmatrix}, \quad (8.16)$$

which has been derived in the previous section can in fact be rewritten as a set of two, one dimensional Schrödinger equations

$$\frac{d^2 E_x}{dz^2} + \left(\frac{\omega}{c}\right)^2 (n_o + S_{11}) E_x = \left(\frac{\omega}{c}\right)^2 S_{12} E_y, \quad (8.17)$$

$$\frac{d^2 E_y}{dz^2} + \left(\frac{\omega}{c}\right)^2 (n_o + S_{22}) E_y = \left(\frac{\omega}{c}\right)^2 S_{21} E_x, \quad (8.18)$$

where the elements of the matrix  $S(z)$  is given by

$$S(z) = \begin{pmatrix} S_{11} & S_{12} \\ S_{21} & S_{22} \end{pmatrix} = \Delta n \begin{pmatrix} \cos^2(\phi) & \cos(\phi) \sin(\phi) \\ \sin(\phi) \cos(\phi) & \sin^2(\phi) \end{pmatrix}. \quad (8.19)$$

In practice, these two coupled time-independent Schrödinger equations describe two orthogonal waves which propagate in a layer in the direction of the  $z$ -axis. Also, in practice, these coupled time independent Schrödinger equations have a unique pair of solutions which propagate in the medium when the frequency of the used light is much smaller than the width of the sample.

As is known, an analytical solution for the two coupled time independent Schrödinger equations is in general not possible due to the form of the potential [60]. One of our goals in writing this section is to provide a model with an exact analytical solution for the two coupled time independent Schrödinger equations.

From an application point of view, an exact analytical solution is the most powerful tool to check the accuracy of a numerical computational program. In the coming subsections, the analytical solution together with a numerical solution will be presented in three different media.

### 8.2.1 The Solution of the Schrödinger equation with a vanishing potential

As mentioned in the previous section, our goal is to find an exact analytical solution for the time independent Schrödinger equation in closed form. To proceed with this aim, we will consider three different media which are the isotropic medium, anisotropic medium with a fixed transmission axis and anisotropic medium with a twisted transmission axis. This section will deal with the first medium, which is the isotropic medium and the remaining two media will be considered later on the coming sections.

When the medium is isotropic then the potential  $S(z)$  of the two coupled Schrödinger equations will vanish. As a consequence of this, the Schrödinger equation will reduce to two uncoupled Schrödinger equations known also as the Helmholtz equation

$$\frac{d^2 E_x}{dz^2} + \left(\frac{\omega}{c}\right)^2 n_0 E_x = 0, \quad (8.20)$$

$$\frac{d^2 E_y}{dz^2} + \left(\frac{\omega}{c}\right)^2 n_0 E_y = 0. \quad (8.21)$$

The solution is a transmission matrix which can be easily worked out. This solution is known in optics as the Jones matrix for an optical device with refractive

index  $n_0$

$$U(z) = \begin{pmatrix} e^{-i\frac{\omega}{c}n_0z} & 0 \\ 0 & e^{-i\frac{\omega}{c}n_0z} \end{pmatrix}. \quad (8.22)$$

This solution, the Jones matrix, will connect the input electric field components of the light to the output ones. In fact, the input polarization of the electric field components will remain unchanged as it passes through the optical device, since the eigenvalues of the solution are the same.

### 8.2.2 The Solution of the Schrödinger equation with a constant potential

A careful analysis of the Spectral equation shows that there are two special cases in which the Schrödinger equation will reduce to two uncoupled equations. The first case is when the potential is given by

$$P(z) = \begin{pmatrix} 1 & 0 \\ 0 & 0 \end{pmatrix}, \quad (8.23)$$

and the second case is when the potential is

$$P(z) = \begin{pmatrix} 0 & 0 \\ 0 & 1 \end{pmatrix}. \quad (8.24)$$

These potentials tell us that the transmission axis will stay along one direction throughout the medium. The uncoupled Schrödinger equation for the above mentioned potentials are

$$\frac{d^2 E_x}{dz^2} + \left(\frac{\omega}{c}\right)^2 n_e E_x = 0, \quad (8.25)$$

$$\frac{d^2 E_y}{dz^2} + \left(\frac{\omega}{c}\right)^2 n_0 E_y = 0, \quad (8.26)$$

and

$$\frac{d^2 E_x}{dz^2} + \left(\frac{\omega}{c}\right)^2 n_0 E_x = 0, \quad (8.27)$$

$$\frac{d^2 E_y}{dz^2} + \left(\frac{\omega}{c}\right)^2 n_e E_y = 0, \quad (8.28)$$

respectively. The unique solution for these equations is a transmission matrix which connects the input electric field components to the output ones. In the remainder of this section, we will consider one case and the second one will be almost similar.

When the transmission axis is along the  $x$ -axis then the transmission matrix is given by

$$U(z) = \begin{pmatrix} e^{-i\frac{\omega}{c}n_e z} & 0 \\ 0 & e^{-i\frac{\omega}{c}n_0 z} \end{pmatrix}. \quad (8.29)$$

This solution of the two uncoupled Schrödinger equations is indeed the Jones matrix for a device with fixed director along the  $x$ -axis. In fact, several valuable pieces of information can be gathered from this solution:

- First of all, the solution shows that the wave traveling along the  $x$ -axis propagates slower than the wave traveling along the  $y$ -axis for a positive birefringence  $\Delta n > 0$  and the opposite is true for a negative birefringence  $\Delta n < 0$ .
- The zeros, off diagonal elements, indicate that there is no coupling between the two waves which are traveling in the medium.
- Also, since the eigenvalues of the solution are not the same any more, unlike the vanishing potential case, the state of polarization of the incoming electric field components will change as they travel through the medium.

### 8.2.3 The Solution of the Schrödinger equation with a non-vanishing potential

The previous two sections show that there are some special cases in which the spectral equation in matrix form can be resolved into two uncoupled equations. However, when the potential depends on the space variable, then there will be coupling between the orthogonal components. Precisely speaking, there will be energy exchange between the two plane waves as they travel in the medium.

According to the research conducted by [61], there is no analytical solution to the spectral equation. The main reason is that the potential is a function of position. This research [61] studied the evolution of the state of polarization and the coupling between the equations through the Zeroth-order approximation solution. This approximation solution was introduced by Huang [60]

$$E_x(z) = \cos\left\{\frac{\tan^{-1}(2Q(z))}{2}\right\}W_x(z) + i \sin\left\{\frac{\tan^{-1}(2Q(z))}{2}\right\}W_y(z), \quad (8.30)$$

$$E_y(z) = i \sin\left\{\frac{\tan^{-1}(2Q(z))}{2}\right\}W_x(z) + \cos\left\{\frac{\tan^{-1}(2Q(z))}{2}\right\}W_y(z). \quad (8.31)$$

According to the Gel'fand-Levitan and Marchenko results[60], the solutions of the spectral equation in one dimension

$$\frac{d^2U}{dz^2} + \lambda^2U = V(z)U, \quad (8.32)$$

obeying the  $U(0) = 1$  and  $U'(0) = ik$ , can be written as:

$$U(z, k) = \exp(ikz) + \int_{-x}^x K(z, y) \exp(iky) dy. \quad (8.33)$$

Our approach to studying the coupling and the evolution of the state of polarization of the spectral equation in matrix form is quite different. This approach which has been presented in details in the previous chapters shows that the solution of the spectral equation in matrix form

$$\frac{d^2 P(z)}{dz^2} + \lambda^2 P(z) = V(z)P(z), \quad (8.34)$$

obeying  $P(0)=I$  and

$$U'(0) = \begin{pmatrix} k_1 & 0 \\ 0 & k_2 \end{pmatrix}, \quad (8.35)$$

where  $k_1 = \frac{\omega n_e}{c}$  and  $k_2 = \frac{\omega n_0}{c}$ , has the following representation:

$$P(z) = \begin{pmatrix} \cos \theta(z) e^{-i \frac{\omega}{c} n_e z} & -\sin \theta(z) e^{-i \frac{\omega}{c} n_0 z} \\ \sin \theta(z) e^{-i \frac{\omega}{c} n_e z} & \cos \theta(z) e^{-i \frac{\omega}{c} n_0 z} \end{pmatrix}. \quad (8.36)$$

The solution of the spectral equation, is the transfer matrix for a device with axis of anisotropy along the  $x$ -axis at the first boundary. At the second boundary, the axis of anisotropy is rotated through an angle  $\theta(z)$  from the  $x$ -axis. The solutions in terms of electric fields with initial polarization  $(E_x(i), E_y(i))$  are

$$E_x(z) = \cos \theta(z) e^{-i \frac{\omega}{c} n_e z} E_x(i) - \sin \theta(z) e^{-i \frac{\omega}{c} n_0 z} E_y(i), \quad (8.37)$$

$$E_y(i)(z) = \sin \theta(z) e^{-i \frac{\omega}{c} n_e z} E_x(i) + \cos \theta(z) e^{-i \frac{\omega}{c} n_0 z} E_y(i). \quad (8.38)$$

In fact, the solution of the spectral equation gives us some valuable pieces of information such as:

- The off diagonal elements indicate that there is a coupling between the waves traveling through the medium.

- The wave which propagates along the  $y$ -axis travels with its maximum velocity at the beginning of the sample and starts to slow down to reach its minimum velocity by the end of the sample and the opposite is true for the wave traveling along the  $x$ -axis.
- Both of the waves will travel with the same velocity when the axis of anisotropy is 45 degrees from the  $x$ -axis.

### 8.3 Inverse problem for Berreman

This section is devoted to study the linearized inverse problem. To begin with that, the solution of the homogenous Berreman equation

$$\frac{d\psi}{dz} + \frac{i\omega}{c}M(z)\psi = 0, \quad (8.39)$$

can be expressed means of a transfer matrix which connect the initial data to the final data

$$\psi(z) = U(z, z_o)\psi(z_o). \quad (8.40)$$

However, for a nonhomogeneous Berreman equation

$$\frac{d\psi}{dz} + \frac{i\omega}{c}M(z)\psi = S(z), \quad (8.41)$$

the solution will have an extra term and the new form of the solution is

$$\psi(z) = U(z, 0)\psi(0) + \int_0^z G(z, \tilde{z})S(\tilde{z})d\tilde{z}. \quad (8.42)$$

where is the Green's function for inhomogeneous problem with zero initial condition. For the sake of simplicity of our analysis, we shall denote the integral

operator which contains the Green's function by  $\mathcal{G}(\mathcal{S})$ .

Now let us consider a slight perturbation in the material parameter  $\epsilon \rightarrow \epsilon + \delta\epsilon$ . As a consequence of that the Berreman matrix will change from  $M$  to  $M + \delta M$  and the corresponding Berreman field should satisfy

$$\frac{d(\psi + \delta\psi)}{dz} = -\frac{i\omega}{c}(M(z) + \delta M)(\psi + \delta\psi). \quad (8.43)$$

If we take the unperturbed Berreman matrix as the initial guess, then the above perturbed Berreman matrix will reduce to

$$\frac{d\delta\psi}{dz} = -\frac{i\omega}{c}(M(z)\delta\psi + \delta M\psi + \delta M\delta\psi), \quad (8.44)$$

or

$$\left(\frac{d}{dz} + \frac{i\omega}{c}M(z)\right)\delta\psi = -\frac{i\omega}{c}(\delta M\psi + \delta M\delta\psi). \quad (8.45)$$

Note that this differential equation is similar to nonhomogeneous Berreman equation. By using equation (8.57), this differential equation can be written in operator form as

$$\delta\psi = -\frac{i\omega}{c}\mathcal{G}[\delta\mathcal{M}\psi + \delta\mathcal{M}\delta\psi] \quad (8.46)$$

$$= -\frac{i\omega}{c}(\mathcal{G}[\delta\mathcal{M}\psi] + \mathcal{G}[\delta\mathcal{M}\delta\psi]), \quad (8.47)$$

or

$$\left(I + \frac{i\omega}{c}\mathcal{G}[\delta\mathcal{M}]\right)\delta\psi = -\frac{i\omega}{c}\mathcal{G}[\delta\mathcal{M}\psi]. \quad (8.48)$$

A similar argument is used by the Calderón [11] in Electrical Impedance Tomography (EIT)

$$\delta\psi = -\frac{i\omega}{c}\left(I + \frac{i\omega}{c}\mathcal{G}[\delta\mathcal{M}]\right)^{-1}\mathcal{G}[\delta\mathcal{M}\psi], \quad (8.49)$$

provided that the operator norm satisfies

$$\|\frac{\omega}{c}\mathcal{G}[\delta\mathcal{M}]\| < 1, \quad (8.50)$$

in some norm. The coming section will discuss the convergence of the power series.

## 8.4 Linearized inverse problem for Berreman

We start this section by the following claim:

If the norm of operator for the perturbed Berreman matrix  $\delta M$  in  $L^\infty$  satisfies

$$\|\delta M\|_\infty < \frac{c}{\|\mathcal{G}\|_\omega}, \quad (8.51)$$

then the final data for the linearized inverse problem is given by

$$\delta\psi(d) = \frac{-i\omega}{c} \int_0^d G(d, z) \delta M(z) \delta\psi(0) dz. \quad (8.52)$$

If we take a sufficiently small perturbation of Berreman matrix to make sure the norm of the operator is  $\|\frac{\omega}{c}\mathcal{G}[\delta\mathcal{M}]\| < 1$ , then we can deal with the linearized inverse problem of

$$\delta\psi = -\frac{i\omega}{c} (I + \frac{i\omega}{c}\mathcal{G}[\delta\mathcal{M}])^{-1} \mathcal{G}[\delta\mathcal{M}\psi]. \quad (8.53)$$

Let us pause to see what kind of power series we have. The power series of the above equation is a convergent power series of operators and hence it is the Taylor series. The linear term is indeed the Fréchet derivative of the forward problem.

By deleting all nonlinear terms in  $\delta M(z)$  from the Neumann series

$$(I + \frac{i\omega}{c}\mathcal{G}[\delta\mathcal{M}])^{-1} = I + (\frac{-i\omega}{c}\mathcal{G}[\delta\mathcal{M}]) + (\frac{-i\omega}{c}\mathcal{G}[\delta\mathcal{M}])^2 + \dots \quad (8.54)$$

we obtain the following equation

$$\delta\psi = -\frac{i\omega}{c}\mathcal{G}[\delta\mathcal{M}\psi]. \quad (8.55)$$

This equation can be rewritten in a differential form as

$$(\frac{d}{dz} + \frac{i\omega}{c}\delta M)\delta\psi = -\frac{i\omega}{c}\delta M\psi, \quad (8.56)$$

and the solution of the final data is given by

$$\delta\psi(d) = \frac{-i\omega}{c} \int_0^d G(d, z)\delta M(z)\delta\psi(0)dz. \quad (8.57)$$

## 8.5 Summary

In this chapter, we have showed that the Maxwell equations can be reduced into an eigenvalue problem. This eigenvalue problem has exactly the same form as the second order Schrödinger equation in Quantum Mechanics,

From optics point of view, the eigenvalues of this spectral equation gives us the information about the refractive indexes of the sample whereas the potential gives us the orientation of the optical axis inside the sample. Different potentials has been considered and discussed.

Finally, this chapter treats the inverse problem and its corresponding linearized problem of Berreman model by considering perturbation about the Berreman matrix.

# Chapter 9

## Conclusions and future work

### 9.1 conclusion

The Jones matrix formalism may be conveniently used to analyze the propagation of light in isotropic and anisotropic media. However, as it is known that the Berreman model produces more exact solution of the Maxwell equations. One of the main difficulties with the Berreman model is that the model consists of four differential equations that is four traveling waves and these waves may coupled as they travel for some types of media. The coupling between the waves makes it impossible to obtain the analytical solution for the forward problem.

It is quite natural in the field of inverse problem to study the solution of the forward problem before approaching the inverse problem. At the outset of this investigation we expected that the forward problem was fully understood and there is nothing to do. It turns out that this is not the case.

By solving the forward problem, we obtained the following interesting results. A relationship between the diagonal elements of the dielectric tensor exists and this relationship has a fixed value everywhere in the sample regardless of the twist

and tilt angles of the director.

One of the interesting results in uniaxial media with vanishing tilt angle is that there is only one distinguishable eigen-direction. This idea results in reducing the the Maxwell equation into a system which contains only the electric field components. This system gives us the tool to project the other eigenspace to visualize the directions of the principal axes.

In fact, the  $2 \times 2$  system has exactly the same form of the Schrödinger equation in Quantum Mechanics. Further investigations showed that this system contains some information encoded in the eigenvalues and the corresponding potential. For instance, the orientation of the director inside the sample is encoded in the potential as we explained in this thesis. This system works for both normal and oblique incidence and the elements of the any incident angles have been worked out in this thesis.

Finding the solution for the  $2 \times 2$  differential equation was one of the main challenge when there is a coupling between the system of differential equations that this when the potential is non-vanishing. By combining the Schrödinger theory and Floquet's theory we were able to come up with new method to solve the  $2 \times 2$  differential equation. The method is termed in this thesis "the rotational frame method". By using the idea of rotational frame, we were able to obtain an analytical solution for the  $2 \times 2$  system. This is interesting since it gives us a tool to study convergence of the Berreman approximated solution for inhomogeneous anisotropic medium. This tool can be used since both Berreman and  $2 \times 2$  system produce the same traveling modes in any infinitesimal layer. Our study showed that the Berreman approximated solution will converge to the analytical solution but will not improve the accuracy after some number of partitions when the Maugin condition is just satisfied. It turns out that the error in the Berreman

approximated solution is a function of both wave length used light beam and the length of the medium. In another wards, for a fixed medium, Berreman approximated solution can improve the accuracy if we decrease the wave length of the used light beam.

Finally, a similar argument used by Calderón in (EIT) has been used to analyze the inverse problem for the Berreman model. His argument gives us the tool to study the convergence of the Neumann series. As a consequence of that we manage to linearize the inverse problem and obtain the solution that connects the final data with the initial data.

## 9.2 Future work

From Maxwell's equations and Berreman model, we have shown in detailed how to derive the  $2 \times 2$  system of differential equations which works for both normal and oblique incidents. As a continuation, we will consider two cases:

### 9.2.1 Non-vanishing tilt angles

In this thesis, we have not considered the case in which the tilt angle is not vanishing. In such situation, the Maxwell equations can not be reduced into a  $2 \times 2$  system of differential equations which depends only on the electric field components. The main reason is that the principal axes will not be normal to the direction of variations and as a result of that the dielectric tensor will have extra components compared with the case considered in this thesis.

In fact, this is a much more difficult problem since the magnetic field components will be coupled with the electric field components. This coupling between the

---

components make it difficult to eliminate the magnetic field components and we would like to investigate this case in the future.

### 9.2.2 Reconstruction of the potential

One of the results we obtained in this thesis is that the derivation allows us to encode the orientation of the director inside the sample into the potential of the Schrödinger equation. This equation has been studied in Quantum Mechanics and some results have been published. In one dimension, the inverse problem for this equation is to recover the potential from the scattering data. This problem has been investigated by I. M. Gel'fand and B. M. Levitan. In matrix form, a potential work has been done by Marchenko and others in this area and some results has been established and published to recover the potential of the Schrödinger equation. The reconstruction of the potential is indeed the recovering the optical axis of the sample and this leads to recover the dielectric tensor. Some work needed to investigate the application of the Marchenko results on our model.

# Bibliography

- [1] I. Abdulhalim. Analytic propagation matrix method for linear optics of arbitrary biaxial layered media. *Journal of Optics A: Pure and Applied Optics*, 1:646–653, July 1999.
- [2] I. Abdulhalim. Exact  $2 \times 2$  matrix method for the transmission and reflection at the interface between two arbitrarily oriented biaxial crystals. *Journal of Optics A: Pure and Applied Optics*, 1:655–661, July 1999.
- [3] I. Abdulhalim. Analytic propagation matrix method for anisotropic magneto-optic layered media. *Journal of Optics A: Pure and Applied Optics*, 2:557–564, August 2000.
- [4] D. Andrienko. Introduction to liquid crystals. *International Max Planck Research School, Modelling of Soft Matter*, September 2006.
- [5] M. Bechi and P. Galatola. Berreman-matrix formulation of light propagation in stratified anisotropic chiral media. *Eur. Phys.*, 8:399–404, May 1999.
- [6] D. W. Berreman. Optics in stratified and anisotropic media:  $4 \times 4$ -matrix formulation. *Optical Society of America*, 62(4), April 1972.
- [7] D. W. Berreman and T. J. Scheffer. Bragg reflection light from single-domain

- cholesteric liquid-crystal films. *Physical review letters*, 25(9):577–581, August 1970.
- [8] S. L. Blakeney, S. E. Day, and J. N. Stewart. Determination of unknown input polarisation using a twisted nematic liquid crystal display with fixed components. *Optics Communications*, 214:1–8, September 2002.
- [9] B. H. Bransden and C. J. Joachain. *Introduction to Quantum Mechaics*. Longman Group UK Limited, 1989.
- [10] D. E. Budil, Z. Ding, G. R. Smith, and K. A. Earle. Jones matrix formalism for quasioptical EPR. *Journal of Magnetic Resonance*, 144(1):20–34, May 2000.
- [11] A. P. Calderón. On an inverse boundary value problem, in seminar on numerical analysis and its applications to continuum physics. *Rio de Janeiro, Editors W.H. Meyer and M.A. Raupp, Sociedade Brasileira de Matematica*, pages 65–73, 1980.
- [12] C. J. Chen, A. Lien, and M. I. Nathan.  $4 \times 4$  and  $2 \times 2$  matrix formulations for the optics in stratified and biaxial media. *Opt. Soc. Am. A*, 14:3125–3134, June 1997.
- [13] P. G. De Gennes and J. Prost. *The physics of liquid crystals*. Oxford University Press, 1993.
- [14] C. Gu and P. Yeh. Dynamic equation for the polarization state in inhomogeneous anisotropic media. *Applied Optics*, 33(1):60–63, January 1994.
- [15] H. Hammer and W. R. B Lionheart. Reconstruction of spatially inhomogeneous dielectric tensors through optical tomography. *Journal of Optical Society of America A*, 22(2):250–255, February 2005.

- 
- [16] M. Honma and T. Nose. Polarization-independent liquid crystal grating fabricated by microrubbing process. *Japan Society of Applied Physics*, 42(11):6992–6997, November 2003.
- [17] M. Honma, M. Ogasawara, and T. Nose. Polarization-independent liquid-crystal grating with microscale alignment pattern. *Icicetrans. Electron*, E88-C(11):2099–2105, November 2005.
- [18] S. Huard. *Polarization of light*. John Wiley and sons, 1997.
- [19] D. K. Hwang and A. D. Rey. Computational modelling of light propagation in textured liquid crystals based on the finite-difference time-domain (FDTD) method. *Liquid Crystals*, 32(4):483–497, April 2005.
- [20] M. Kawamura, Y. Goto, and S. Sato. A two-dimensional pretilt angle distribution measurement of twisted nematic liquid crystal cells using Stokes parameters at plural wavelengths. *The Japan Society of Applied Physics*, 43(2):709–714, February 2004.
- [21] W. Klaus, Y. Suzuki, M. Tsuchiya, and T. Kamiya. Optical characterization of homogenous nematic liquid crystal cells based on the liquid crystal continuum model. *Applied Physics*, 34(11):6116–6124, November 1995.
- [22] E. E. Kriezis and S. J. Elston. A wide angle beam propagation method for the analysis of tilted nematic liquid crystal structure. *Modern Optics*, 46(8):1201–1212, Feb 1999.
- [23] M. P. C. M. Krijn. Electromagnetic wave propagation in stratified anisotropic media in the presence of sources. *Optics Letters*, 17:163–165, August 1992.
- [24] D. O. Krimer, G. Demeter, and L. Kramer. Influence of the backflow effect

- on the orientational dynamics induced by light in nematics. *The American Physical Society*, 71(5):051711–1–051711–10, May 2005.
- [25] B. M. Levitan and I. S. Sargsjan. *Introduction to spectral theory: selfadjoint ordinary differential operators*. The American Mathematical Society, 1975.
- [26] X. LI, X. Dai, M. Jin, F. Jia, X. Chen, X. Li, and S. Xie. A novel method of automatic polarization measurement and its application to the higher-order PMD measurement. *Optics Communications*, 215:309–314, 2003.
- [27] A. Lien. A detailed derivation of Jones matrix representation for twisted nematic liquid crystal displays. *Liquid Crystals*, 22(2):171–175, Sep 1997.
- [28] P. J. Lin-Chung and S. Teitler.  $4 \times 4$  matrix formalisms for optics in stratified anisotropic. *Journal of Optical Society of America A*, 1(7):703–705, July 1984.
- [29] W. R. B. Lionheart and C. J. P. Newton. Analysis of the inverse problem for determining nematic liquid crystal director profiles from optical measurements using singular value decomposition. *New Journal of Physics*, 9(63), March 2007.
- [30] E. Hallstig, T. Martin, L. Sjöqvist, and M. Lindgren. Polarization properties of a nematic liquid-crystal spatial light modulator for phase modulation. *Journal of Optical Society of America A*, 22(1):177–184, January 2005.
- [31] P. McIntyre and A. W. Snyder. Light propagation in twisted anisotropic media: Application to photoreceptors. *Optical Society of America*, 68(2):149–157, February 1978.
- [32] V. Ya. Molchanov and C. V. Skrotskii. Matrix method for the calculation of

- the polarization eigenstates of anisotropic optical resonators. *Soviet Journal of Quantum Electronics*, 1(4):310–330, January 1972.
- [33] M. Monerie and L. Jeunhomme. Polarization mode coupling in long single-mode fibres. *Optical and Quantum Electronics*, 12:449–461, May 1980.
- [34] E. N. Montbach and P. J. Bos. Control of dispersion in form birefringent-based holographic optical retarders. *Optical Engineering*, 44:124001, May 2005.
- [35] X. Nie, T. X. Wu, Y. Lu, Y. Wu, X. Liang, and S. T. Wu. Dual-frequency addressed infrared liquid crystal phase modulators with submillisecond response time. *Molecular Crystals and Liquid Crystals*, 454:123/525–133/535, 2006.
- [36] Y. Ohtera, H. Yoda, and S. Kawakawi. Analysis of twisted nematic liquid crystal Fabry-Perot interferometer (TN-FPI) filter based on the coupled mode theory. *Optical and Quantum Electronics*, 32:147–167, 2000.
- [37] C. Oldano. Electromagnetic-wave propagation in anisotropic stratified media. *Physical Review A*, 10:6014–6020, November 1989.
- [38] H. L. Ong. Reducing the Berreman  $4 \times 4$  propagation matrix method for layered inhomogeneous anisotropic media to the Abeles  $2 \times 2$  matrix method for isotropic media. *Journal of Optical Society of America A*, 8(2):303–305, February 1991.
- [39] R. Ozaki, M. Aoki, H. Moritake, K. Yoshino, and K. Toda. Evaluation of nematic liquid crystal director orientation in vicinity of glass substrate using shear horizontal wave propagation. *The Japan Society of Applied Physics*, 45(5B):4662–4666, May 2006.

- 
- [40] O. A. Peverini, D. Olivero, C. Oldano, D. K. G. de Boer, R. Cortie, R. Orta, and R. Tascone. Reduced-order model technique for the analysis of anisotropic inhomogeneous media: application to liquid-crystal displays. *Journal of Optical Society of America A*, 19(9):1901–1909, September 2002.
- [41] M. Schubert. Polarization-dependent optical parameters of arbitrarily anisotropic homogeneous layered systems. *Physical Review B*, 53(8):4265–4274, February 1996-II.
- [42] F. Schwabl. *Advanced Quantum Mechanics*. Springer-Verlag Berlin Heidelberg, 2000.
- [43] V. A. Sharafutdinov. *Integral geometry of tensor fields*. 1994.
- [44] L. ShiFang. Jones-matrix analysis with Pauli matrices: application to ellipsometry. *Optical Society of America*, 17(5):920–926, May 2000.
- [45] J. H Shirley. Solution of Schrödinger equation with a Hamiltonian periodic on time. *Physical Review*, 138(4B):979–987, May 1965.
- [46] S. Stallinga. Berreman  $4 \times 4$  matrix method for reflective liquid crystal displays. *applied physics*, 85, December 1999.
- [47] S. Stallinga. Equivalent retarder approach to reflective liquid crystal displays. *Journal of Applied Physics*, 86(9):4756–4766, November 1999.
- [48] Yu. P. Svirko and N. I. Zheludev. *Polarization of light in nonlinear optics*. John Wiley and sons, 1998.
- [49] A. N. Tikhonov and V. Y. Arsenin. *Solutions of ill-posed problems*. V. H. Winston and sons, 1977.

- 
- [50] V. A Tkachenko. *Spectral operator theory and related topics*. The American Mathematical Society, 1994.
- [51] M. Tsutsumi. Periodical linear systems and a class of nonlinear evolution equations. *Proceedings of the Japan Academy*, 51(8):645–649, October 1975.
- [52] E. Vogelzang, H. A. Ferwerda, and D. Yevick. A numerical reconstruction of permittivity profile of a stratified dielectric layer. *Optica Acta*, 31(5):541–554, 1984.
- [53] W. E. Wiesel and D. J. Pohlen. Cononical Floquet theory. *Celestial Mechanics and Dynamical Astronomy*, 58:81–96, 1994.
- [54] H. Wobler, G. Hasa, M. Pritsch, and D. A. Mlynakl. Faster  $4 \times 4$  matrix method for uniaxial inhomogeneous media. *Optics*, 6(9):1554–1557, September 1988.
- [55] H. Wohler and M.E. Becker. Numerical modelling of LCD electro optical performance. *Opto-Electronics Review*, 10:23–33, 2002.
- [56] K. L. Woon, M. O’Neill, G. J. Richard, M. P. Aldred, and S. M. Kelly. Stokes-parameter analysis of the polarization of light transmitted through a chiral nematic liquid-crystal cell. *Optical Society of America*, 22(4):760–766, April 2005.
- [57] M. Yamauchi. Jones-matrix models for twisted-nematic liquid-crystal devices. *Optical Society of America*, 44(21):4484–4493, July 2005.
- [58] F. H. Yu and H. S. Kwok. Comparison of extended Jones matrices for twisted nematic liquid-crystal displays at oblique angles of incidence. *Optics*, 16(8):2772–2780, November 1999.

- 
- [59] Y. Zhou, Z. He, and S. Aato. A novel method for determining the cell thickness and twist angle of a twisted nematic cell by Stokes parameter measurement. *The Japan Society of Applied Physics*, 36(5A):2760–2764, May 1997.
- [60] C. Zhu. Exact analytical solution for coupled time-independent Schrödinger equations with certain model potential. *Journal of Physics*, 29:1293–1303, 1996.
- [61] X. Zhu and R. Jain. Detailed analysis of evolution of the state of polarization in all-fiber polarization transformers. *Optics Express*, 14(22):10261–10277, October 2006.